

A STUDY OF THE THROUGHFEED CENTRELESS GRINDING PROCESS  
WITH PARTICULAR REFERENCE TO THE SIZE ACCURACY

CLIFTON GOODALL

A thesis submitted in partial fulfilment of the  
requirements of the Council for National Academic  
Awards for the degree of Doctor of Philosophy

July 1990

Liverpool Polytechnic (School of Engineering and  
Technology Management) in collaboration with the  
Torrington Company



C.Goodall.

A study of the throughfeed centreless grinding process with particular reference to the size accuracy.

Synopsis.

A model of the throughfeed centreless grinding process was developed and a computer program based on the model was written. Emphasis was placed on the workpiece sizing mechanism although provisions were made to include the workpiece rounding mechanism. The results from the simulation were supported by experimental observations.

Experimental studies identified two major trends in the size variation of a stream of consecutively ground workpieces. One was associated with a once per revolution error in the trued shape of the regulating wheel whilst the other was attributed to the precession ratio of the regulating wheel spindle bearings. The error in the trued shape of the regulating wheel was due to the interaction between the trueing tool and the regulating wheel, and the response of the regulating wheel system to temperature variations. A number of solutions were proposed.

Expressions were developed to describe the conventionally trued regulating wheel form in throughfeed centreless grinding. Those expressions were then used to illustrate the effect of changing trueing parameters on the generated regulating wheel form. In turn, alternative regulating wheel trueing philosophies, for example, trueing the regulating wheel with the grinding wheel, were analysed in terms of their applicability to throughfeed centreless grinding.

The combined effect of the size, roundness and geometric form of a centreless ground workpiece on its diametral measurement in a Two point gauge was studied. Measured size and effective size were shown to be functions of the relationship between the coordinate system of the workpiece and that of the measurement device. A size gauging methodology specific to centreless ground workpieces was developed.

A detailed study was made of the primary components of a precision throughfeed centreless grinding machine and their contribution to the generated workpiece form. The necessity for additional tuning of a machine set-up was shown to be dependent on a number of machine setting errors and expressions were developed to quantify them. Some machine components were redesigned to minimise those errors.

## Acknowledgements.

The author is greatly indebted to his Director of studies, Professor W.B.Rowe, for his insight, guidance and encouragement in all aspects of the programme. Many thanks are also extended to Dr.D.Brough who, in the role of second supervisor, brought additional depth to the research effort.

As an industrial sponsor, the Torrington Company provided strong support for the programme for which the author is deeply grateful. Special thanks are extended to Mr.W.S.Pete, the industrial supervisor, whose experience and perception proved invaluable.

Thanks are also extended to Mr.A.Dunmore (Research Technician) for his contribution to the experimental programme and to Liverpool Polytechnic's School of Engineering and Technology Management for the use of the computing and laboratory facilities.

Finally, many thanks to my parents, and to my wife Patricia for all her support.

### The Author.

Clifton Goodall was born in 1958 and joined Ocean Transport and Trading's four year Engineer Cadetship Scheme in 1975. During this period he gained an Ordinary National Diploma in Mechanical Engineering and an Ordinary National Diploma Endorsement in Mechanical/Marine Engineering.

On completing his indentures, he enrolled on a sandwich degree course at Liverpool Polytechnic, where, four years later, he was awarded an honours degree in Mechanical Engineering by the Council for National Academic Awards. The industrial training periods were undertaken with the United Kingdom Atomic Energy Authority's Safety Reliability Directorate and with the National Institute for Agricultural Engineering.

In 1983 he was appointed as a research assistant in the Department of Mechanical, Marine and Production Engineering, Liverpool Polytechnic, and in 1986 took up his current position as a research engineer with the Torrington Company.

He was elected a Graduate of both the Institution of

Mechanical Engineers and the Institution of Production Engineers in 1983.

Related studies.

The author spent three weeks at the Torrington Company's Dahlonga production facility reviewing needle roller manufacture in general and the throughfeed centreless grinding process in particular. Visits were also made to the production facility in Coventry.

The author attended a number of conferences, seminars and machine tool shows as well as visiting the major centres for grinding research in the United Kingdom.

Attendance at lectures in postgraduate and honours degree courses presented by Liverpool Polytechnic's Department of Mechanical, Marine and Production Engineering were also part of the programme of related studies.



A study of the throughfeed centreless grinding process  
with particular reference to the size accuracy.

	Page Number.
Synopsis.	i
Acknowledgements.	ii
The Author.	iii
Related studies.	iv
Contents.	v
List of Figures.	ix
List of Tables.	xi
Nomenclature.	xii
 Chapter 1.	
Introduction.	
 1.1 Historical aspects.	1
1.2 Description of the throughfeed centreless grinding process.	3
1.3 Definition of the problem and broad aims of the programme.	5
1.4 Scope of the programme.	6
1.5 The nomenclature of the throughfeed centreless grinding process.	9
 Chapter 2.	
Basic investigation of workpiece size errors in the throughfeed centreless grinding process.	
 2.1 Introduction.	11
2.2 The Cincinnati 230-10 centreless grinder.	11
2.3 Investigation of the machine setting errors.	12
2.4 Redesign of the lower slide clamp.	17
2.5 Pre-grind preparation of workpieces.	18
2.6 Development of a system for capturing consecutively ground workpieces.	19
2.7 Basic grinding experiments.	21
2.8 Discussion of results from initial experiments.	23
2.9 Factors that affect the shape of the consecutive workpiece size plots.	25
2.10 Primary factors affecting size holding in the throughfeed centreless grinding process.	28

### Chapter 3. Workpiece metrology.

3.1	Introduction.	30
3.2	Literature survey.	31
3.3	Development of a methodology for measuring the size of a needle roller.	37
3.3.1	The gauging system.	37
3.3.2	Determining the minimum number of measurements necessary to classify the size of a workpiece.	38
3.3.3	Analysing the interaction between the gauge operator and the gauge.	41
3.3.4	A methodology for gauging centreless ground workpieces.	48
3.4	Measurement of size variation within a blank (unground workpiece).	50
3.5	Summary.	51

### Chapter 4. The regulating wheel.

4.1	Introduction.	53
4.2	Obtaining the optimum regulating wheel shape.	54
4.3	Centreless grinder set-up to achieve the optimum regulating wheel shape for throughfeed grinding cylindrical workpieces.	58
4.3.1	Dresser angle (Cincinnati Milacron).	62
4.3.2	Profile bar (Lidköping).	62
4.4	Development of expressions for the trued regulating wheel shape.	64
4.5	Regulating wheel shape when trued using the grinding wheel.	69
4.6	Effect of throughfeed angle, trueing angle and diamond offset on the grinding gap contour.	72
4.7	Physical constraints on correcting the regulating wheel profile.	75
4.8	Feasibility of using a ground regulating wheel in throughfeed centreless grinding.	76
4.9	Summary.	77

## Chapter 5.

Part to part size variation and the centreless grinding machine system.

5.1	Introduction.	79
5.2	Size variation.	80
5.3	Errors in the trued shape of the regulating wheel.	82
5.4	Investigation of the source of the once per revolution error in the trued shape of the regulating wheel.	85
5.5	The interaction between the diamond tool and the regulating wheel.	88
5.6	Thermal considerations.	94
5.7	Machine stiffness.	101
5.8	Grinding forces.	105
5.9	Conventionally trued regulating wheel versus a ground regulating wheel.	108
5.10	Summary.	110

## Chapter 6.

Simulation of the throughfeed centreless grinding process: workpiece sizing mechanism.

6.1	Introduction.	116
6.2	Review of previous models of the centreless grinding process.	116
6.3	Basic concept used in the development of a throughfeed centreless grinding model.	119
6.4	Considerations when modelling the throughfeed centreless grinding process.	121
6.4.1	Variation in the throat angle.	122
6.4.2	Grinding below centre.	123
6.4.3	Variation in throughfeed rate and workpiece rotational speed.	125
6.4.4	Dynamic effects.	126
6.5	Initial version of a model of the sizing mechanism in the throughfeed centreless grinding process.	127
6.5.1	Regulating wheel axial form.	127
6.5.2	Depth of cut per workpiece revolution.	127
6.5.3	Regulating wheel system runouts.	129
6.5.4	Initial workpiece shape.	130
6.5.5	Workpiece diameter.	130



6.6	General description of the computer program written to simulate the throughfeed centreless grinding process.	131
6.7	Results of the computer simulation.	135
6.8	Summary.	136

## Chapter 7.

### Discussion and conclusions.

7.1	Discussion.	138
7.2	Conclusions.	145

## Chapter 8.

Further Work.	148
---------------	-----

## References.

## Figures.

## Tables.

## List of Figures.

1. The throughfeed centreless grinding system.
2. Effect of grinding gap geometry on workpiece axial form.
3. Variation in throat angle in throughfeed centreless grinding.
4. Regulating wheel housing pivot point in relation to regulating wheel centre - 'below offset' effect.
5. Regulating wheel housing pivot point in relation to regulating wheel centre - angular effect.
6. Plot of consecutive workpiece size variation.
7. Plot of number of consecutive workpieces per size variation cycle versus frequency of occurrence.
8. Measurement of an iso-diametric shape (5 lobed).
9. Two-point measurement.
10. Taylors Principle and iso-diametric workpieces (after Loxham).
11. Operator variability - Operator 1 versus Operator 2.
12. Operator variability - Operator 1 versus Operator 3.
13. Within workpiece size variation.
14. Creation of the shape of the regulating wheel for different height positions (after Meis).
15. Relationship between workpiece diameter and regulating wheel shape (after Meis).
16. Generation of regulating wheel form: no part height.
17. Generation of regulating wheel form: with part height.
18. Generation of regulating wheel form when using dresser profile bar.
19. Regulating wheel dresser profile bar.
20. Regulating wheel viewing plane.
21. Ground regulating wheel axial profile - theoretical shape.
22. Ground regulating wheel axial profile - actual shape.
23. Effect of changing throughfeed angle on regulating wheel axial profile.
24. Effect of changing trueing angle on regulating wheel axial profile.
25. Change in rake and drag angles during regulating wheel trueing.
26. Regulating wheel surface runout (outboard) and outboard bearing temperature against time.
27. Regulating wheel surface runout (outboard) against time.
28. Effect of a three minute feed stoppage.
29. Effect of a momentary feed stoppage.
30. Rough cut size variation.
31. Finish cut size variation.



32. Size variation with conventionally dressed regulating wheel.
33. Size variation with plunge ground dressed regulating wheel.
34. Visual representation of the equation of constraint (after Rowe).
35. Condition for tapered regulating wheel.
36. Flow chart of the simulation of the throughfeed centreless grinding process.
37. Graphical results of computer simulation for  $K = 0.3$ .
38. Graphical results of computer simulation for  $K = 0.7$ .

## List of Tables.

1. Back-pressure evaluation.
2. Surface roughness of Tube and Non-Tube parts (early runs).
3. Surface roughness of Tube and Non-Tube parts (later runs).
4. Out-of-roundness of Tube and Non-Tube parts (early runs).
5. Out-of-roundness of Tube and Non-Tube parts (later runs).
6. Size measurements over one workpiece revolution.
7. Multiple shot measurement of a needle roller.
8. Operator variability - 20 piece sample size: Operator 1 versus Operator 2.
9. Operator variability - 20 piece sample size: Operator 1 versus Operator 3.
10. Operator variability - 20 piece sample size: Operator 2 versus Operator 3.
11. Operator variability - 20 piece sample size: Operator 1 versus Operator 1.
12. Operator variability - 10 piece sample size: Operator 1 versus Operator 2.
13. Operator variability - 10 piece sample size: Operator 1 versus Operator 3.
14. Operator variability - 10 piece sample size: Operator 1 versus Operator 1.
15. Computed regulating wheel shape when ground with grinding wheel.
16. Workpiece diameter change as a function of axial location.
17. Effect of changing throughfeed angle on regulating wheel axial profile.
18. Effect of changing trueing angle on regulating wheel axial profile.



## Nomenclature.

For any given parameter, where possible, the symbol used in this programme is shown first. The primary nomenclature systems are [1] England (Rowe), [2] Japan (Miyashita) and [3] W.Germany (Aachen University).

$\alpha[3], \alpha_R[3]$	:Throughfeed angle.
$\alpha[1], \phi_1[2][3]$	:Angle between the grinding wheel contact normal and the workblade contact normal.
$\alpha_s[3], \alpha_{dr}[3]$	:Regulating wheel trueing angle.
$\alpha_v$	:Regulating wheel viewing angle.
$\beta[3], \alpha'[1], \theta[2]$	:Workblade angle.
$D_s[3], D_g[1], d_g[2]$	:Grinding wheel diameter.
$D_R[3], d_r[2], D_c[1]$	:Regulating wheel, control wheel diameter.
$D_w[3][2][1], d_w[3]$	:Needle roller diameter, nominal.
$D_{WMP}$	:Single plane mean diameter of a needle roller.

$D_{ws}$	:Single diameter of a needle roller.
$\delta_1[1]$	:The magnitude of a negative error on the workpiece at the point where contact is made with the workblade.
$\delta_2[1]$	:The magnitude of a negative error on the workpiece at the point where contact is made with the regulating wheel.
$\gamma [3][2], \beta[1]$	:Included angle between the grinding wheel contact normal and the regulating wheel contact normal.
$\gamma_s[3], \beta[2]$	:Grinding wheel tangential angle.
$\gamma_R[3], \alpha[2]$	:Regulating wheel tangential angle.
$g[3]$	:Dislocation of the workpiece centre in direction of a normal line relative to the grinding wheel.



$g_1[3]$	:Dislocation of the workpiece centre as influenced by the workblade.
$g_2[3]$	:Dislocation of the workpiece centre as influenced by the regulating wheel.
$h[3][1], H[2]$	:Workpiece height above centre.
$h_0[3]$	:Workpiece/regulating wheel contact height above centre.
$h_1[3]$	:Regulating wheel diamond offset.
$h_v$	:Regulating wheel viewing height above centre.
$K[1]$	:Machining elasticity parameter.
$K_B$	:Workblade shape factor.
$K_m[1]$	:Machining factor.
$K_R$	:Regulating wheel shape factor.
$K_{-}[1]$	:Elasticity factor for the machine elements.

$l_R$	:Regulating wheel length.
$l_g, B_{\text{eff}}[3]$	:Grinding wheel length, effective grinding wheel width.
$l_w, l_{w\text{eff}}[3]$	:Needle roller length (nominal), effective roller length.
$N_g[3][2]$	:Grinding wheel rotational speed.
$n_R[3], N_R[2]$	:Regulating wheel rotational speed.
$n_w[3][2], N_w[2]$	:Workpiece rotational speed.
$\theta[1], \phi[2]$	:Angle measured between an original line rotating with the workpiece and the grinding wheel contact normal.
$\phi_2[3][2]$	:Workpiece rotating angle between the contact points at the grinding wheel and at the regulating wheel.
$P[1], F_n$	:Normal force in grinding.
$R(\theta)[1]$	:The apparent reduction in radius at the same position as $r(\theta)$ .



$r(\theta)[1]$	:Reduction in radius from the workpiece reference circle in a direction determined by the angle $\theta$ .
$r_s[3][2]$	:Grinding wheel radius.
$r_k[3]$	:Regulating wheel concavity radius.
$r_R[3], r_r[2]$	:Regulating wheel radius.
$r_w[3]$	:Workpiece radius.
$S[1]$	:True depth of cut.
$v[1]$	:Ratio relating $\alpha$ to $\alpha'$ and $\beta$ according to $\alpha = \pi/2 - \alpha' - v\beta$ .
$V_A[3], V_t[3]$	:Throughfeed or axial speed.
$V_R[3][2]$	:Regulating wheel surface speed.
$V_s$	:Grinding wheel surface speed.
$V_w[3]$	:Workpiece surface speed.
$X(\theta)[1]$	:The magnitude of the feed motion of the grinding wheel normal to the workpiece at the angle $\theta$ .
$x(\theta)[1]$	:Wheel/workpiece/system deflection.

$X_{DU}, Y_{DU}, Z_{DU}$	:Dressing unit/dresser
$X_D, Y_D, Z_D[3]$	coordinate system.
$X_M, Y_M, Z_M[3]$	:Centreless grinder
	(machine) coordinate
	system.
$X_R, Y_R, Z_R[3]$	:Regulating wheel coordinate
	system.
$X_V, Y_V, Z_V$	:Viewing plane coordinate
	system.
$X_W, Y_W, Z_W[3]$	:Workpiece coordinate
	system.

## Chapter 1.

### 1.0 Introduction.

#### 1.1 Historical aspects.

Prior to the Industrial Revolution, the grinding of materials was confined to the sharpening and polishing of tools and implements. With the Industrial Revolution came the demand for mass production and in turn the development of machine tools. It was not however until much later that the need arose for precision ground parts and with it the development of grinding machines. Various people are credited with inventing the centreless grinding machine although the term centreless can be applied to machine tools that bear little resemblance to the modern accepted definition of centreless grinding. In 1915 the German-American Lewis Heim, through the invention of the regulating wheel and workblade, developed the basic concept of centreless grinding. The radial form of the workpieces produced on those early centreless grinders were, in classic centreless grinding traditions, odd lobed and not very round on account of the flat topped workblades and zero part heights. Further development of the process by



Francis Sanford led to the Sanford patents and in 1922 The Cincinnati Grinding Company began manufacturing centreless grinding machines. At about the same time, the centreless grinding process was also being developed elsewhere, and in Europe, Lidköping Machine Tools manufactured its first centreless grinding machine in 1922 (Reference 1).

Over the years, additional research and development led to the introduction of various refinements to the basic design resulting in significant improvements in the quality aspects of centreless ground parts. The role of the centreless grinding machine has also been expanded from traditional finishing to first cut/large stock removal operations. It is nevertheless the ability of a throughfeed centreless grinding machine to mass produce high precision circular parts in a continuous manner that has consolidated its position as a vital machine tool particularly in the anti-friction bearing industry.

## 1.2 Description of the throughfeed centreless grinding process.

The grinding wheel, regulating wheel and workblade form the core of a centreless grinding machine as shown in Figure 1. The workpiece is supported by the regulating wheel and workblade whilst being ground by the grinding wheel. The absence of centres or formal work holding devices means that the workpiece is free to round-up in an independant fashion under the feedback effect of its radial support.

In throughfeed centreless grinding, as the name implies, workpieces, under the action of an inclined regulating wheel, move axially through the machine in a controlled manner, their radial form being the result of the inter-relationship between the grinding wheel, regulating wheel and the workblade whilst their axial form is a function of the grinding gap geometry and/or the alignment of the workpiece guides. Figure 2 shows examples of grinding gap geometries which in this case are those necessary for producing barrel and hour-glass shaped workpieces.

In common with plunge/infeed centreless grinding, optimum workpiece roundness is a function of the throat angle and the workblade angle. However, unlike plunge/infeed centreless grinding, the throughfeed centreless grinding process is essentially three dimensional and consequently the throat angle is not constant but varies axially through the machine. This is illustrated in Figure 3.

Of primary importance in the throughfeed centreless grinding process is the requirement to impart a particular shape to the regulating wheel in order to guide and control the workpieces as they move through the machine. This shape is generated by moving a dressing tool in a precise manner and at a particular orientation with respect to the axis of rotation of the regulating wheel. The regulating wheel shape in throughfeed centreless grinding is discussed in detail in Chapter 4.

In addition to the centreless grinding machine itself, consideration must also be given to its support systems, for example material handling, since successful throughfeed centreless grinding depends on establishing and maintaining a cohesive train of workpieces through the grinding zone.



### 1.3 Definition of the problem and broad aims of the programme.

Historically, as evident by the number of publications, research efforts have concentrated on the plunge centreless grinding process and in particular workpiece roundness generation (References 2,3,4,5,6 and 7). This has meant that the throughfeed centreless grinding process and especially its size holding capability has received scant attention. At first sight it might appear that the throughfeed centreless grinding process is inherently capable of holding good size. However, in practice, a forty millionths of an inch size spread has been observed in a fifty piece sample lot of needle rollers which, at current production rates, represents less than five seconds of machining/grinding time.

In order to explain these observations, a research programme was initiated that would concentrate on the identification and analysis of the variables that control the basic size holding capability of the throughfeed centreless grinding process in needle roller grinding. Such a fundamental study of workpiece

diameter variation would complement the numerous studies to date on workpiece roundness generation in the centreless grinding process.

#### 1.4 Scope of the programme.

The programme of study was divided into three main areas; literature review, experimental aspects and theoretical aspects.

The literature review involved a study of the relevant publications to date on centreless grinding and related topics. Specialist knowledge was also obtained through conversations with Torrington Company personnel and via access to the Torrington Company's research department's test reports. The literature review also addressed the problem of the many varied and incomplete nomenclatures for the centreless grinding process.

Where necessary, new process definitions and nomenclature were developed.

In terms of the experimental aspects, the loan, by the Torrington Company, of a Cincinnati Milacron 230-10 centreless grinding machine required that experience be gained in the set-up and operation of a centreless

grinder in the throughfeed mode. In addition, a thorough understanding of the machine system was crucial in order to appreciate the role played by the various machine elements and their significance in terms of part to part size variation. Potential machine setting errors were identified and expressions developed to quantify them. Where necessary the performance of machine components was improved through redesign. This study of the machine system was extended to cover support systems and procedures such as material handling and the pre-grind preparation of the workpieces, both of vital importance in ensuring a continuous throughfeed action within the grinding zone.

Having developed a good understanding of the machine system, it was then possible to investigate the nature of the observed part to part size variation. A number of experiments were devised and in turn a list of the primary factors affecting size variation in the throughfeed centreless grinding process was compiled. Based on these results, target areas for more detailed analysis and experimentation were identified. In support of the experimental programme it was necessary to develop data gathering techniques that could capture



the part to part size variation within a stream of consecutively ground workpieces.

The analysis of the experimental data called for the ability to effectively evaluate the diameter of test workpieces, which in turn led to a study of the metrology of needle rollers. This study was concerned with the technique for gauging the diameter of needle rollers, gauging error sources and their effects, and the rationalization of the interdependence of workpiece radial geometry and size when making diametral measurements with a Two point gauge.

The bulk of the theoretical work was concerned with the development of a model of the workpiece sizing mechanism in the throughfeed centreless grinding process. General expressions were formulated and a computer program based on this model was then written.

Expressions were also developed to define the required regulating wheel form in throughfeed centreless grinding. These expressions were then used to evaluate alternative regulating wheel truing philosophies. This work was supported by experimental studies.

### 1.5 The nomenclature of the throughfeed centreless grinding process.

A literature survey revealed that research into the throughfeed centreless grinding process had been conducted primarily in Europe and accordingly a basic nomenclature, principally West German in origin, had developed. The result was that in many instances the German nomenclature came to be accepted as the standard. Officially however, ISO Standards ISO 3002 1982(E) (Reference 8) does not define any throughfeed centreless grinding terms. Definitions and terms for centreless external cylindrical grinding machines are presented in DIN 69718 Part 3 (Reference 9) but no nomenclature is provided.

Conversely, the plunge centreless grinding process had received attention worldwide and alternative nomenclatures, principally Rowe in England and Miyashita in Japan, had evolved. Traditionally, in plunge centreless grinding, the nomenclature adopted depended on which primary source the author used, for example, Subramanya Udupa (Reference 10) used Rowe's model (Reference 4) in his studies of centreless

grinding. The result was that various nomenclatures have therefore been perpetuated but no standard established.

The approach adopted in this research programme was to use the German nomenclature for throughfeed centreless grinding as well as providing, wherever necessary, original definitions. However, since Rowe's model of the centreless grinding process was used as the basis for this programme's model of the throughfeed centreless grinding process, then, in that instance, this was reflected in the choice of nomenclature. A comprehensive listing of the nomenclature used in this programme together with the variations for the three primary nomenclature systems, England, Japan and W.Germany, are presented at the front of this thesis.



## Chapter 2.

### 2.0 Basic investigation of workpiece size errors in the throughfeed centreless grinding process.

#### 2.1 Introduction.

The objective of the first phase of the research programme was to formulate a list of the primary factors affecting the size holding capability of the throughfeed centreless grinding process. In order to do this it was necessary to establish some baseline data on the nature and magnitude of the workpiece size errors. This involved a study of the set-up and operation of a throughfeed centreless grinding machine, the development of techniques for measuring the size variation of a stream of consecutively ground workpieces and the manufacture of precision throughfeed centreless ground workpieces in accordance with existing practices.

#### 2.2 The Cincinnati 230-10 centreless grinder.

All of the experimental work was performed on a Cincinnati 230-10 centreless grinder loaned by the

Torrington Company. This machine had previously undergone a considerable amount of re-engineering and therefore reflected much of the Torrington Company's philosophy towards throughfeed centreless grinding.

The Cincinnati 230-10 formed the core of a precision throughfeed centreless grinding system comprising material handling, grinding fluid and gauging systems. After mounting the grinding and regulating wheels and installing a tooling package, the 230-10 was set-up to throughfeed centreless grind needle rollers (0.1 inches nominal diameter) in accordance with procedures developed by the Torrington Company's research department.

### 2.3 Investigation of the machine setting errors.

When setting up a throughfeed centreless grinder, the normal procedure is to calculate the values of the machine set-up parameters, for example, the workpiece height above centre and the regulating wheel trueing angle, based on the grinding parameters, for example, the workpiece diameter and the throughfeed angle. This set-up data is then transferred to the grinding machine where the required grinding gap geometry is achieved.

Based on the theoretically derived set-up data for a 0.1 inch diameter straight needle roller, it was not possible to achieve the desired grinding gap geometry on the Cincinnati 230-10 without considerable refinement. This was not unexpected since in practice, the initially set grinding gap geometry may require some further refinement on account of the machine scales not having the necessary resolution demanded by grinding theory. Furthermore, discrepancies also exist because, when calculating the theoretical set-up data, it is not practical to determine for each set-up the current grinding and regulating wheel diameters. The result is that having achieved the desired grinding gap geometry, the values of the settings as read off the machine's scales may differ from those derived mathematically.

It should be pointed out that failure to achieve the desired grinding gap geometry may be caused by factors other than those just outlined. Errors in the straightness of dresser profile bars, the inability of the dresser to reproduce the form of the dresser profile bar, poor dressing tool quality, a warped workblade and poor system stiffness amongst others will all contribute to inappropriate grinding gap geometries.

In this case, a large discrepancy was found between the value of the throughfeed angle as read off the machine's scale and the desired value. The problem was traced to the throughfeed setting angle scale which was found to be in error by one degree.

This finding prompted a systematic evaluation of the various machine setting scales and an analysis of their effect on the grinding gap geometry. Measurements were made of the distance from the machine slide datum surface to the wheel centres (that the height above centre be accurately set) and of the position of the regulating wheel pivot point with respect to the regulating wheel spindle hub. The axial location of the grinding wheel and regulating wheel with respect to each other is important in throughfeed centreless grinding and must be such that firstly their end faces be aligned and secondly that the regulating wheel centre (radial plane that divides the regulating wheel symmetrically) and regulating wheel housing pivot point are coincident. In practice these requirements are satisfied by either placing suitably dimensioned spacer rings between the regulating wheel and the regulating wheel spindle hub or by means of the spindle adjustment provided on some types of centreless grinding machines.



An analysis showed that if the regulating wheel housing pivot point was to the left of the regulating wheel centre and the regulating wheel was tilted down at the front, then the result was an inherent below offset effect. If the pivot point was to the right of the regulating wheel centre then an inherent above offset effect was created. The amount of inherent offset can be found from the expression:-

$$\text{Offset} = x \sin \alpha \quad (1)$$

where  $x$  = distance from regulating wheel housing pivot point to the regulating wheel centre.

$\alpha$  = throughfeed angle.

The condition of an inherent below offset effect is illustrated in Figure 4.

Also of interest was the relationship between the regulating wheel housing pivot point and the throughfeed angle setting scale. It can be shown that an error may be introduced depending on the degree of coincidence between the regulating wheel centre and the regulating wheel housing pivot point. Again, if the regulating wheel housing pivot point is to the left of

the regulating wheel centre then the set throughfeed angle will be less than the desired throughfeed angle (refer Figure 5a). Conversely it will be greater in the case where the regulating wheel housing pivot point is to the right of the regulating wheel centre (refer Figure 5b). The actual set angle can be found from:-

$$\text{Angle set} = \arctan\left(\frac{(x_1 \pm x_2) \tan \alpha}{x_1}\right) \quad (2)$$

here  $x_1$  = distance from the regulating wheel housing pivot point to the throughfeed setting scale.

$x_2$  = distance from regulating wheel housing pivot point to regulating wheel centre.

$\alpha$  = throughfeed angle

(+ when to right, - when to left)

Inserting actual measurements taken from the Cincinnati 230-10 centreless grinder into expressions 1 and 2 revealed an inherent below offset of 0.0218 inches and a set angle of 3 degrees 51 seconds and 38 minutes based on a desired throughfeed angle of 4 degrees. As

discussed earlier, throughfeed angle setting scales do not have the resolution to discriminate accurately between 4 degrees and 3 degrees 51 minutes and 38 seconds but nevertheless the exercise illustrated some of the problems in attempting to 'dial-in' a set-up on a throughfeed centreless grinder.

#### 2.4 Redesign of the lower slide clamp.

When throughfeed centreless grinding on the Cincinnati 230-10 it is usual to lock the upper slide to the lower slide (fix the position of the workblade with respect to the regulating wheel) whilst leaving the lower slide free to move with respect to the machine bed in order to compensate for grinding wheel wear. A serious weakness in the design of the Cincinnati 230-10 was the slide clamping system. It was found that the lower slide clamp did not bite immediately but allowed up to 0.04 inches play making it impossible to set the correct distance between the workblade and the regulating wheel. A new lower slide clamp was therefore designed, manufactured and fitted resulting in a reduction in the play to 0.0005 inches and better.

## 2.5 Pre-grind preparation of workpieces.

Successful throughfeed centreless grinding depends on delivering a cohesive stream of workpieces to the grinding machine. In order to do this, the workpiece feeding system must be properly set-up, but more importantly, the workpieces must be clean and slick. It was found that when grinding blanks (unground) or pre-ground workpieces, severe feed problems resulted from the presence of a sticky residue on the surface of the workpieces. This residue was made up of grinding coolant, abrasive grains, grinding swarf and tramp oil. Simple washing of the workpieces proved ineffective since it made them clean but not slick. The solution was a drying barrel which was designed, manufactured and used to tumble and dry the workpieces after first washing them in a chemical cleaner. The barrel consisted of a cylindrical frame covered with a piece of fine mesh steel netting. The workpieces were first submerged in a cleaning solution and then placed in the barrel. The barrel, supported on vee blocks, was rotated, whilst simultaneously, air from a blower was directed at the tumbling mass of workpieces. The result was dry, clean workpieces whilst the rotation of the



barrel created a workpiece on workpiece action that increased their slickness.

## 2.6 Development of a system for capturing consecutively ground workpieces.

In order to investigate part to part size variation it was necessary to capture and gauge consecutively ground workpieces. In simple terms, this was achieved by connecting a length of tubing to the exit end of the workblade. Recent developments however now permit the study of part to part size variation by observing the suitably conditioned output of a post process size gauge.

A requirement of the collecting tube was that it allowed workpieces to flow freely without creating a 'back pressure' which would have a detrimental effect on the workpieces still within the grinding gap. This back pressure was caused by workpieces stacking up in the tube as a consequence of either too small or too large a bore size and/or a fluid dampening effect caused by grinding coolant filling up the tube. After experimenting with a number of different materials and tube bore sizes, the ideal was found to be a length of

copper tubing. The back pressure problem was alleviated by drilling a series of vent holes along the length of the tube and by arching the tube so that the workpieces flowed down a gradient.

An experiment was performed as a means of estimating the degree of back pressure present. This procedure involved counting the number of workpieces collected over a five second period with and without the collecting tube attached. The results (Table 1) showed that on average there was little effect. As a matter of course, the back pressure evaluation procedure was a feature of each grinding test.

Another cause for concern was the effect on the dimensional characteristics of the workpieces as a result of the abrasive action of sliding along the collecting tube. A visual examination of the parts during the initial grinding trials revealed that workpieces exiting the collecting tube had an inferior surface texture. Measurements made of the surface finish of a few workpieces randomly selected from a group of workpieces collected over a five second period confirmed this (Table 2), but, it soon became apparent, that as the collecting tube's internal surface wore so

the surface texture of the workpieces improved (Table 3). An explanation for the inferior surface texture was that abrasive grains shed by the grinding wheel and moved along by the coolant and throughfeed action were picked up and held by the initially rough internal surface of the collecting tube. As the tubes internal surface wore so its ability to retain the loose abrasive diminished and in turn its effect on workpiece surface texture. Table 4 suggests that the abrasive action within the un-worn collecting tube must have been severe since it significantly affected workpiece roundness. Whilst roundness can also be affected by back pressure, a back pressure evaluation test showed no evidence of this. Table 5 shows data collected with and without a worn collecting tube. Although there is scatter in the data, the differences are generally less and the averages are comparable.

## 2.7 Basic grinding experiments.

The objective of the first set of experiments was to collect consecutively ground workpieces and measure their sizes. Using this data, graphs of consecutive workpiece size could be plotted and examined for any cyclical variations or trends. Such a plot is shown in Figure 6.

The experimental procedure consisted of setting up the Cincinnati Milacron 230-10 centreless grinder in a throughfeed grinding mode consistent with the requirements of grinding heat treated AISI 52100 workpieces. The collecting tube was attached to the exit end of the workblade, and, once steady state grinding conditions had been achieved, a stream of consecutively ground workpieces was collected by disconnecting one end of the tube from the workblade whilst simultaneously blocking off the other end. After removing, in order, the workpieces from the tube, they were dried and placed in individually labelled envelopes which in turn were placed in the metrology area in preparation for gauging. The ground workpieces were gauged for size according to the procedure described in Chapter 3 section 3.3.4.

Consecutive workpiece size data was collected during tests in which the throughfeed rate was varied - regulating wheel speeds of 100, 200 and 300 revolutions per minute (r/min), and in which blanks (unground) and pre-ground workpieces were ground. In all the tests, the stock removal was held at 0.002 to 0.0025 inches on a 0.1 inch nominal diameter needle roller. Other features of the programme were the monitoring of wheel



speeds, both grinding and regulating, and the evaluation of the degree of slippage – difference between the theoretical and measured throughfeed rates.

## 2.8 Discussion of results from initial experiments.

The interpretation and analysis of the consecutive workpiece size variation plot as shown in Figure 6 revealed two distinctive trends. These are illustrated in Figure 7 which is a plot of number of workpieces per cycle versus frequency for the data in Figure 6. This plot clearly shows two distributions, one centred around three workpieces per cycle and the other at six workpieces per cycle. The plot in Figure 6 is also characterised by two distinct phases, the first phase dominated by three workpiece cycles and the second phase by six workpiece cycles. The transition from three to six workpiece cycles is accompanied by an increase in the range of the size variation.

Based on a throughfeed rate of 324 parts per minute at a regulating wheel speed of 100 r/min, then it can be calculated that the throughfeed rate in parts per regulating wheel revolution was 3.24. The conclusion therefore is that regulating wheel surface runout had

a significant effect on part to part size variation. The explanation for the six workpiece cycles lies in the fact that the regulating wheel spindle was supported by rolling element bearings which precessed every 2.2 revolutions. The precession ratio of a rolling element bearing is the number of times that the spindle must rotate in order that one rolling element (roller) make a complete orbit within the outer race. This was equivalent to a throughfeed rate of 7.13 parts per regulating wheel spindle bearing precession. Hence the regulating wheel spindle bearing precession ratio was also a major contributor to part to part size variation.

The reason for the increased size variation with the transition from three parts to seven parts per cycle was not understood. Possible explanations centred on the asynchronous behaviour of either the regulating wheel spindle bearings and/or the grinding wheel spindle bearings. Both spindles were straddle supported, the regulating wheel spindle bearings as already stated were rolling element whilst the grinding wheel spindle bearings were Cincinnati Milacron Filmatics. It is known that in centreless grinding, the action of two spindle bearings either 'fighting' each

other or orbiting results in workpiece taper or a cyclical trend in a plot of consecutive workpiece sizes (Reference 11).

In the initial experimental programme, regulating wheel surface runout was identified through the technique of capturing and gauging streams of consecutively ground workpieces and analysing the data for evidence of cyclical trends. Errors in the trued shape of the regulating wheel may also be measured directly off the surface of the wheel and this is discussed further in Chapter 5.

## 2.9 Factors that affect the shape of the consecutive workpiece size plots.

A number of factors other than regulating wheel runout will influence the shape and nature of the consecutive workpiece size plots, although to a much lesser degree. Interruptions in the flow of workpieces to the grinding zone will have an influence on the shape of the plot. These interruptions may be caused by poor set-up of the workpiece feeding device, sticky parts, mixed workpieces, poor machine set-up or incorrect coolant application.

The selection and application of coolant is important as regards lubrication of the workpiece/workblade interface where increased friction affects the throughfeed rate through the formation of a wear groove on the surface of the workblade. Poor flushing of the grinding zone and/or incorrect coolant selection/maintenance can result in the build up of a sticky residue on the workblade surface. Excessive coolant volume is however also detrimental since it hampers the free flow of workpieces at workblade entrance and exit. This was observed during the initial grinding trials.

Another phenomenon associated with the volume of coolant present in the grinding zone is the creation of a hydrodynamic wedge. In needle roller grinding, workpiece speeds in excess of 25,000 r/min are not uncommon and it is thought that the amount and distribution of coolant in combination with the high workspeeds causes the workpieces, especially small needle rollers, to move up off the workblade whereupon they make contact with and ride along the underside of the top workblade. The result is floaters or strays, recognisable by their unground appearance or larger than average diameter. Floaters are also the result of



the regulating wheel losing its regulatory ability in which case the workpieces quickly accelerate up to the grinding wheel surface speed, lose contact with the lower workblade and ride along the underside of the top workblade.

The tendency for workpieces to 'pop-up' off the workblade is increased when utilising greater part heights. In this case the 'hold-down' force generated by the grinding wheel is insufficient. In the initial grinding tests, it appeared that the 'hold-down' force was sufficient since no floaters were observed. Further evidence for this was the fact that the grinding wheel appeared to drive the regulating wheel via the workpieces; regulating wheel speed increases of 2 to 10 r/min and grinding wheel speed decreases of 20 to 25 r/min were observed. Other factors that affect the hold down force are stock removal; type of abrasive and dynamic effects such as wheel out of balance.

All of these factors will combine to affect the slippage - difference between the theoretical and the actual (measured) throughfeed rates. During the initial grinding tests the average slippage was 12%.

## 2.10 Primary factors affecting size holding in the throughfeed centreless grinding process.

Whilst any variation in the grinding gap will result in a change in the size of throughfeed ground workpieces, that variation can be separated into two effects - short term and long term. Regulating wheel surface runout and regulating wheel spindle bearing precession are examples of short term effects whilst grinding wheel wear is an example of a long term effect. Of particular interest in this research programme were the short term effects - those that occurred in less than five seconds of operating time. With this in mind, the primary factors affecting size holding in the throughfeed centreless grinding process are:-

1. Regulating wheel surface runout - once per revolution error in the trued shape of the regulating wheel.
2. Regulating wheel spindle bearing precession - repeatable, but not once per revolution, error associated with the precession of the rolling elements of the regulating wheel spindle bearings.

3. Asynchronous behaviour of the grinding wheel and regulating wheel straddle supported spindles - result of bearing 'pairs' fighting each other.

4. Machine stiffness - relative motion within the grinding wheel/regulating wheel/workblade system as a result of forcing functions such as:-

- Inconsistent throughfeed.

- Initial workpiece size variations.

Following the completion of the basic grinding experiments, the decision was made to replace the regulating wheel spindle package. The second phase of the experimental programme is covered in Chapter 5.

## Chapter 3.

### 3.0 Workpiece metrology.

#### 3.1 Introduction.

It was of concern in this research programme to detect and measure workpiece size variations arising from the machining (grinding) process and not from the method or technique by which the workpieces were measured. In attempting to measure the diameter of workpieces to within 10 microinches or less, it was soon apparent that the interdependence of size, roundness and geometric form produced different results when gauging the same workpiece. These within-workpiece size variations were a source of great frustration to the gauge operator who had difficulty presenting a single number that adequately described the size of the workpiece. The objective therefore was to develop a methodology for gauging centreless ground workpieces that would not only satisfy good gauging practices, but provide the gauge operator with the feedback necessary to ensure a high degree of confidence in the results. A literature survey together with a series of experiments formed the basis from which this methodology evolved.



### 3.2 Literature survey.

From a theoretical standpoint, size and shape can be defined for any section by means of the Fourier series (Reference 12) which has the general form:

$$r(x) = \frac{1}{2}A_0 + \sum_{n=1}^{\infty} A_n \cos nx + \sum_{n=1}^{\infty} B_n \sin nx \quad (3)$$

where  $A_0$  = base diameter.

$A_n, B_n$  = perturbations from the base diameter.

Therefore, in principle, an out-of-roundness measurement system together with the appropriate computer software could be used as a comparator to provide information on the size of components. In practice, however, this is extremely difficult to achieve and consequently distinct methodologies have been developed to measure the size and out-of-roundness of components. Unfortunately this approach has its limitations as recognised by Dagnall (Reference 13) who stated that 'whilst size and out-of-roundness are generally recognised as two different quality characteristics of a component and as such are measured quite differently and separately, the out-of-roundness of a component does however have a practical effect on

the measurement of its diameter and can make such measurements very misleading'. This sentiment was echoed by Loxham (Reference 14) who wrote that 'this relationship between size and out-of-roundness adopts greater significance with the demand for higher accuracy since errors of form which were previously ignored because they were a small percentage of the total work tolerance now assume paramount importance'.

The apparent relationship between size and out-of-roundness is sometimes used in the monitoring of the centreless grinding process where large within-workpiece size variations are interpreted as being indicative of poor roundness. Despite the convenience of this technique, the results obtained are not very accurate and are heavily influenced by the gauge contact points/angle of the vee-block and the degree of lobing on the workpiece. British Standard 3730 (Reference 15) contains details of procedures and tables by which the radial deviation of a workpiece may be determined from Two and Three point gauging techniques.

Another issue in the metrology of centreless ground workpieces is that the term size conjures up a

different mental image than that of the term diameter. Size is defined as the proportions, dimensions, amount or extent of something, for example, the size of an egg. Diameter is defined as a straight line connecting the centre of a geometric figure especially a circle or sphere with two points on the perimeter or surface and/or the length of such a line. This generalised association of diameter with the length of a chord passing through the centre of a circular form makes the statement 'the diameter of an egg is .....

appear ridiculous. In practice therefore, the term diameter is only used to define objects that are circular or round. The centreless grinding process has a propensity for generating iso-diametric workpieces i.e. workpieces whose 'diameter' remains constant but whose geometric form is not round but consists of circumferential undulations or lobes that are odd in number.

The effect of the geometric form of a workpiece on its size is important where distinction must be made between 'measured' size and 'effective' size. Dagnall (Reference 13) defined the measured size of a component as the diameter (or chord) as measured between a pair of parallel faces, whilst the effective size was the diameter of either a hole or a shaft to fit that

component. Differences between measured size and effective size are exhibited by iso-diametric shapes. For example a three lobed workpiece having a measured size of 25 mm would have an effective size of 28.9mm. Figure 8 illustrates the measured size and the effective size of an iso-diametric shape. For such workpieces a general rule of thumb is that the effective size is equal to the measured size plus half the radial deviation. For example in the case of a three lobed part of effective size 2.310 inches, measured size 2 inches and radial deviation 0.62 inches, then the calculated effective size is 2 plus a half of 0.62, which equals 2.31 inches.

The method most commonly used for measuring the size (mid-length diameter) of needle rollers is the Two point measurement technique (Figure 9), defined in BS 3730 Part 3 (Reference 15) as 'measurement between co-axial anvils, one fixed and one moving in the direction of measurement'; Dagnall's definition of measured size. BS 5773 Part 6/ISO 6193-1980 (Reference 16) defines  $D_{ws}$  - the single diameter of a needle roller as 'the distance between two tangents to the needle roller surface parallel to each other and in a plane perpendicular to the needle roller axis i.e. a



radial plane'. It can be stated that  $D_{ws}$  in effect defines the measured size, and as a diameter it does not necessarily pass through the centre of the workpiece shape.

To obtain the effective size, a circumscribing circle defined by the effective diameter must be centred on the centre of the iso-diametric shape. This action is one of the fundamental concepts of out-of-roundness measurement i.e. the axis of rotation of the gauge must be independant of that of the workpiece being measured. By observing this principle, an iso-diametric shape can be identified, which may not have been the case if the workpiece had been rotated in a vee-block. In summary, the measured size of a workpiece is obtained when the coordinate system or shape of the workpiece is a feature of its size measurement, whilst its effective size is obtained when the coordinate system of the workpiece is independant of that of the measurement device.

The impact of measured size and effective size on the application of Taylors Principle in quality inspection was discussed by Loxham (Reference 14). The inspection of a cylinder toleranced with a minimum and a maximum

diameter is addressed by Taylors Principle. A full form gauge would check the maximum metal condition whilst a Two point gauge would check the minimum metal condition. Loxham stated that two problems in applying Taylors Principle in the case of a cylinder would be firstly the difficulties in manufacturing a ring gauge to check the maximum metal condition and secondly, that an odd lobed part could be outside the tolerance of the minimum metal condition yet be acceptable when gauged with a Two point gauge as per Taylors Principle (Figure 10). Loxham added that there are workpieces whose diameter tolerances are not intended to satisfy Taylors Principle.

As with odd lobed workpieces, even lobed workpieces will also have a measured and effective size. Unlike odd lobed workpieces however, the measured size is not constant but varies depending on how the workpiece is presented to the Two point gauge. In addition, the maximum measured size will be the effective size which is not the case with iso-diametric shapes. The diameter of an even lobed workpiece may be specified as the mean of the maximum and minimum measured sizes. This is defined in BS 5773 Part 6/ISO 6193 1980 (Reference 16) as the single plane mean diameter of a needle roller

$D_{WMP}$  - 'the arithmetical mean of the largest and the smallest actual single diameters of the needle roller in a single radial plane'. The value for  $D_{WMP}$  can be seen to have no physical representation since it lies somewhere between the maximum and the minimum measured size.

### 3.3 Development of a methodology for measuring the size of a needle roller.

#### 3.3.1 The gauging system.

The needle rollers were gauged using a Two point electronic comparator which featured an LVDT (mounted between leaf springs), interchangeable stylus tips and a synthetic sapphire platen (Figure 9). The output from the comparator was fed to a digital column gauge whose maximum resolution was 5 microinches. The system was calibrated by placing a master standard between the stylus tip and the platen.

Since it was not practical to use an adjustable support or stop as shown in Figure 9, then the measured size of the needle roller was interpreted as the captured dimension of the chord of the cross section of the

needle roller presented between the stylus tip and the platen. The term captured was used since it was an instantaneous and unique measurement which was dependent on a number of factors.

### 3.3.2 Determining the minimum number of measurements necessary to classify the size of a workpiece.

Without a knowledge of the workpiece's geometric form, the following three possibilities are likely in the event of a single shot size measurement; the workpiece is perfectly round, the workpiece is odd lobed or the workpiece is even lobed. If the workpiece is rotated slightly and then re-gauged, an identical reading will rule out the third possibility. How many times then should a needle roller be gauged in order to obtain a reasonable understanding of its size?

In practice the approach adopted on both rough and finish ground workpieces is the single shot measurement i.e.  $D_{ws}$ . It is argued that over the long run the values average out i.e. when comparing the  $D_{ws}$  (single shot) to the  $D_{wmp}$  (multiple shot) the 'underestimates' balance the 'overestimates'.



As discussed earlier, one of the problems with the single shot measurement was the uncertainty of whether or not the result adequately described the size of the workpiece. This was usually confirmed by additional measurements. The needle roller selected as the standard for the research programme had a nominal diameter of 0.1 inches and a length of 0.7 inches. Owing to the size of the needle roller, it was found that multiple measurement shots produced misleading results as thermal effects due to the handling of the workpiece began to take over.

An experiment was devised aimed at determining the minimum number of measurements necessary to classify the size of a workpiece.

The size variation within a pre-ground blank was evaluated by gauging the part over one revolution (360 degrees) and observing its variation. Using a felt pen, a line was drawn along the axis of a roller at one end to establish a reference line. With the reference line orientated uppermost, the roller was pushed between the stylus tip and platen of a calibrated Two point gauge. After taking a reading, the roller was rotated slightly and a second measurement made. This process was

repeated until the reference line had rotated through 360 degrees and was once again uppermost. After some initial difficulty, it was possible to get good size repeatability (75 microinches above the datum (master setting)) at the reference positions i.e. 0, 360, 720 degrees e.t.c.; the actual angular positions between the reference positions were chosen at random and, due to practical limitations, not recorded. The results are shown in Table 6, the maximum diameter being 95 microinches (above datum), the minimum 75 microinches and the mean 85 microinches.

The next stage of the experiment involved gauging the workpiece a number of times, each time a different, randomly chosen chord was presented to the stylus of the Two point gauge; refer to Table 7. The first result, equivalent to a single shot measurement, was 85 microinches, adding credibility to the single shot measurement philosophy. Subsequent measurements were 80, 80 and 80 microinches, and it was not until the fifth measurement that a 90 microinch reading was captured, and the ninth before 95 microinches was captured. In total, fifteen random measurements were made, the minimum reading of 75 microinches (from the 360 degree tests) was never captured.

Based on these results a  $D_{WMP}$  of 87.5 microinches (above datum) was calculated for the random orientation test compared with a  $D_{WMP}$  of 85 microinches from the more ordered 360 degree tests. The  $D_{WMP}$  (random tests) for measurements 1 to 4 was 82.5 microinches and for measurements 5 to 7, 85 microinches. Whilst the first (single shot) measurement from the random tests was coincidentally identical to the value of  $D_{WMP}$  determined in the 360 degree tests i.e. 85 microinches (above datum), the data suggested that with a minimum of five measurements a more confident statement of the size of a workpiece was possible.

### 3.3.3 Analysing the interaction between the gauge operator and the gauge.

When gauging to resolutions of 10 microinches or less, good repeatability could only be achieved if the operator acquired a deftness of touch or a 'feel' for gauging such a workpiece. Generally, operators acquired the necessary skills through increased familiarity with the gauge and through gauging workpieces. Techniques evolved which were either unique or transferable between operators. An example of uniqueness was the thermal effect that different operators had on the

gauging system. This affected the time that it took the gauge to stabilise thermally when different pairs of hands were introduced into the gauging zone at the start of a gauging run.

These thermal effects were addressed by a series of experiments performed by the Torrington Company on the thermal stability of the comparator which revealed that the gauge was thermally unstable, varying on average 6.5 microinches per degree Fahrenheit. In one test, with an ambient temperature of 71 to 72 degrees Fahrenheit, the display changed by an average of 20 microinches when a warm pair of hands was placed in a position near the gauge comparable with that adopted during workpiece measurement (Reference 17). Experience has also shown the gauge to be thermally sensitive to the speed with which workpieces are gauged, variations in gauging speed resulting in wave patterns in consecutive workpiece size variation plots. The conclusions to be drawn are therefore that the gauge must be at a uniform temperature of  $68 \pm 1^\circ$  Fahrenheit, dummy parts should be gauged prior to starting gauging proper in order to warm up the gauge, and that parts should be gauged at a uniform and steady pace.



During gauging, the gauge operator was able to develop an appreciation for the cleanliness of the gauge through monitoring any resistance to motion or stickiness when moving the workpiece across the platen and under the stylus tip. Since the axial profile of the workpiece was employed as a locational surface against the platen then a dirty platen would affect the measured size. Likewise, the use of the workpieces axial profile as a locational surface would also provide feedback to the operator on whether the workpiece was bent.

As a means of quantifying gauge operator 'feel', a series of reproducibility and repeatability tests were devised. Subsequent to these tests the author became aware of statistically designed repeatability and reproducibility studies specifically designed for such an application. Unfortunately, the format of the original data was such that it prevented the use of these procedures. Typically, repeatability and reproducibility values for the comparator used in this programme were of the order of 5 to 10 microinches.

Operator variability was assessed by using three operators; operator 1 (experienced) was used as the

control and the other operators, operator 2 (experienced) and operator 3 (inexperienced) were compared to the control. Twenty consecutively labelled workpieces were gauged, each workpiece being gauged five times and the mean diameter  $D_{WMP}$  evaluated. Each operator, for a given workpiece, would therefore experience the same variability. Steps were taken to maintain a constant ambient temperature and, prior to each gauging run, the gauge was brought into thermal equilibrium with each operator through the gauging of some dummy parts.

It was discovered, that when gauging to resolutions of millionths of an inch, if the gauge operator was aware of any trend in the data as exhibited by previously measured workpieces then a result could be produced consistant with that trend. To avoid that happening, each gauge operator was isolated from previous results and an independant source was used to record each reading.

It was hoped that by taking all these precautions, then the differences between the data sets would be as a result of operator variability.

The results of the operator variability tests are presented graphically in Figures 11 and 12. Figure 11 is a comparison of the two experienced operators and shows that both plots exhibit similar trends and match each other quite closely up to part number 14, after which they are displaced relative to each other. The reason for this was that the door to the gauging room was accidentally opened during the gauging of part 14 and the resultant shift between the two plots is on account of a change in the ambient temperature.

A statistical software package (Statgraphics) was used to compare the means of the paired operators (Tables 8,9,10,11,12,13 and 14). Depending on the null and alternative hypothesis selected, the t statistic was calculated and compared with the t critical statistic based on the number of degrees of freedom and the confidence level. Having made the comparison, the null hypothesis  $H_0$  was either accepted or rejected. Comparing the experienced operators and using the complete data set of 20 workpieces (Table 8) with the null hypothesis that the means were equal versus the alternative hypothesis that they were not, at an alpha of 0.05, the significance level was 62.1% and the null hypothesis was not rejected. A similar analysis but

with consideration of only the first 10 workpieces (Table 12), i.e. before the temperature shift, produced a significance level of 91.3%, the null hypothesis again not being rejected.

Figure 12 illustrates greater variability between the experienced operator (1) and the inexperienced operator (3) although the plots again exhibit similar trends. Statistically, the significance level over 20 workpieces (Table 9) was 45.7% ( $H_0$  not rejected) and over 10 workpieces (Table 13), 62.1% ( $H_0$  not rejected).

In conclusion, whilst there was variability between the experienced and inexperienced operator, it was not statistically significant; the variability between operators who had developed the necessary gauging skills was negligible as testified by a 91.3% significance level.

The data was structured such that it was possible to make comparisons not only within a data set but, by comparing the two data sets of the standard (operator 1), across time periods. The tests were conducted in two different time periods; the first period involving



the experienced operators, then a change over period followed by the second period involving the inexperienced operator. The data sets (10 piece sample size) for operator 1 had a significance level of 49.2% (Table 14). The fact that within a time period (Table 12) operators 1 and 2 (experienced) had negligible variability (91.3% significance level) whilst across time periods operator 1 had greater variability suggests the presence of an external effect, most probably temperature.

The evidence therefore strongly indicates that attempts must be made to maintain a constant ambient temperature across time periods thereby allowing comparison between different data sets. In this investigation however, it was size variations or the size range within a data set i.e. within a time period that was important and not the absolute size. Consequently size ranges within time periods may be compared with those from within other time periods on condition that the ambient temperature within each time period remained constant. However, since gauge stability/linearity at different ambient temperatures is an unknown quantity then it is recommended that temperature fluctuations across time periods also be minimised.

#### 3.3.4 A methodology for gauging centreless ground workpieces.

The results of the various investigations into the metrology of needle rollers led to the development of a methodology as outlined below:

-Prior to gauging, the workpieces, master and gauge were left in the gauging room for 24 hours. The temperature within the gauge room varied between 20°C (68°F) and 22°C (71.6°F).

-The platen and stylus tip were cleaned with methanol prior to gauging and again during gauging at regular intervals, the frequency of which depended on the operators interpretation of any stickiness or resistance to motion experienced when moving the workpiece through the gauge, or by visual examination of the platen for evidence of a film.

-Before starting gauging proper, a few dummy workpieces were measured in order to stabilise the gauge. The reason for this was that it had been noticed that the gauge was initially unstable on account of the thermal variation caused by the sudden presence of the operators hands within the gauging zone.

-Initially the gauge was reset (using the master standard) after gauging each workpiece, but, after a period of time, it was only reset after gauging every fifth workpiece.

-During gauging, a steady rhythmic technique was developed. This prevented the warming up and cooling down of the gauge in response to variations in the gauging speed. The whole batch of workpieces was gauged at one sitting. Interruptions or distractions to the operator were discouraged.

-Each workpiece was gauged five times. The process consisted of pushing the workpiece under the stylus tip until the peak reading was detected, pushing the workpiece on a little further until the indicator (analogue or digital) started to move downwards and then pulling the workpiece back through the gauge, once again observing the peak reading. This procedure was then repeated after first rotating the workpiece in order to present a different chord between the stylus and the platen. On the third go around, the workpiece was again rotated prior to gauging but only made one forward pass under the stylus. Using this technique, the readings could be cross referenced with each other

and there was minimum workpiece handling. The maximum and minimum values were recorded and the  $D_{WMP}$  evaluated. The data was not examined for any trends or cyclical patterns until the last reading had been taken in order to resist the temptation to identify patterns in the data and thereby bias the results.

#### 3.4 Measurement of size variation within a blank (unground workpiece).

In throughfeed centreless grinding it is common practice to make multiple grinding passes, the size spread and roundness of the workpieces improving with each pass. This suggests that incoming workpiece quality is an important consideration; it has been shown (Reference 4) that the geometric form of a ground workpiece was influenced by the interaction between the set-up of the centreless grinder and the geometric form of the unground workpiece.

In production there is little need to accurately determine the diameter of a blank - if such a thing were possible. The nominal diameter ( $D_w$ ) was used to select grinding parameters and was evaluated by gauging five or so workpieces with a micrometer and calculating the average.



It is known that drawn or extruded parts take their shape from the dies, and at Torrington it has been found that the wire extrusion dies on the needle roller production lines wear to a two lobed shape. This translates to the blanks whose geometric forms are invariably also two lobed. As expected, when measuring blanks, large variations in size were observed within each workpiece if the workpiece was gauged several times and each time it was rotated slightly prior to gauging. Figure 13 clearly shows the within workpiece size spread as obtained in a 360 degree test; the size spread for the batch was 0.001 to 0.002 inches. Similar tests on ground rollers revealed within part size spreads of 10 to 20 microinches; the average radial deviation of these parts was 30 microinches.

### 3.5 Summary.

The Two point diameter gauging technique is based on using the workpiece's geometric form as a reference surface. By making the coordinate system of the gauge dependent on that of the workpiece then the dimensional result will be the measured size but not necessarily the effective size. Within-workpiece size variations were therefore variations in the measured size as a

result of the interaction between the coordinate system of the gauge and the workpiece's geometric form.

Having understood this, it was then possible to develop a methodology for gauging needle rollers that presented the gauge operator with feedback on the geometric form of the workpiece being gauged. This resulted in a more confident statement of the size of that workpiece.

A reliable and repeatable needle roller size gauging process was shown to be dependent on both the quality of the equipment and on the operator developing a controlled gauging technique. Such a technique should not only recognise and thereby minimise the potential impact of temperature variations by pre-warming the gauge prior to gauging and by gauging at a steady rate, but should be sensitive to the effect of the gauge's cleanliness on the workpiece's measured size through monitoring any stickiness or resistance to motion when moving the workpiece across the platen and under the stylus tip.

## Chapter 4.

### 4.0 The regulating wheel.

#### 4.1 Introduction.

In throughfeed centreless grinding, the regulating wheel, as its name implies, is the most important element in guiding and moving the workpiece within the grinding gap (Reference 18). The regulating wheel regulates both the rotational speed of the workpiece and its axial speed through the machine. In addition, the physical position of the regulating wheel with respect to the grinding wheel and workblade contributes significantly to the geometric requirements necessary for optimum workpiece rounding and size control. To satisfy these regulatory functions, the regulating wheel must be shaped such that it provides uninterrupted contact with the workpiece along the length of the grinding gap (Reference 18). The usual shape is that of a hyperboloid (Figure 14) which has been shown mathematically by Meis (Reference 18) to 'fulfil the function of a regulating wheel'.

The hyperboloid is generated by passing a cutting tool, generally a single point diamond, along a straight line

at an angle to, but in a plane parallel to, the regulating wheel axis of rotation. The axial cross section through the regulating wheel is, in general, a symmetric hyperbola with radius  $r_w$  (concavity radius) at the narrowest radial cross section as shown in Figure 14 (Reference 18). The axial location of the narrowest radial cross section with respect to the regulating wheel mid-point is a function of the diamond offset as well as the trueing angle. It follows from this that examples will exist where the axial location of the narrowest radial cross section is outside of the physical envelope of the regulating wheel and that in such cases the concavity radius will have no real representation (Reference 18). From Figure 14 it can be seen therefore that, depending on the machine set-up parameters, the regulating wheel is either a symmetric or a truncated hyperboloid (Reference 18).

#### 4.2 Obtaining the optimum regulating wheel shape.

The action of trueing the regulating wheel by moving the diamond tool along a straight line at an angle to the regulating wheel axis of rotation produces a line on the surface of the regulating wheel that is in a plane parallel to the plane containing the axis of



rotation of the regulating wheel. If the regulating wheel is then inclined with respect to the grinding wheel through an angle equal to that between the diamond tool path and the regulating wheel axis of rotation, then uninterrupted contact between the workpiece and the regulating wheel is achieved within the grinding gap. This condition only holds true however for workpiece diameters of zero. As the workpiece diameter increases there is interference between the circumferential profiles of the regulating wheel and workpiece resulting in a gap ( $\Delta r_R$ ) at the centre of the hyperboloid as seen in Figure 15 (Reference 18); the regulating wheel concavity appears to be excessive.

It was Slonimski (Reference 19) who first recognised this and who proposed that the correct regulating wheel shape was in fact 'a line equidistant to a hyperbola at a distance  $r_k + r_w$  from the axis of rotation' (Reference 18). Slonimski developed an empirical expression which refined the shape of the regulating wheel by defining an angle  $\alpha_s$  between the path of the diamond tool and the axis of rotation of the regulating wheel.

$$\alpha_3 = \frac{\alpha}{\sqrt{(1+D_w)} D_R} \quad (4)$$

This had the effect of retaining the requisite hyperbolic regulating wheel shape but reducing the concavity.

In addition to the trueing angle, modifications must also be made to the expressions used to determine the diamond offset. As the workpiece diameter increases, the regulating wheel/workpiece contact point assumes a value less than  $h$  (the workpiece height above centre) (refer Figure 1). The parameter  $h_0$  now defines the height above centre of the regulating wheel/workpiece contact point and is found from:

$$h_0 = \frac{h}{1+D_w D_R} \quad (5)$$

The diamond offset,  $h_1$ , is then found from:

$$h_1 = \frac{h_0 \sin \alpha_3}{\sin \alpha} \quad \text{or} \quad h_1 = \frac{h_0 \alpha_3}{\alpha} \quad (6)$$

In throughfeed centreless grinding the parameter  $h_1$  is not normally evaluated, the diamond offset being dictated by  $h_0$ . In needle roller throughfeed centreless grinding the difference between  $h_0$  and  $h_1$  is in the range 0.0015 inches, and between  $h$  and  $h_0$ , 0.003 inches.

Meis (Reference 18) developed a mathematical expression for determining the exact shape of the regulating wheel that guaranteed guiding a workpiece of any diameter along a straight line. He then went on to compare the exact shape of the regulating wheel with that of the non-corrected case (trued at angle  $\alpha$  and diamond offset  $h$ ) and corrected case (trued at angle  $\alpha_3$  and diamond offset  $h_1$ ). His analysis showed that the corrected regulating wheel shape was a significant improvement over the non-corrected shape in terms of generating a linear workpiece path that was straight and parallel to the grinding wheel axis. Although the corrected regulating wheel shape was for all practical purposes perfectly acceptable, it still exhibited excessive workpiece path curvature at larger workpiece diameters. Meis concluded that this error was more dependent on  $\alpha$  than larger workpiece diameters and suggested that a further reduction in  $\alpha_3$  would be appropriate for

values of  $\alpha$  greater than six degrees. In general,  $\alpha$  values of six degrees and above are considered extreme in throughfeed centreless grinding and consequently Slonimski's correction factor is perfectly adequate.

#### 4.3 Centreless grinder set-up to achieve the optimum regulating wheel shape for throughfeed grinding cylindrical workpieces.

Although variations exist, the two most common regulating wheel trueing/dressing systems are those featured on Cincinnati Milacron and Lidköping centreless grinders. Both of these systems involve moving a cutting tool with respect to the regulating wheel axis of rotation, but differ in the way that they correct the regulating wheel profile to account for different workpiece diameters. These two systems are discussed in more detail in sections 4.3.1. and 4.3.2..

When trueing the regulating wheel, the diamond tool is often offset by an amount equal to or less than the workpiece height above centre. As stated previously, this action results in an axial displacement of the regulating wheel's narrowest cross section and therein the formation of a truncated hyperboloid. Depending on



the application, the truncated hyperboloid offers advantages on account of the variation in the workpiece axial speed through the grinding zone. Where such considerations are not important, the use of diamond offset is expensive in terms of set-up time and in regulating wheel life/usage.

Trueing a regulating wheel without using diamond offset involves first selecting the correct dressing angle  $\alpha_z$  and then fine tuning the grinding gap by swivelling the regulating wheel (symmetric hyperboloid)/workblade in a horizontal plane with respect to the grinding wheel. Meis (Reference 18) proposed a variation on this theme which involved generating a symmetric hyperboloid by inclining the regulating wheel in two planes, one vertical and one horizontal, and trueing with zero diamond offset. The regulating wheel was first trued at an angle equivalent to the throughfeed angle  $\alpha$  and with zero diamond offset. The throughfeed angle  $\alpha$  was then reduced to  $\alpha'$  according to the expression:

$$\tan \alpha' = \tan \alpha \sqrt{1 - \left( \frac{h}{r_w + r_k} \right)^2} \quad (7)$$

Finally the regulating wheel was swivelled with respect to the workblade through an angle  $\delta'$  found from:

$$\tan\delta' = \frac{h}{r_w + r_k} \tan\alpha \quad (8)$$

By this method a symmetric regulating wheel shape was generated which, from his analysis, Meis had shown better satisfied the theoretical shape necessary to guide a workpiece along a straight line. This was particularly evident at extreme values of  $\alpha$  and  $h$ . Meis went on to explain the advantages of the symmetric regulating wheel shape, such as the absence of interference with the workblade at workpiece exit. This meant that larger throughfeed angles could be used and/or more rigid workblades employed. In addition, wider regulating wheels could be employed and in turn wider grinding wheels hence more workpiece rotations within the grinding zone (improved workpiece roundness) for a given cutting rate. Also, by utilising a regulating wheel that is wider than the grinding wheel, additional workpiece guidance and support at entrance to and exit from the grinding zone may be achieved.

In practice, the set-up of a centreless grinder in the

throughfeed mode is a combination of theory (calculated set-up parameters) and operator skill (fine tuning to achieve the desired grinding gap). Generally, the operator does not understand the theoretical expressions for the trueing angle  $\alpha_s$  or diamond offset  $h_1$ , does not know the current regulating or grinding wheel diameters or the value of  $r_w$ , because of the absence of finely graduated scales cannot accurately set  $\alpha$  or  $\alpha_s$ , and finally, for convenience, uses one machine set-up to grind as wide a range of workpiece diameters as possible (Reference 20). Fine tuning of the grinding gap is therefore an inevitable aspect of setting up a centreless grinder in the throughfeed mode, given that the machine has first undergone a 'rough' set-up in accordance with optimum geometric considerations.

An alternative method for trueing/dressing the regulating wheel involved using the grinding wheel in the plunge grind mode. This approach was featured on early Herminghausen centreless grinders and resurfaced recently in a paper by Hashimoto (Reference 21). This method is presented in detail in section 4.5. The traditional regulating wheel trueing systems, Cincinnati and Lidköping, will now be discussed in more detail.

#### 4.3.1 Dresser angle (Cincinnati Milacron).

On Cincinnati centreless grinders, the regulating wheel trueing/dressing unit is attached to the regulating wheel spindle housing. When the regulating wheel spindle housing is inclined to the desired throughfeed angle ( $\alpha$ ), the dresser unit comes with it and consequently the line of action of the diamond tool is parallel with as opposed to inclined to the axis of rotation of the regulating wheel. This condition is corrected for by then swivelling the dressing unit to the trueing angle ( $\alpha_{\Sigma}$ ). Cincinnati use the Slonimski expression to calculate  $\alpha_{\Sigma}$  and have developed tables which show for a given 'incline angle of the regulating wheel' and D/d ratio (regulating wheel diameter/workpiece diameter) the recommended regulating wheel trueing angle setting (Reference 22). Having established  $\alpha_{\Sigma}$ , a further table is provided for obtaining the 'set over of the diamond point' for a given 'height of work centre above wheel centre line' and D/d ratio.

#### 4.3.2 Profile bar (Lidköping).

On Lidköping centreless grinders the regulating wheel



trueing/dressing unit is a feature of the machine bed/regulating wheel housing and consequently when the regulating wheel spindle is inclined to angle  $\alpha$  the diamond tool line of action also assumes an angle  $\alpha$  with respect to the regulating wheel axis of rotation. The optimum regulating wheel profile may be achieved by two methods. The first involves using a suitably shaped regulating wheel dresser cam/profile bar such that the diamond tool generates a shallower hyperbolic contour. This is equivalent to trueing at an angle  $\alpha_z$ . The second method relies on first inclining the regulating wheel axis to the trueing angle  $\alpha_z$  and then inclining the now trued regulating wheel to the desired throughfeed angle  $\alpha$  (Reference 20).

The second method is sometimes used when setting up Cincinnati centreless grinders. If for some reason the regulating wheel profile is not optimal then the situation can be corrected by changing the throughfeed angle as opposed to the more time consuming option of changing  $\alpha_z$  and retrueing.

#### 4.4 Development of expressions for the trued regulating wheel shape.

The relationship between the dressing unit coordinate system and the regulating wheel coordinate system is shown in Figure 16. The diamond tool moves along an axis ( $X_{DU}$ ) in a plane parallel to but at an angle  $\alpha_3$  to the regulating wheel axis of rotation ( $X_R$ ). The two planes are separated by a distance  $r_k$  (the concavity radius). The diamond offset is zero. From Figure 16 with reference to the regulating wheel coordinate system, since the regulating wheel rotates about the  $X_R$  axis then in order to generate a regulating wheel form at point B from centre O the diamond tool must be located at point D from centre O.

$$AB = r_k \quad (9)$$

$$BD = X_R \tan \alpha_3 \quad (10)$$

The regulating wheel radius ( $r_R$ ) at distance OB is therefore:

$$r_R = AD \quad (11)$$

and

$$AD^2 = AB^2 + BD^2 \quad (12)$$

Substituting 9, 10 and 11 into 12 yields:

$$r_R^2 = r_k^2 + X_R^2 \tan^2 \alpha_3 \quad (13)$$

Expression 13 may be represented in the dressing unit coordinate system through the transformation:

$$X_R = \cos \alpha_3 \quad (14)$$

$$X_{DU}$$

giving

$$r_R^2 = r_k^2 + X_{DU}^2 \sin^2 \alpha_3 \quad (15)$$

Figure 17 introduces the diamond offset  $h_1$ , which as explained earlier has the effect of shifting  $r_k$  along  $X_R$ . An above centre diamond offset is considered; the same approach can be used for a below centre diamond offset. From Figure 17:

$$EF = \frac{h_1}{\cos \alpha_3} \quad (16)$$

and

$$FB = X_R \tan \alpha_3 \quad (17)$$

and from

$$AE^2 = (EF+FB)^2 + AB^2 \quad (18)$$

$$r_R^2 = r_k^2 + \left( X_R \tan \alpha_3 + \frac{h_1}{\cos \alpha_3} \right)^2 \quad (19)$$

in the regulating wheel coordinate system. In the dressing unit coordinate system:

$$r_R^2 = r_k^2 + \left( X_{DU} \sin \alpha_3 + \frac{h_1}{\cos \alpha_3} \right)^2 \quad (20)$$

Figure 18 addresses the situation where a regulating wheel dresser cam/profile bar is used. Again the diamond offset is set at zero.

$$AE = r_k + y' - y \quad (21)$$



$$EC = X_{DU} \sin \alpha \quad (22)$$

hence,

$$r_R^2 = (X_{DU} \sin \alpha)^2 + (r_k + y' - y)^2 \quad (23)$$

From Figure 19,  $y$  is determined for any position  $X_{DU}$  and a given  $y'$ :

$$y = (r_k + y') - \sqrt{((r_k + y')^2 - X_{DU}^2)} \quad (24)$$

If the diamond offset is now considered then:

$$r_R^2 = (X_{DU} \sin \alpha + \frac{h_1}{\cos \alpha})^2 + (r_k + y' - y)^2 \quad (25)$$

Expressions 23 and 25 are represented by expressions 26 and 27 respectively in the regulating wheel coordinate system:

$$r_R^2 = (X_R \tan \alpha)^2 + (r_k + y' - y)^2 \quad (26)$$

$$r_R^2 = (X_R \tan \alpha + \frac{h_1}{\cos \alpha})^2 + (r_k + y' - y)^2 \quad (27)$$

Having developed expressions for the diameter of the regulating wheel along its axis of rotation, the next stage was to develop expressions with which to view the regulating wheel profile in any plane and at any angle with respect to  $X_R$ . From Figure 20:

$$Y_v^2 = r_R^2 - (X_M \sin \alpha_v)^2 \quad (28)$$

$$X_M = \frac{X_R}{\cos \alpha_v} \quad (29)$$

In most cases,  $h_v$  will be numerically equivalent to  $h_o$  and can therefore be found from expression 5. If a viewing plane at a height  $h_v$  is now introduced then:

$$Y_v^2 = r_R^2 - \left( \frac{X_M \sin \alpha_v + h_v}{\cos \alpha_v} \right)^2 \quad (30)$$

Armed with these expressions, it was possible to construct, for a given set of parameters, the theoretical regulating wheel profile as seen by a workpiece within the grinding zone. These expressions may also be incorporated into a simulation of the throughfeed centreless grinding process.

#### 4.5 Regulating wheel shape when trued using the grinding wheel.

A paper by Hashimoto (Reference 21) proposed a wheel trueing method whereby the regulating wheel was trued by the grinding wheel. The results showed that this method had a higher trueing accuracy (by one order) and hence greater grinding accuracy, gave improved out-of-roundness and surface finish, excellent wheel life, and more stable friction characteristics between the wheel and workpiece.

By applying Hashimoto's wheel trueing proposal to the throughfeed centreless grinding process it can be deduced that when the regulating wheel is trued by the grinding wheel the resulting profile on the regulating wheel is the same as that required to ensure uninterrupted contact with a workpiece whose diameter is equal to that of the grinding wheel used in the trueing process. The explanation for this lies in the assumption that the grinding wheel is a cylinder, with an abrasive surface, whose shape remains constant throughout the trueing process. Since the grinding wheel abrades the regulating wheel then a profile is generated on the regulating wheel which ensures full

axial contact with the grinding wheel. It is therefore possible to compute the regulating wheel profile when trued using a grinding wheel by simply inserting the diameter of the grinding wheel as the workpiece diameter in the expressions for calculating  $D_R$ . In addition, it is also to be expected that due to the absence of a diamond offset the resulting ground regulating wheel shape will be a hyperboloid symmetric about the regulating wheel mid axis point where  $r_R$  is equal to  $r_w$  and the plane of minimum cross section exists.

Utilising a personal computer spreadsheet package (Lotus 1-2-3) and expressions 15 and 30 developed in section 4.4, the 'ground' regulating wheel shape was computed based on measurements of  $D_R$ ,  $D_S$  and  $\alpha$  taken from a Cincinnati 230-10 centreless grinder. The computed values of  $r_R$  and  $Y_v$  are presented in Table 15 with the resultant axial profile, as seen by a workpiece, plotted in Figure 21. By joining the two extreme points with a straight line it was possible to estimate the regulating wheel crown which in this case was 0.0035 inches.

In order to verify the theoretical results, a 230-10



Cincinnati centreless grinder was set up to plunge grind the regulating wheel. The process involved first inclining the regulating wheel to the desired throughfeed angle and then swivelling the regulating wheel housing until the grinding and regulating wheel spindle axes were parallel. The regulating wheel was then plunge ground as per the procedure described by Hashimoto (Reference 21) until it had cleaned up across the whole of its face. After replacing the workblade, the grinding gap was evaluated by plunge grinding a row of workpieces that had been placed along the workblade. For each workpiece, its axial location and pre and post ground diameters were recorded. The throughfeed motion of the workpieces was prevented by blocking off the exit tube.

The experimental results are presented in Table 16. The plot of axial position (workpiece number) versus diameter change is shown in Figure 22, from which the regulating wheel crown was determined to be 0.0025 inches. The plot also shows that the regulating wheel and grinding wheel spindle axes were not parallel but slightly skewed i.e. the wheels were slightly open at entrance. The theoretical and experimental values for the regulating wheel crown showed good correlation

especially in the light of the difficulties experienced in obtaining accurate measurements of the grinding and regulating wheel diameters.

#### 4.6 Effect of throughfeed angle, trueing angle and diamond offset on the grinding gap contour.

In throughfeed centreless grinding the shape of the grinding gap is a function of the orientation and profile of both the grinding wheel and the regulating wheel. The grinding wheel may be trued straight or portions of its profile tapered in order to satisfy production constraints such as large initial size variations i.e. lead in tapered zone, or particular workpiece profile, sizing, roundness or surface finish requirements i.e. sparkout zone. These various grinding wheel profiles are complimented by the crown and swivel of the regulating wheel. The regulating wheel profile is a function of the throughfeed angle  $\alpha$ , the trueing angle  $\alpha_3$  and the diamond offset  $h_1$ .

The regulating wheel itself may be considered to have both a macro and a micro profile as illustrated in Figure 21. The macro profile is a function of the general orientation of the regulating wheel with

respect to the grinding wheel. Superimposed on this profile is the micro profile or regulating wheel crown. Generally the macro profile is controlled by swivelling the lower slide (Cincinnati Milacron centreless grinders) whereas the micro profile is a function of the set-up parameters.

Although a smaller diamond offset could be used, the common approach to correcting a high regulating wheel crown is either to reduce the throughfeed angle or to increase the trueing angle. Both of these methods have the same effect, that is they reduce the difference between the throughfeed angle and the trueing angle. The result is that the straight line profile associated with the trueing angle moves nearer the throughfeed angle and hence the regulating wheel profile within the grinding gap is 'smoothed' out.

Using the same basic data as in Table 15, the theoretical regulating wheel profile, as seen by a workpiece, in the grinding gap in a horizontal plane was computed for different throughfeed angles (Table 17). These are shown in Figure 23, where, by reducing the throughfeed angle, the regulating wheel profile within the grinding gap was flattened out. It is

important to note that the macro profile is not of interest since it can be accommodated for by swivelling the regulating wheel housing. In addition, the symmetric hyperboloid shape associated with zero diamond offset is apparent when the regulating wheel axis is parallel to the grinding wheel axis, i.e. at  $\alpha=0^\circ$ .

Working from Slonimski's expression, it can be calculated that for the given parameters in the case of the ground regulating wheel, a 4 degree throughfeed angle dictates that the trueing angle should be 2.33 degrees. By inclining the regulating wheel to 2.33 degrees a straight profile is to be expected. This is confirmed in Figure 23. Therefore, in order to provide optimum guidance for a workpiece with a diameter of 21.188 inches, a regulating wheel that is inclined at a 4 degree throughfeed angle must be trued at a 2.33 degree angle.

The alternative to decreasing the throughfeed angle is to increase the trueing angle in order to correct for a high regulating wheel crown. This has the effect of reconditioning the regulating wheel shape to accept a workpiece with a different diameter. Increasing the



trueing angle generates a regulating wheel shape suited to decreasing workpiece diameters. Figure 24 (Table 18) shows the effect on the regulating wheel profile of trueing at different values of  $\alpha_z$ . The plot is of the grinding gap viewed in a horizontal plane at the workpiece height. As expected, the high crown condition was corrected by reducing the difference between  $\alpha_z$  and  $\alpha$ . Figure 24 also illustrates the difference between changing  $\alpha_z$  and changing  $\alpha$ . By changing  $\alpha$ , the fixed regulating wheel shape was inclined until a straight line appeared at the necessary value of  $\alpha_z$  based on  $D_w$ . By changing  $\alpha_z$  the regulating wheel shape was changed to suit a different  $D_w$  and consequently as  $\alpha_z$  increased the profile straightened out. When  $\alpha_z$  was 4 degrees, it was equivalent to the throughfeed angle  $\alpha$  which was the condition necessary to guide a workpiece of diameter zero, hence the straight regulating wheel profile.

#### 4.7 Physical constraints on correcting the regulating wheel profile.

It has been shown that the regulating wheel profile can be modified by changing  $\alpha$  and  $\alpha_z$ . An attempt was made to use this approach to modify the profile of the

ground regulating wheel. By setting  $\alpha$  to 4 degrees, a straight line regulating wheel profile existed at an  $\alpha_s$  of 2.33 degrees. Using Slonimski's expression, a straight line profile at 4 degrees is achieved by plunge grinding the regulating wheel at an angle of 6.86 degrees. Unfortunately, restraints within the design of the regulating wheel housing prevented setting  $\alpha$  to 6.86 degrees. Similarly, interference between the regulating wheel and the workblade at exit prevented the use of a 2.33 degree throughfeed angle.

#### 4.8 Feasibility of using a ground regulating wheel in throughfeed centreless grinding.

Despite the advantages reported by Hashimoto, the ground regulating wheel concept is not practical in throughfeed centreless grinding. The major disadvantage is that the generated regulating wheel profile is only suited to the guidance of a workpiece whose diameter is equivalent to that of the grinding wheel. A detailed knowledge of the regulating wheel micro and macro profiles appeared to offer a solution but did so without due regard to the physical restraints imposed by the design of the centreless grinding machine. Another disadvantage is the increase in set-up time

associated with removing the tooling in order to plunge grind the regulating wheel.

Finally, great caution must be exercised when plunge grinding a rubber regulating wheel due to the rapid loading of the grinding wheel and the reverse torque imposed on the regulating wheel drive system.

#### 4.9 Summary.

Working from the two most common approaches to trueing a regulating wheel, namely Cincinnati Milacron and Lidköping, expressions were developed by which the trued axial profile of a regulating wheel could be determined and then in turn viewed. Such expressions may be incorporated into a simulation of the throughfeed centreless grinding process. In addition, they afford the researcher the opportunity to analyse the effect of various trueing philosophies on the generated regulating wheel form.

Using the above described expressions, a regulating wheel trueing method proposed by Hashimoto i.e. plunge grinding it with the grinding wheel, was evaluated in terms of the generated regulating wheel profile and how

it related to the throughfeed centreless grinding process. It was shown that this approach did not generate the optimum regulating wheel profile for the throughfeed grinding of workpieces other than those with a diameter equivalent to that of the grinding wheel.

The regulating wheel form was described in terms of a macro and a micro profile. The effects of the parameters  $\alpha$  and  $\alpha_3$  on the regulating wheel profile were analysed. This led to a greater understanding of the regulating wheel form generating process and prompted a re-examination of the plunge grind regulating wheel trueing method. The results showed that whilst this may be possible theoretically, physical constraints within the design of the centreless grinder and production problems in terms of increased set-up time seriously questioned the validity of its application.



## Chapter 5.

### 5.0 Part to part size variation and the centreless grinding machine system.

#### 5.1 Introduction.

The initial grinding experiments described in Chapter 2 revealed regulating wheel surface runout and precession of the regulating wheel spindle bearings as major contributors to part to part size variation. Whilst any relative motion between the grinding wheel and regulating wheel surfaces would affect size holding, the nature of the part to part size variations was very specific as represented by cycles repeating with a frequency of 0.75 to 5 Hertz. These observations narrowed the focus of the programme to certain potential causes, for example, grinding wheel wear could be discounted. Likewise, although runout of the surface of the grinding wheel was also measured and found to be once per revolution in nature, the relative speed of the grinding wheel at 20 to 25 Hertz was not as influential as that associated with the runout of the regulating wheel surface.

In order to better understand the cyclical size variations, a literature survey was conducted from which a reasoned approach was formulated for further investigating the experimental observations reported in Chapter 2. This work is described in this chapter as are the experiments derived from this activity.

## 5.2 Size variation.

In a rare article on size variation in centreless grinding, Loxham (Reference 14) reported that, when throughfeed centreless grinding, the chart of an automatic post process size recorder showed a pronounced wave pattern superimposed on the approximate uniform grinding wheel wear trace. A similar finding when plunge centreless grinding was reported by Willmore in an unpublished paper (Reference 23) where it was referred to as the 'saw tooth' effect and a hypothesis based on the dulling of the grinding wheel grits was advanced as the cause. Some correlation was found between components with poor roundness and reduced size, and, by monitoring the static deflections and vibration level of the grinding machine it was found possible, in some cases, to predict the apparent onset of the effect. It was suggested that the

progressive dulling of the grinding wheel active grits resulted in an increase in the radial cutting force thereby deflecting the grinding wheel spindle and in turn increasing the diameter of the ground workpiece. At some force level the wheel 'self-dressed' and there was an increase in the vibration level and by association the roundness errors. The grinding wheel now cut freer resulting in a reduction in the radial cutting force, the grinding wheel spindle deflection and in turn the workpiece size. This 'self-dressing' action of the grinding wheel was only temporary; the wheel soon assumed a stable cutting condition and the whole cycle repeated as reflected in the 'saw tooth' size effect. Summerfield (Reference 24) also observed a 'staircase' size effect when 240 workpieces were plunge centreless ground consecutively and measured for size.

Loxham did not provide an explanation for the effect that he observed. However, even though the 'saw tooth' effect observed by Loxham was shorter term than those reported by Willmore and Summerfield, that is it was superimposed on the plot of grinding wheel wear, it appeared to be a function of grinding wheel wear and as such was classified, in the context of this investigation, as long term in nature.

### 5.3 Errors in the trued shape of the regulating wheel.

Hashimoto (Reference 21) stated that grinding accuracy depended primarily on suppressing variations in the grinding depth and that in this context a major factor was the runout of the regulating wheel periphery at the contact point with the workpiece. He attributed this to two factors, the first was runout of the regulating wheel spindle whilst the second was a shape error of the trued regulating wheel. Hashimoto found that the runout of a regulating wheel trued with a single point diamond was worse than that of the regulating wheel spindle itself; 7.8 microns peak to peak compared with 0.15 microns, and proposed a new trueing method whereby the regulating wheel was trued by the grinding wheel; the ground regulating wheel runout was measured at 0.62 microns peak to peak.

Whilst Hashimoto confined his ground regulating wheel analysis to the effect on workpiece surface finish and out-of-roundness, the findings were applicable to size holding; the relationship between regulating wheel runout and part to part size variation was not examined probably because only the plunge centreless grinding process was considered. The implication from



Hashimoto's work was clearly that the conventional method of trueing the regulating wheel with a single point diamond did not result in an accurately trued shape. The error was once per revolution which was consistent with the observed part to part size variations described in Chapter 2.

Research into conventional dressing methods by Yokogawa (Reference 25) showed that a wheel out-of-roundness condition could result from dressing with a single point diamond tool and taking a reverse pass across the wheel at the same depth. This condition was dependent however on a low overlap ratio and the ensuing wheel shape was elliptical, a twice per revolution runout pattern.

The importance of the regulating wheel shape was also stressed by Rowe (Reference 4) in his study of the rounding action in centreless grinding. Rowe stated that an irregularity on the workpiece's radial form would have a much greater effect on the generated workpiece form at the grinding wheel if it made contact with the regulating wheel rather than the workblade. Errors in the trued shape of the regulating wheel therefore further complicate the rounding mechanism in

centreless grinding.

Nakkeeran (Reference 26) investigated the effect of regulating wheel form errors on workpiece roundness and roughness in plunge centreless grinding. A simulation based on Rowe's equation of constraint (Reference 4) was developed which included a term for an irregularity on the regulating wheel surface. Irregularities in the form of projections and flats were investigated as well as a case that featured the actual roundness deviations of a regulating wheel. In the latter case, the simulation returned a 7.2 micron workpiece roundness error as opposed to 1.07 microns for a theoretically perfect regulating wheel. The magnitude of the workpiece roundness error was found to be sensitive to the number of flats on the regulating wheel and the workpiece/regulating wheel diameter ratio.

Nakkeeran also investigated slip between the workpiece and the regulating wheel and stated that it was caused by variations in the grinding force which in turn were due to regulating wheel and workpiece form errors and workpiece movement. Experimental studies revealed that slip was predominantly controlled by the roughness of the regulating wheel. It was also found that the

roundness error of the regulating wheel was initially high following a fresh dress but improved during the course of the subsequent grinding run. An explanation based on the removal of loose particles from the wheel originating in the dressing operation and the settling of regulating wheel surface irregularities under the pressure of the grinding process was presented. Like Hashimoto, Nakkeeran confined his analysis to the plunge centreless grinding process and the effect on workpiece roundness errors.

#### 5.4 Investigation of the source of the once per revolution error in the trued shape of the regulating wheel.

In attempting to explain the source of the error in the trued shape of the regulating wheel, a possible explanation was the rotational accuracy of the regulating wheel spindle. One method for evaluating spindle performance involves eccentrically mounting two pickups 90 degrees apart and observing the 'zone of non-repeatability' on an oscilloscope. Such an approach provides information on the three main undesirable spindle motions - radial, angular and axial (Reference 27). The fact that a zone of non-repeatability exists proves that these primary motions, either individually

or collectively, do not repeat from revolution to revolution.

The regulating wheel spindle bearings were Torrington designed 'hollow rollers'; a full discussion of hollow roller bearing inaccuracies was presented by Bhateja (Reference 28). In a hollow roller bearing the zone of non-repeatability is a function of three frequency components - higher than, equal to and lower than the shaft rotational frequency. As with most precision bearings, the zone of non-repeatability of a hollow roller bearing may be of the order of 20 microinches, however the total runout of a spindle featuring two or more hollow roller bearings will be a function of the precession ratios of the individual bearings and consequently an assessment of the composite runout will require analysis over a large number of spindle rotations. It is possible that such a behaviour of the hollow roller bearing straddle supported regulating wheel spindle is described by the third cycle observed in the consecutive size plots of Figures 29 and 31.

It is improbable however that a once per revolution error in the spindle system will result in a similar error in the trued regulating wheel radial form since



it will be 'trued out'. This may be explained by considering a spindle that orbits about an elliptical path. A regulating wheel mounted on that spindle will be trued to an elliptical shape (radial plane) by a single point diamond tool. If that diamond tool is then replaced by a displacement transducer, no runout will be observed and the regulating wheel will 'appear' to be perfectly round.

This scenario however does not take into account the relative motion between the regulating wheel system and the diamond tool due to wheel vibration. Rowe (Reference 29) described the application of the Abbe principle to dresser siting and stated that ideally the dressing tool should be located as closely as possible in the same position and manner as the workpiece. Since this was impossible to achieve, it appeared that the next best position was opposite the grinding point. This philosophy is present in the location of the regulating wheel dresser on Lidkoping centreless grinding machines; Cincinnati on the other hand locate their regulating wheel dresser at the two o'clock position. In this respect, Hashimoto's approach to trueing the regulating wheel with the grinding wheel satisfied this requirement (Reference 21).

When studying regulating wheel runout it was soon apparent that when the dressing tool was replaced by a displacement transducer a runout was observed. A possible explanation was that the diamond tool was 'trueing-in' a once per revolution error and the source of the error lay in the interaction between the diamond tool and the regulating wheel system.

#### 5.5 The interaction between the diamond tool and the regulating wheel.

Maden (Reference 30) studied the effect of single point diamond dressing of Aluminium Oxide grinding wheels. His findings were however also applicable to regulating wheel dressing/trueing. The geometry of a single point diamond is described by two parameters - the rake angle and the drag angle. Typically the diamond tool is inclined towards the wheel such that the diamond points in the direction of rotation of the wheel. This is referred to as the drag angle and is defined as the angle measured between the axis of the diamond tool and a radial line passing through the wheel centre. The drag angle, normally 5 to 15 degrees, serves to reduce the possibility of cleavage or fracture of the diamond tool due to shock or induced vibration. The rake angle

is defined as the angle between the upper surface of the diamond and a radial line passing through the point of contact with the wheel face. It is normally  $-65$  to  $-70$  degrees. The rake angle is the more important since it is a function of the diamond geometry and the drag angle. Maden found that as the rake angle fell below  $-65$  degrees and the drag angle below  $5$  degrees, the radial component of the dressing force increased and with it a corresponding decrease in the stability of the dressing process.

Armed with this information, a study was made of the regulating wheel diamond tool orientation on the Cincinnati Milacron 230-10 centreless grinder. The drag angle was measured and found to be  $-2$  degrees; the diamond tool was therefore pointing against the direction of rotation of the wheel. Subsequent consecutive workpiece size variation tests showed no reduction in the magnitude of the regulating wheel surface runout despite modifying the diamond tool holder to suit a  $10$  degree rake angle. Nevertheless, correct orientation of the single point diamond tool will result in some degree of 'self-reconditioning' thereby increasing tool life.

Further studies of the regulating wheel trueing process revealed a unique situation as regards variation in both the rake and drag angles with respect to axial position. Since the diamond tool moves at an angle to the axis of rotation of the regulating wheel then diamond orientation with respect to the wheel is constantly changing as is the line of application of the dressing force. This is illustrated in Figure 25. These changes however are not dramatic; it can be calculated that for a 12 by 10 by 6 inch regulating wheel trued symmetrically at an angle of 3 degrees, the rake and drag angles each change by 5 degrees from one end to the other.

Kaliszer (Reference 31) also investigated the interaction between the diamond tool and the wheel. In a study of the effect of dressing upon grinding performance, he investigated the form error of a grinding wheel as a result of the dressing action on the basis of known dressing forces and the rigidity of the system. Errors in the trued shape of the grinding wheel were dependent on the variation in spindle deflection due to variations in the dressing forces which in turn were linked with non-uniformity in the wheel hardness. This variation in wheel hardness was



estimated at plus or minus half a hardness grade and in Kaliszer's paper equivalent to a 0.8 Newton variation in dressing force. When dressing with a single point diamond the result was a grinding wheel form error of about 0.02 microns (0.8 microinches) which is insignificant.

Bhateja (Reference 32) discussed variations in wheel hardness and showed that the frequency of wheel dressing (wheel wear rates) and component size holding capability in the throughfeed centreless grinding process was fairly sensitive to the hardness variations of both wheels. For example, two A80 S2R regulating wheels with E Moduli of 27.93KN/mm<sup>2</sup> (wheel A) and 19.96 KN/mm<sup>2</sup> (wheel B) were evaluated under identical conditions. The results showed that the grinding wheel wear rates were 0.5 microns/minute (A) and 2.5 microns/minute (B); this can be explained by considering the systems dynamic stiffness.

With one exception, Bhateja concentrated on within batch as opposed to within wheel variations. The exception concerned two grinding wheels which had within wheel variations of 0.22 and 0.3 KN/mm<sup>2</sup>. By comparison with the grinding wheels, Bhateja found that

the variations were far greater between regulating wheels. For one particular regulating wheel specification (A80 S2R) for the 35 wheels tested, the E Modulus varied by 9.37 KN/mm<sup>2</sup>. Interestingly, the variation was 1.57 KN/mm<sup>2</sup> between twelve A120 S2R wheels. Given the average within batch variation of the A80 S2R wheels, it is not unreasonable to expect within wheel variations greater than those measured for the grinding wheels. This would suggest that the within regulating wheel hardness variation be of the order of several grades, resulting in a larger trueing error than that reported by Kaliszer (Reference 31) for the case of the grinding wheel. It also appears that a move towards finer grit sizes - 120, 180 - for regulating wheels would offer advantages not only from the viewpoint of smaller E Modulus variations but also as regards workpiece stability - a less 'rocky' axial regulating wheel profile. Finer grit regulating wheels also offer thermal advantages as explained in section 5.6.

The trueing accuracy is thus a function of the response of the single point diamond dressing system to variations in resistance to dressing brought about by the characteristics of the regulating wheel such as its

homogeneity, mounted rigidity, grade and bond and the orientation of the diamond dressing tool. Amongst the principal elements are the dresser rigidity and 'lift pressure' and therein its ability to maintain contact with the wheel at the pre-set dress depth. All these factors will ultimately dictate the nature of the error in the regulating wheel radial form.

The compliance of the rubber regulating wheel is an important element in the work rounding mechanism of centreless grinding particularly with regard to regenerative effects (Reference 33). In some applications, for example when grinding components with slots, excessive compliance of the rubber regulating wheel is detrimental to achieving good quality and a vitrified (less compliant) regulating wheel is used (Reference 34). One of the items reported by Hashimoto (Reference 21) was that the ground regulating wheel had a longer life and a contact stiffness three times greater than a conventionally trued regulating wheel. During grinding, the regulating wheel is subjected to radial forces in much the same way as during dressing and can therefore be considered to respond in a similar fashion. Such a response will have obvious implications as regards part to part size variation.

## 5.6 Thermal considerations.

In order to reduce set-up time, regulating wheels are dressed at high speeds, typically 500 to 900 r/min. One of the problems with changing speed is that the heat balance within the regulating wheel system also changes (Reference 11). An examination of the thermal balance along a straddle supported regulating wheel spindle would reveal five sources of heat input - the outboard bearing, the inboard bearing, the regulating wheel spindle gearbox/drive unit and the heat generated by the trueing/dressing action. The fifth source is heat radiated from the grinding wheel spindle bearings; it is usual to have both wheels rotating during wheel trueing/dressing. Conversely, the regulating wheel system will be cooled externally through the application of coolant (cutting fluid) during the trueing/dressing operation, and, depending on the type of spindle bearing, internal cooling may be provided by the bearing lubrication system. In the authors experience, coolant supply to the regulating wheel dresser is rarely adequate and in many instances regulating wheels are dressed/trued dry. It is also presumptuous to expect the coolant to find its way out of the grinding zone and on to the spindle bearing



housings. In many cases, internal cooling of the spindle bearings is also inadequate; many regulating wheel spindle bearings are grease packed on account of the low operating speeds. The problem of thermal stability has been addressed by some centreless grinding machine manufacturers through the introduction of cold shields, increased lubricant flow and lubricant temperature (refrigeration) control systems.

The effect of temperature changes within the regulating wheel system is further complicated by the presence of dissimilar materials, for example, the steel shaft and the rubber regulating wheel, and their respective thermal properties. Heat generated within the regulating wheel spindle bearings will tend to move out along the spindle and radially into the machine frame. Since rubber is a poor heat conductor then the regulating wheel will be ineffective as a heat sink and consequently there will be little heat dissipation from that portion of the spindle contained within the bore of the regulating wheel.

For rubber, the coefficient of thermal expansion varies depending on the type and amount of filler incorporated in the basic rubber gum. Increasing the filler content

reduces the coefficient (Reference 35); the thermal sensitivity of coarser grain regulating wheels is greater than that of finer grain wheels (Reference 11). Obtaining an accurate figure for the coefficient of thermal expansion of a rubber regulating wheel is difficult, with most estimates in the range 20 to 60 microinches per degree Celsius per inch.

The problem of estimating the effect of a temperature change on the dimensions of a rubber regulating wheel is compounded by a number of factors unique to elastomers. Rubber is virtually incompressible and its form, when subjected to a load, is dictated by a shape factor. In centreless grinding, the rubber regulating wheel is held between two clamping flanges or rings causing the unrestrained portion of the wheel to bulge. Rubber is also susceptible to stress relaxation - loss of stress when held at a constant strain over a period of time, and strain relaxation or creep - gradual increase in deformation under constant load with time. Returning to thermal effects, whilst rubber under no strain will expand when heated, rubber under load behaves differently on account of the Joule effect and will therefore tend to contract (Reference 35).

Through consideration of all these factors, the potential scenario when a regulating wheel system is subjected to a temperature change during dressing/trueing could include all or some of the following - a variation in the spindle rotational accuracy as a result of a change in the bearing preload; spindle radial and axial contraction or growth as a result of a distortion of the machine frame; a shift in the axial loading on the regulating wheel as a consequence of distortions of the clamping rings. The possibility therefore exists that a regulating wheel could be dressed true with reference to a particular thermal condition and then later assume a different form in response to another thermal condition.

Experiments were devised and techniques developed to test this hypothesis. A regulating wheel was trued in accordance with standard procedures. After trueing, the regulating wheel rotational speed was reduced to 20 r/min. and a displacement transducer (LVDT), fitted with a carbide ball tip, was placed against the surface of the wheel. The output from the LVDT was fed to a conditioning unit and then to one channel of a two channel chart recorder. A piece of reflective tape was attached to the regulating wheel and used to generate a

once per revolution signal via an optical tachometer which reported to the remaining channel of the chart recorder. Finally, a temperature probe with a digital readout was attached to the outboard bearing housing. Measurements were then made of regulating wheel surface runout (outboard) and bearing temperature (outboard) against time after trueing/dressing. The regulating wheel was not rotating between measurements. The data is shown graphically in Figure 26. The regulating wheel runout plot approximates an exponential function and can thus be described by the expression:

$$\text{Runout} = A(1 - e^{-t/T}) \quad (31)$$

where  $A$  is a constant,  $t$  is time in minutes and  $T$  is the time constant in minutes. If the plot in Figure 26 is extended to the origin then it can be described adequately by the expression:

$$\text{Runout} = 135(1 - e^{-t/25}) \quad (32)$$

Figure 27 shows another plot of regulating wheel runout versus time for the same centreless grinder but on a different occasion. If the origin is set at 63



microinches then it can be described by the expression:

$$\text{Runout} = 56(1 - e^{-t/20}) \quad (33)$$

The plots in Figures 26 and 27 are interesting in a number of respects. The first is an increase and then levelling off of the regulating wheel runout at some maximum value. This is indicative of steady state conditions and is echoed in the equilibrium condition exhibited by the outboard bearing temperature plot. In a classical sense, it illustrates the lagging response of a system to a temperature change and may be described by an exponential function. When the regulating wheel speed is increased to dressing speed, the spindle bearing temperature will rise and in time the heat generated will diffuse into the spindle and surrounding machine frame.

Depending on the length of the dressing operation, the regulating wheel system may achieve some measure of thermal equilibrium and possibly dimensional stability. In any event, the regulating wheel is trued with respect to the prevalent conditions of dimensional stability and attains a particular degree of roundness.

After dressing, the reduction in regulating wheel speed initiates further thermal changes and as the temperature falls the regulating wheel runout increases until thermal equilibrium and dimensional stability are once more attained. This is the point of maximum runout.

A second respect is that Figure 26 shows the magnitude of the runout reduces further immediately after dressing. This implies that not only does the regulating wheel system continue to change dimensionally but those changes reduce the regulating wheel form error. No explanation is offered for this observation.

In Figure 26 the inclusion of the outboard bearing temperature plot tends to confuse the situation. The rise in bearing temperature immediately following dressing is accounted for by the action of stopping the spindle and with that the flow of lubricant to the bearing.

A final respect refers to a phenomenon known by some as 'Monday morning regulating wheel' (Reference 11). This term is used to describe the unstable grinding

conditions experienced when a grinding machine is first turned on following shut down over a weekend. Stable grinding conditions are usually achieved some one to two hours after initial start-up. It is suggested that the plots in Figures 26 and 27 offer evidence of this phenomenon. Whilst there may be no apparent justification for blaming the regulating wheel for the initial period of instability, it is nevertheless interesting that one time constant ( $T$ ) is 20 to 25 minutes and therefore  $3T$  is equivalent to 60 to 75 minutes.

#### 5.7 Machine stiffness.

In addition to regulating wheel surface runout and precession of the regulating wheel spindle bearings, part to part size variation is also a function of the compliance of the machine tool. In throughfeed centreless grinding, a simple procedure for evaluating machine compliance is to perform a 'pinch-out' test. Pinch-out is a measure of the static stiffness of the grinding wheel and the regulating wheel systems and is the variation in the distance between the grinding wheel and regulating wheel surfaces when workpieces are first introduced to the grinding zone or as a stream of

parts exits the grinding zone. Whilst pinch-out may not be evaluated in a formal sense, it is nevertheless an intuitive part of the strategy for operating a throughfeed centreless grinding machine.

Pinch-out affects size holding in two ways. Excessive pinch-out causes considerable part to part size variation as the system responds to the forcing functions of large initial size variations and throughfeed interruptions. This in turn increases the number of grinding passes necessary to achieve the desired size tolerance. It also limits the degree of compensation available within the grinding zone. On the other hand, a small amount of pinch-out permits accurate compensation but the energy created in the grinding process must now be absorbed by the workpiece. It has been shown (Reference 36) that increasing the stiffness (reducing the pinch-out) of the regulating wheel slide by clamping the lower slide to the machine bed (upper slide is clamped to the lower slide) on a Cincinnati centreless grinder resulted in a 2 to 1 increase in the part to part size variation. By increasing the stiffness of the regulating wheel system, the stream of workpieces was forced to absorb dimensional changes within the grinding zone, for



example, errors in the trued shapes of the grinding and regulating wheels, resulting in an increase in the part to part size variation.

With the Cincinnati Milacron 230-10 centreless grinding machine set-up for throughfeed grinding and operating under steady state conditions, throughfeed interruptions were simulated by blocking the flow of workpieces to the machine. From a knowledge of the throughfeed rate and the length of the collecting tube, it was possible to capture the effect of a feed stoppage within a stream of consecutively ground workpieces. The results are shown in Figures 28 and 29; Figure 28 represents a feed stoppage of two to three minutes whilst Figure 29 represents a momentary feed stoppage.

Figure 28 clearly shows the machine responding elastically to the feed stoppage; from a size variation of 25 to 30 microinches, the average size ramps up following the feed stoppage to a new mean, and a size variation of 40 to 50 microinches. It has been argued (Reference 11) that this response is not purely pinch-out but also the dimensional response of the system to thermal changes brought about by an

alteration in the flow pattern of the coolant within the grinding zone due to the absence of workpieces. In Figure 29, the effect of a feed stoppage appears minimal, but the point at which it occurs is nevertheless discernable.

The effect of initial size variations is illustrated in Figures 30 and 31. Figure 30 shows the grinding machine response when grinding blanks (first cut) and Figure 31 when grinding first cut parts (second cut). Under similar conditions of stock removal and throughfeed rate, the initial size variation was 0.001 to 0.002 inches on first cut and 0.0001 to 0.0002 inches on second cut. The data shows that the size spread on first cut averaged 75 microinches, whilst on the second cut it was 30 microinches. The experiments therefore demonstrated the effect of initial size variations on size holding in the throughfeed centreless grinding process.

The plots in Figures 29, 30 and 31 are clearly dominated by the regulating wheel surface runout cyclical pattern. There is, however, evidence of another cyclical pattern which can be seen in Figure 29 running from part number 3 to part number 25, and part number

25 to 50, and in Figure 31 from part number 10 to 35. This cyclical pattern accounts for 10 to 20 microinches of size variation over 20 to 30 consecutive parts. It is suggested that this cycle was associated with orbitting of the grinding wheel Filmatic straddle supported spindle or the composite effect of the precession runouts of the roller bearings in the regulating wheel straddle supported spindle.

In this section, the response of the machine system to forcing functions such as feed stoppages and initial size variations has been shown to affect part to part size variation in the short term. This places the onus on the production process to ensure that the centreless grinder receives an uninterrupted supply of raw material of the required dimensional characteristics that will enable it to produce acceptable quality.

## 5.8 Grinding forces.

In throughfeed centreless grinding the workpiece is held within the grinding zone (against the regulating wheel and the workblade) by the tangential component of the grinding force. This force, also referred to as the 'cut pressure', is important since it controls

workpiece stability and hence quality; insufficient cut pressure results in 'floaters' - workpieces that float along the top of the workblade and exit the grinding zone either unground or larger than the nominal size.

Factors that influence the vertical movement of the workpiece are workpiece height above centre and workspeed. This was reported in a paper published by Subramanya Udupa (Reference 37). Another factor is workblade angle; increasing it will increase the hold down force. A limiting factor however will be the attendant increase in the horizontal component of the force acting on the workblade, the frequency and amplitude of which may result in workpiece 'lift-off'. It is also thought that workspeed, which in needle roller grinding may exceed 30,000 r/min, causes the formation of a hydrodynamic coolant wedge between the workblade and the workpiece thereby increasing the risk of floaters. Such hydrodynamic effects have been reported by Smits (Reference 11). The effect of coolant on the frictional conditions within the grinding zone were discussed by Subramanya Udupa (Reference 38) but his observations were limited to variations in workspeed and axial feed rate and their effect on workpiece roundness and surface finish.



Any increase in the normal force will also tend to push the workpiece up and out of the grinding zone. This may arise from dulling of the grinding wheel or increased infeed. For a given set of conditions, different grinding wheels will produce different magnitudes of normal force, for example, Silicon Carbide has a higher cut pressure than Aluminium Oxide (Reference 11).

Hashimoto, in his paper on regulating wheel trueing accuracy (Reference 21), presented a plot showing the variation in the normal force synchronised with the rotation of the regulating wheel; variation in the grinding depth as a result of regulating wheel runout.

As discussed in section 5.5, the response of the regulating wheel system will also be affected by variations in the normal force. It can therefore be appreciated that limiting the variation in the normal force will increase workpiece stability within the grinding zone and thereby minimise part to part size variation.

## 5.9 Conventionally trued regulating wheel versus a ground regulating wheel.

Despite the problems associated with achieving the optimum regulating wheel profile (refer Chapter 4 section 4.8) an attempt was made to throughfeed centreless grind workpieces using a ground regulating wheel. The regulating wheel was plunge ground according to the procedure described by Hashimoto (Reference 21). As expected, the appearance of the ground regulating wheel was very striking; the wheel's surface being very smooth and highly polished.

The experimental data in Figures 32 and 33 was obtained by means of the previously discussed technique of capturing a stream of consecutively ground workpieces and measuring their individual sizes. In this series of tests the stock removal on diameter was 0.0025 inches. Figure 32 is a consecutive workpiece size plot featuring the new regulating wheel spindle system and a conventionally trued regulating wheel. The decision was made to replace the original regulating wheel spindle package following the data obtained in the Basic Grinding Experiments (refer Chapter 2) which suggested that there was excessive precession of the hollow

roller bearings. Figure 32 is characterised by two to three part cycles of amplitude 15 to 40 microinches and the occasional six to seven part cycle of amplitude 30 to 40 microinches. Figure 33 is the consecutive workpiece size plot for the 'ground' regulating wheel and again there were two distinct cycles. The first one occurred every two to three parts with a spread of 15 to 25 microinches whilst the second occurred every seven parts with a spread of 30 to 40 microinches. The seven part cycles can be clearly seen in Figure 33 from part number 77 to part number 111.

The plot in Figure 33 implied two things; the first was that the new regulating wheel spindle system also exhibited precession of the bearings, although 30 to 40 microinches was typical of the quality achievable at that time; and second that in this case the precession of the bearings contributed a greater portion to the part to part size variation than the regulating wheel runout. The data attributed some 15 to 25 microinches (0.375 to 0.625 microns) to regulating wheel surface runout which compared favourably with Hashimoto's figure of 0.62 microns peak to peak (Reference 21). Therefore, by plunge grinding the regulating wheel, those errors associated with the spindle rotational

frequency were effectively 'sparked-out'. The consecutive workpiece size plot (Figure 33) still showed evidence of the regulating wheel form error but the plot was now dominated by the error associated with the precession ratio of the regulating wheel spindle bearings and independant of the regulating wheel trueing technique.

#### 5.10 Summary.

Whilst any variation in the depth of cut would affect the grinding accuracy of the throughfeed centreless grinding process, this investigation found that as regards part to part size variations, those variations were very specific in nature as represented by cycles repeating with a frequency of 0.75 to 5 Hertz. Two major factors were identified as causal effects, an error in the trued shape of the regulating wheel and the precession ratio of the regulating wheel spindle bearings.

The error in the trued shape of the regulating wheel was once per revolution and resulted in a cyclical size variation that repeated at a frequency equivalent to the throughfeed rate in parts per regulating wheel



revolution. Two causes for the error in the trued shape of the regulating wheel were presented.

The first was the interaction between the single point diamond trueing tool and the regulating wheel system, and concerned the inability of the trueing tool to maintain contact with the regulating wheel at the preset depth due to variations in the radial component of the trueing force. These variations were brought about by spindle deflections, dresser deflections, changes in the orientation of the trueing tool with respect to the regulating wheel and the non-uniformity of the regulating wheel.

By using the grinding wheel to 'plunge' true the regulating wheel, Hashimoto (Reference 21) was able to reduce the amplitude of the once per revolution regulating wheel form error. This approach countered the effect of system deflections by effectively 'sparking-out' the regulating wheel shape. Whilst this trueing method cannot generate the regulating wheel form necessary for throughfeed centreless grinding, experimental results confirmed the reduction in the magnitude of the regulating wheel surface runout.

The magnitude of the radial component of the trueing force was dependent on the trueing tool's rake and drag angles. In regulating wheel trueing, it was shown that the orientation of the diamond tool with respect to the regulating wheel changed as the tool moved axially along the wheel resulting in changes in the rake and drag angles and in turn the stability of the trueing process.

The trueing force was also affected by variations in the regulating wheel hardness which was dependent on the manufacturing process and the regulating wheel composition. Finer grit regulating wheels offered advantages in terms of smaller E Modulus variations, a less rocky axial profile and better thermal stability.

The second cause for the error in the trued shape of the regulating wheel was that the regulating wheel was very sensitive to changes in the thermal balance within the centreless grinding machine's envelope. To minimise set-up time it is common practice to increase the regulating wheel speed during trueing which has the effect of upsetting the centreless grinding machine's thermal equilibrium. The response of a rubber regulating wheel to temperature changes is

unpredictable since it depends on the type and amount of filler incorporated into the basic rubber gum and the loading conditions to which the wheel is subjected. Variations in the magnitude of the regulating wheel surface runout were observed and described in terms of an exponential function. Emphasis on thermal stability of machine tools is gaining commercial acceptance and is increasingly reflected in the design of modern centreless grinding machines.

Owing to the importance of the regulating wheel in moving the workpiece through the grinding zone and as a locational element both in the workpiece roundness generation feedback control loop and in controlling the dimensions of the workpiece, it is essential that it be correctly 'conditioned' prior to commencing grinding operations. The regulating wheel system therefore represents an area of opportunity for improving the quality of throughfeed centreless ground workpieces.

The second major factor to affect part to part size variation was the precession ratio of the regulating wheel's spindle bearings. This resulted in cyclical size variations that repeated at a frequency equivalent to the throughfeed rate in parts per 2.2 regulating

wheel revolutions. Reducing the impact of machine tool spindle runout on part to part size variation will be a function of future advances in spindle manufacturing technology.

The experimental results also identified a third cyclical pattern that repeated every 20 to 30 parts throughout the plot of consecutive workpiece size variations. The source of this variation was not identified, but a hypothesis was formulated based on the orbitting of the straddle supported spindles and/or the composite effect of the precession ratios of each spindle bearing package.

In addition to the cyclical effects, workpiece size variation was also shown to be dependent on the response of the centreless grinding machine to variations in throughfeed rate and incoming workpiece initial sizes. The static stiffness of the machine may affect workpiece size holding in a number of ways. High static stiffness will force the workpieces to absorb dimensional changes within the system such as spindle runout whereas low static stiffness will increase the number of grinding passes necessary to achieve the desired size tolerance.



Finally, the size holding capability of the throughfeed centreless grinding process is also dependent on the degree of control exercised over the workpiece within the grinding zone. Lack of control will result in the workpiece moving up off the workblade and 'floating' through the grinding zone. This can be as a result of factors such as abrasive type, a dull grinding wheel - increased normal grinding force, excessive workpiece height above centre, incorrect workblade angle, and high workspeeds - creation of a hydrodynamic coolant wedge beneath the workpiece.

## Chapter 6.

### 6.0 Simulation of the throughfeed centreless grinding process: workpiece sizing mechanism.

#### 6.1 Introduction.

This chapter describes the development of a model of the throughfeed centreless grinding process. Emphasis was placed on the workpiece sizing mechanism and consequently the model reflects much of the work described in earlier chapters.

#### 6.2 Review of previous models of the centreless grinding process.

A number of researchers have developed models of the centreless grinding process most notably Dall (Reference 2), Yonetsu (Reference 3), Gurney (Reference 5), Rowe (References 4, 29 and 39), Becker (Reference 40), Miyashita (References 7, 41 and 42) and Reeka (Reference 6). Amongst the later researchers who utilised these primary models were Chien (Reference 43), Frost (References 44 and 45), Subramanya Udupa (References 10, 46 and 47), Spragget (Reference 48),

Nakkeeran (Reference 26) and Schreitmuller (Reference 49).

Although these models concentrated primarily on the plunge or infeed centreless grinding process and more particularly the work rounding mechanism, some of the published material was applicable to the throughfeed centreless grinding process. An example was the paper by Subramanya Udupa (Reference 10) which was a three dimensional geometric analysis of the plunge centreless grinding process. Another example was Nakkeeran (Reference 26) who included in Rowe's equation of constraint the effect of a regulating wheel irregularity but confined his analysis to plunge centreless grinding and workpiece roundness errors.

With one exception, an extensive literature survey failed to identify any models or simulations of the throughfeed centreless grinding process. That exception was Meis (Reference 50) who developed a geometric model of the grinding gap in order to simulate the movement of a workpiece during the throughfeed centreless grinding process. Having developed an expression for the exact shape of the regulating wheel necessary for optimum workpiece axial guidance, Meis set out to

investigate various regulating wheel shapes and how they affected the path taken by the workpiece through the grinding gap. The workpiece coordinates were first established with respect to the grinding wheel, regulating wheel and the workblade for the zero position of the workpiece at the grinding gap entrance. The workpiece was then moved axially through the grinding gap whilst new values for the workpiece diameter and workpiece centre point coordinates were determined. In the simulation, the workpiece was modelled as a number of slices with each slice considered as a perfect circle. The model ignored radial deviations and assumed the system to be rigid. The output of the simulation was a plot of workpiece centre coordinates against axial distance through the grinding gap where deviations between the workpiece path and one parallel to the grinding wheel axis were of primary interest.

Meis expressed reservations about the integrity of a model of the throughfeed centreless grinding process on account of the complexity of the interactions between the many factors prevalent in the process as well as the computing power necessary to adequately describe the workpiece form.



### 6.3 Basic concept used in the development of a throughfeed centreless grinding model.

The equation of constraint developed by Rowe (Reference 4) formed the basis from which a model of the workpiece sizing mechanism in the throughfeed centreless grinding process was developed. With reference to Figure 34, the basic equation of constraint was stated as:-

$$r(\theta) = K[X(\theta) - K_R \cdot r(\theta - \pi + \beta) + K_B \cdot r(\theta - \alpha) - r(\theta - 2\pi)] + r(\theta - 2\pi) \quad (34)$$

$$\text{where } K_B = \frac{\sin \beta}{\sin(\alpha + \beta)} \quad (35)$$

$$K_R = \frac{\sin \alpha}{\sin(\alpha + \beta)} \quad (36)$$

The system's response was expressed by the machining-elasticity parameter,  $K$ , defined as the ratio of the true depth of cut to the apparent depth of cut. The value of  $K$  may be determined experimentally, but is typically in the range 0.3. Rowe defined the true depth of cut as:-

$$S(\theta) = r(\theta) - r(\theta - 2\pi) \quad (37)$$

Additional effects may be included in the basic equation of constraint such as grinding wheel and regulating wheel spindle runouts.

Alternatively, the equation of constraint may be expressed as:-

$$r(\theta) = X(\theta) + x(\theta) - K_R \cdot r(\theta - \pi + \beta) + K_B \cdot r(\theta - \alpha) \quad (38)$$

where  $x(\theta)$  represents the wheels/workpiece/system deflection. The normal force ( $P$ ) is related to the true depth of cut by the approximate relationship:-

$$P = K_m \cdot f\{S_1(\theta) + S_2(\theta) + S_3(\theta) + \dots S_n(\theta)\} \quad (39)$$

where  $n$  is the number of components within the grinding gap. This force must be balanced by the elastic force of the machine elements:-

$$P = K_e x(\theta) \quad (40)$$

From expressions 38, 39 and 40 :-

$$r(\theta) = x(\theta) + \frac{K_m}{K_a} \cdot f\{S_1(\theta) + S_2(\theta) + \dots + S_n(\theta)\}$$

$$K_a$$

$$- K_R \cdot r(\theta - \pi + \beta) + K_B \cdot r(\theta - \alpha) \quad (41)$$

The inclusion of  $x(\theta)$  permits the simulation of the effect of throughfeed interruptions and/or incoming workpiece size variations. The alternative form of the equation of constraint may be incorporated into more developed forms of the model given that values for  $K_a$  and  $K_m$  are known or estimated.

Finally, the various restrictions described by Rowe were also incorporated such as metal replacement and regulating wheel, grinding wheel and workblade interferences.

#### 6.4 Considerations when modelling the throughfeed centreless grinding process.

Unlike the plunge centreless grinding process which is analysed in terms of two dimensions, the throughfeed centreless grinding process is three dimensional and must be analysed as such. In order to model the throughfeed centreless grinding process, the following

factors need to be considered:-

#### 6.4.1 Variation in the throat angle.

In throughfeed centreless grinding the throat angle  $\gamma$  is not constant but varies axially through the grinding gap (Figure 3). The throat angle is defined as the sum of  $\gamma_R$  and  $\gamma_S$ , and it is the change in the value of  $\gamma_R$  with axial position that is responsible for the variation. The variation in  $\gamma_R$  can be found from the following expression:-

$$\Delta \gamma_R = \sin^{-1} \left( \frac{2l \sin \alpha}{D_R + D_w} \right) \quad (42)$$

In needle roller grinding, a typical value for  $\Delta \gamma_R$  would be five degrees. This variation in  $\gamma_R$  was accommodated in the model by substituting modified values for  $h$  in the expression for  $\gamma_R$ . The value for  $h$  was modified according to expression 43 which was derived using approaches outlined in Chapter 4.

$$h = \frac{1}{\cos \alpha} \left( \frac{h}{\cos \alpha} + \frac{\tan \alpha l_R}{2} \right) \quad (43)$$



In expression 43 the - sign relates to the portion of the regulating wheel from workpiece entrance to the regulating wheel centre whilst the + sign is from the regulating wheel centre to workpiece exit. Expression 43 may be simplified to:-

$$h = h \pm \frac{l_R \sin \alpha}{2} \quad (44)$$

or in terms of  $X_R$  as:-

$$h = h \pm \frac{X_R \sin \alpha}{2} \quad (45)$$

Therefore in order to model the throughfeed centreless grinding process it is necessary to track the axial movement of the workpiece within the grinding gap and from that calculate the value for  $h$  and in turn those for  $\gamma_R$  and  $\gamma$ .

#### 6.4.2 Grinding below centre.

Depending on the values chosen for the throughfeed angle and the workpiece height above centre, the workpiece may enter the grinding gap below the centre

of the regulating wheel. In such a situation Rowe's equation of constraint (Reference 4) must be modified as follows (Reference 46):-

$$r(\theta) = K[X(\theta) - \frac{\sin \alpha}{\sin(\alpha-\beta)} r(\theta-\pi-\beta) - \frac{\sin \beta}{\sin(\alpha-\beta)} r(\theta-\alpha) - r(\theta-2\pi)] + r(\theta-2\pi) \quad (46)$$

and the values for  $\beta$  and  $\alpha$  found from expressions 47 and 48:-

$$\beta = -\sin^{-1} \frac{2h}{D_s + D_w} - \sin^{-1} \frac{2h}{D_r + D_w} \quad (47)$$

$$\alpha = \pi/2 - (\alpha' - v\beta) \quad (48)$$

The throughfeed centreless grinding model must therefore determine whether the workpiece has entered the grinding gap above or below the regulating wheel centre and use the appropriate form of the equation of constraint. If initially the workpiece entered the grinding gap below the regulating wheel centre but during the course of its axial translation moves above the regulating wheel centre then the simulation must

monitor the axial movement of the workpiece and when appropriate employ the relevant equation of constraint.

#### 6.4.3 Variation in throughfeed rate and workpiece rotational speed.

The throughfeed rate  $V_A$  is found from expression 49:-

$$V_A = n_R \pi D_R \sin \alpha \quad (49)$$

In throughfeed centreless grinding the hyperbolic shape of the regulating wheel means that the regulating wheel diameter is not constant but varies axially. In some cases the variation in  $D_R$  is used to advantage particularly when throughfeed grinding bearing rings or workpieces with a length to diameter ratio of less than one. Typically, in needle roller grinding the variation in  $D_R$  is 0.040 to 0.080 inches with the corresponding variation in  $V_A$  being 2.5 to 5.25 inches/minute.

From expression 50 it can be seen that a variation in  $D_R$  will also cause a variation in the rotational speed of the workpiece:-

$$n_w = \frac{n_r D_r \cos \alpha}{D_w}$$

(50)

In addition, as stock is ground off the workpiece,  $D_w$  will also be reduced resulting in an increase in  $n_w$ . Whilst acknowledging that variations in the workpiece axial and rotational speed are inherent in the throughfeed centreless grinding process, it was decided that such variations could reasonably be ignored at this stage of model development in favour of the reduced computer program complexity and computational time.

#### 6.4.4 Dynamic effects.

In preceeding chapters, throughfeed interruptions and incoming workpiece size variations were shown to affect the size holding capability. More advanced versions of the model must therefore simulate the situation where the response of the system to the physical dimensions of a workpiece at one position in the throughfeed stream has repercussions on a workpiece at another position.

Ideally, the model should also cater for workspeed and



its effect on workpiece stability within the grinding zone, for example, hydrodynamic (coolant) lift-off.

#### 6.5 Initial version of a model of the sizing mechanism in the throughfeed centreless grinding process.

##### 6.5.1 Regulating wheel axial form.

In the first model of the throughfeed centreless grinding process, a simple taper was selected for the regulating wheel axial form. This choice immediately defined the position of the regulating wheel surface with respect to the grinding wheel for every axial position within the grinding gap. From this it was possible to determine, for a given workpiece rotation, its kinematically associated axial displacement and in turn its radial infeed towards the grinding wheel.

##### 6.5.2 Depth of cut per workpiece revolution.

From an understanding of the throughfeed centreless grinding process, the following expression for the time spent by the workpiece in the grinding gap was derived:-

$$\frac{l_R}{\pi n_R D_R \sin \alpha \cos \alpha} \quad (51)$$

From expressions 50 and 51, the number of rotations executed within the grinding gap is given by:-

$$\frac{l_R}{\pi D_w \sin \alpha} \quad (52)$$

Further development yields an expression for the time to execute one workpiece revolution:-

$$\frac{D_w}{n_R D_R \cos \alpha} \quad (53)$$

From expressions 49 and 53, the axial distance travelled by the workpiece for one workpiece revolution is:-

$$X_M = \pi D_w \tan \alpha \quad (54)$$

With reference to Figure 35, in the case of a tapered regulating wheel by proportion:-

$$\frac{X_M}{\frac{l_R}{\cos \alpha}} = \frac{Y_M}{\text{DEPTH OF CUT}} \quad (55)$$

Hence the infeed per workpiece revolution is:-

$$Y_M = \frac{(\text{DEPTH OF CUT}) \pi D_w \sin \alpha}{l_R} \quad (56)$$

Expression 56 may in turn be modified in the simulation to give the infeed per workpiece rotational increment. Since the infeed was a function of the regulating wheel axial profile then it was expressed in terms of a component normal to the grinding wheel surface by multiplying it by the parameter  $K_B$ .

### 6.5.3 Regulating wheel system runouts.

To include the effect of regulating wheel system runouts in the simulation, expression 57 (Reference 26) was added to the equation of constraint:-

$$+ \frac{\sin \alpha}{\sin(\alpha + \beta)} \cdot \delta z \quad (57)$$

where  $\delta_z$  is an irregularity on the surface of the regulating wheel. The parameter  $\delta_z$  could be defined to represent either a regulating wheel form error(s) and/or a regulating wheel spindle bearing precession runout. Initially, all runouts were expressed in terms of sine functions although a Fourier series can be developed from the actual data.

#### 6.5.4 Initial workpiece shape.

As with plunge centreless grinding simulations, it was possible to create an initial shape on the workpiece prior to grinding. From Chapter 3 section 3.4, roller blanks were invariably two lobed, and consequently this feature was included in the simulation.

#### 6.5.5 Workpiece diameter.

In the simulation, the workpiece diameter was determined by calculating the average  $r(\theta)$  value, multiplying it by two and subtracting it from the original diameter. Other techniques may be used such as simulating a Two point gauging system whereby the values of  $r(\theta)$  at opposite positions on the workpiece



are determined based on an approach similar to the interference restriction in the equation of constraint.

#### 6.6 General description of the computer program written to simulate the throughfeed centreless grinding process.

In order to simulate the throughfeed centreless grinding process, a computer program was written based on the aforementioned model. The computer language selected was Microsoft QuickBASIC, a powerful personal computer based software package. In keeping with programming convention, the program was written in the form of a main program or module and a number of subprograms.

The program first established the data to be used in the program such as the grinding wheel diameter (GWDIA) and the workpiece height above centre (HACTR). Each workpiece was then given an initial two lobed shape as discussed in section 6.5.4..

The subprogram INFEEED then calculated the amount of infeed of the workpiece towards the grinding wheel per workpiece revolution. In this particular simulation, each workpiece revolution was divided up into 360

increments and consequently INFEEED returned the parameter GWBITE, the infeed per increment to the main module. As discussed in section 6.4.3., the workpiece rotational speed ( $n_w$ ) was assumed constant as was the throughfeed rate ( $V_A$ ). The value of GWBITE was therefore calculated using the initial workpiece diameter and held constant for each axial position within the grinding gap. To represent grinding as opposed to spark out, the value of AMOFIN (AMount OF INfeed) in the equation of constraint was continuously revised by setting it initially equal to GWBITE and then adding GWBITE to it with successive workpiece rotational increments.

The AXial DISTance moved by the workpiece per increment of rotation was designated AXDIST and based, like GWBITE, on an initial workpiece diameter. The program used AXDIST to track workpiece axial progress as well as control the movement of workpieces into and out of the grinding gap.

The first workpiece was then introduced into the grinding gap and a check made to see if it entered above or below the regulating wheel centre. The subprogram GARMOD (GAMma R MOdification) was called

which calculated, for a given axial location, the height of the workpiece centre above the regulating wheel centre, HMOD (Height MODification). Upon return to the main module, HMOD was added to HACTR and tested for the condition of less than zero - indicative of the workpiece entering below centre. The program then proceeded to evaluate the equation of constraint by calling the subprograms BCSHAFAC (Below Centre SHApe FACtors), BCRWINT (Below Centre Regulating Wheel INTerference) and EQNCBC (EQuation of Constraint Below Centre) or alternatively SHAFAC, RWINT and EQNCAC. The subprogram WBINT (Work Blade INTerference) applied to both cases.

The subprograms SHAFAC and BCSHAFAC calculated the workblade ( $K_B$ ) and regulating wheel ( $K_R$ ) shape factors used in the equation of constraint. They also evaluated the parameters BETA - the included angle between the grinding wheel contact normal and the regulating wheel contact normal, and ALPHA - the angle between the grinding wheel contact normal and the workblade contact normal.

The subprograms RWINT, BCRWINT and WBINT checked for interferences at the regulating wheel and workblade as

defined by Rowe (Reference 4).

The subprograms EQNCBC and EQNCAC calculated the regulating wheel system runouts, evaluated the equation of constraint and then tested for grinding wheel interference and metal replacement. This process was then repeated for each of the 360 workpiece increments or ROTational STEPs (ROTSTEP) in turn, after which, the average reduction  $r(\theta)$  was calculated and used to determine the new WorkPiece DIAMeter (WPDIA). This sequence of events continued until AXDIST(workpiece 1) was equivalent to one times WPLGH (WorkPiece LenGth) when a second workpiece was introduced into the grinding gap. The first and second workpieces were then moved through the grinding zone until AXDIST(workpiece 1) was equal to two workpiece lengths. A third workpiece was then introduced, and the whole process repeated with additional workpieces being introduced into the grinding zone as appropriate. When AXDIST(workpiece 1) was equal to the Regulating Wheel WIDTH (RWWID), workpiece 1 was ejected from the grinding zone and underwent no further 'grinding'. Figure 36 shows the flowchart for the computer program.



## 6.7 Results of the computer simulation.

Figures 37 and 38 are graphical representations of the data generated by the computer when simulating the effect of regulating wheel system runouts. In both cases the regulating wheel surface runout and precession runout were equal at 0.00025 and 0.00005 inches respectively, and the workpieces were given an initial two lobed out-of-roundness of 0.00025 inches. In Figure 37, however, the machining-elasticity parameter,  $K$ , was 0.3 whereas in Figure 38 it was 0.7. The workpieces were 'ground' using a typical machine set-up for throughfeed centreless grinding needle rollers.

In common with the experimental data, these plots were characterised by 2, 3 and 4 part cycles. The plot for a  $K$  of 0.7 (Figure 38) had a larger size spread, 21 microinches, compared with that for a  $K$  of 0.3 at 13 microinches. The mean size was also smaller at 0.097196 inches compared with 0.097227 inches. The simulation showed that decreasing the compliance resulted in a larger size spread as the workpieces absorbed the system runouts. This was supported by the experimental data of McCalmont (Reference 36) who reported a 2 to 1

increase in the part to part size variation after having reduced the compliance of the regulating wheel slide (refer Chapter 5 section 5.7).

The computing time for each 'grinding' run was 75 hours during which time 14 workpieces were fully 'ground'. By increasing the number of workpieces ground, it may be possible to identify the third cycle - every 20 to 30 parts - that was observed experimentally (Figures 29 and 31). In this respect, Figure 37 may suggest such a trend on account of the decreasing magnitude of the peaks at consecutive workpiece numbers 5, 9 and 11.

#### 6.8 Summary.

A basic model was developed and a computer program written to simulate the sizing mechanism in the throughfeed centreless grinding process. The model included the effects of regulating wheel surface runout, regulating wheel spindle precession ratio and initial workpiece out-of-roundness. The results showed good correlation with the experimental observations.

Since Rowe's equation of constraint (Reference 4) was used as the basis in the development of the model, then

provisions exist to extend the model to address the roundness generation mechanism.

Development of the model provided a clear insight into both the complexity and the necessary computing power involved in fully modelling the throughfeed centreless grinding process. Whilst full development may not be a viable approach, less developed models, as in this case, will nevertheless still afford the opportunity for a greater understanding of the process as well as provide the basic framework for potential future growth.

## Chapter 7.

### 7.0 Discussion and conclusions.

#### 7.1 Discussion.

As with most machining operations, dimensional accuracy in throughfeed centreless grinding results from the creation of the correct environment through the use of dedicated systems and methodologies. Having established a baseline, additional improvements are effected through further studies and in this context the regulating wheel 'system' was identified as a key area of opportunity.

In throughfeed centreless grinding the regulating wheel is the prime element in controlling and moving the workpiece within the grinding zone. Establishing control over the location of the workpiece is vital if dimensional accuracy is to be achieved. By systematically capturing and gauging streams of throughfeed centreless ground workpieces, cyclical part to part size variation trends were identified. These size variations were caused by displacements of the workpiece centre towards the grinding wheel as a result



of dislocations of one of the two locational surfaces, namely the regulating wheel. Two separate effects were identified, one associated with an error in the trued shape of the regulating wheel and the other with the precession ratio of the regulating wheel spindle bearings.

The error in the trued shape of the regulating wheel was once per revolution and resulted in a cyclical size variation that repeated at a frequency equivalent to the throughfeed rate in parts per regulating wheel revolution. The precession ratio of the regulating wheel spindle bearings resulted in a size variation with a frequency equivalent to the throughfeed rate in parts per 2.2 regulating wheel revolutions.

The error in the trued shape of the regulating wheel centred on the interaction between the trueing tool and the regulating wheel 'system' and concerned the inability of the trueing tool to maintain contact with the regulating wheel at the preset depth as a result of spindle deflections, dresser deflections and the non-uniformity of the regulating wheel. The situation was further complicated by the practice of increasing the regulating wheel spindle speed during trueing which

upset the thermal equilibrium of the system, resulting in a change in the physical dimensions of the regulating wheel contingent upon its particular temperature/load characteristics.

Alternative designs and methods for regulating wheel trueing must be sought which minimise the effect of system deflections and generate a purer regulating wheel radial form. The use of finer grit regulating wheels should be encouraged wherever practical since they offer the advantages of smaller E Modulus variations - better homogeneity, greater thermal stability, and present a less 'rocky' axial profile to the workpiece. Finally, incorporated within the design of the centreless grinding machine must be the ability to respond to different operating conditions without the loss of thermal stability.

In developing alternative designs and methods for regulating wheel trueing, consideration must be given to the special requirements of the regulating wheel form in throughfeed centreless grinding. The development of expressions that described the regulating wheel form necessary for throughfeed centreless grinding opened the way to analysing such

alternatives. The concept of plunge trueing the regulating wheel with the grinding wheel was proposed by Hashimoto (Reference 21) as a way of reducing the error in the trued form of the regulating wheel. Experimental data supported this approach but the process did not generate the optimum regulating wheel form for throughfeed centreless grinding and furthermore greatly increased the set-up time.

Traditionally, the single point diamond tool was used to true the regulating wheel. When using these tools, the radial component of the trueing force was sensitive to changes in the rake and drag angles. Such changes are inherent in the throughfeed centreless grinding regulating wheel trueing process on account of the axial path taken by the trueing tool. Alternative regulating wheel trueing tools may be used as was the case with Hashimoto's grinding wheel (Reference 21). Meis (Reference 50) also addressed the subject of regulating wheel trueing tools but from the viewpoint of reducing set-up time. By using a suitably dimensioned poly-crystalline diamond tool featuring a zero rake angle, smaller trueing forces were predicted in addition to the increase in trueing rates. Hashimoto (Reference 21) reported a threefold increase in the

regulating wheel's contact stiffness when trueing it with the grinding wheel. Schreitmuller (Reference 49) showed that the regulating wheel's contact stiffness was sensitive both to the conditioning method and to the regulating wheel's exposure to coolant. As regards the roundness generation mechanism in centreless grinding, he advised the use of regulating wheels with greater contact compliance since their response to an irregularity on the workpiece produced a smaller offset of the workpiece centre and hence a reduced change in the depth of cut. This finding was also reported by Rowe (Reference 33) and Miyashita (Reference 42). Regulating wheel trueing technology therefore represents an area of opportunity for securing improvements in the quality of throughfeed centreless ground workpieces.

In addition to the aforementioned size variation effects, a third effect was identified when gauging the size of consecutively ground workpieces. Although this effect was cyclical and repeated every 20 to 30 parts, the source of this variation was not identified and could be the subject of a further study.

Other factors that affected the size holding capability



of the throughfeed centreless grinding process included the response of the centreless grinding machine to inconsistencies in the throughfeed rate and to incoming workpiece size variations, and poor throughfeed centreless grinding practices such as excessive workpiece height above centre and a dull grinding wheel, both of which contribute to lack of workpiece control within the grinding zone.

Failure to recognise both the interdependence of size, roundness and geometric form and the effect of the relationship between the coordinate system of the workpiece and that of the measurement device were sources of great frustration when gauging the size of centreless ground workpieces. A standard gauging procedure was established therefore to address those issues and therein provide a more confident interpretation of the data.

The experimental programme together with the development of expressions to describe the regulating wheel form, provided a good understanding of the throughfeed centreless grinding process and formed the basis for the development of a model of the sizing mechanism. The model was based on Rowe's equation of

constraint (Reference 4) and could therefore be extended to address the roundness generation mechanism. From this model a computer simulation was written using the Microsoft QuickBASIC programming language. Using the simulation, it was possible to recreate the effects observed experimentally as regards regulating wheel system runouts.

As with most simulations of this type, the computing time necessary to simulate a modest throughfeed centreless grinding process was found to be enormous, involving some seventy five hours to 'grind' a stream of fourteen workpieces. This must be viewed in the context that the simulation only considered the sizing mechanism, was simple in nature, and restricted primarily to geometric effects. Owing to the complexity of the throughfeed centreless grinding process, it may not be viable to develop a full simulation but rather some intermediate version which nevertheless achieves particular goals or provides new insights. In this regard, the simulation developed here laid the groundwork for further development as necessary.

In conclusion, this study of the size holding capability of the throughfeed centreless grinding

process has expanded the knowledge base in this area of grinding technology and led to the adoption of new methods and procedures by Industry.

### Conclusions.

- (1) Two major factors were identified as being responsible for part to part size variation in the throughfeed centreless grinding process, an error in the trued shape of the regulating wheel and a runout associated with the precession ratio of the regulating wheel spindle bearings.
- (2) The error in the trued shape of the regulating wheel was as a result of the interaction between the trueing tool and the regulating wheel system and dependent on factors such as spindle deflections, dresser deflections, non-uniformity of the regulating wheel and the regulating wheel's response to temperature variations.
- (3) Three recommendations were proposed, investigate alternative designs and methods for regulating wheel trueing, use finer grit regulating wheels, and design centreless grinding machine systems that exhibit less thermal sensitivity.

- (4) Size holding in the throughfeed centreless grinding process was also shown to be dependent on the response of the centreless grinding machine to inconsistencies in the throughfeed rate and to incoming workpiece size variations.
- (5) A study of the form and function of the various elements of the centreless grinding machine established a clear relationship between design and performance and laid the groundwork for a better understanding of the throughfeed centreless grinding process.
- (6) Expressions were developed that described the regulating wheel form necessary for throughfeed centreless grinding. These expressions may be used to evaluate alternative regulating wheel trueing philosophies or incorporated into a simulation of the throughfeed centreless grinding process.
- (7) An alternative regulating wheel trueing method proposed by Hashimoto (Reference 21) which involved plunge 'trueing' the regulating wheel with the grinding wheel was analysed using the aforementioned expressions. Whilst it resulted in a reduction in the regulating wheel surface runout, it did not generate the correct



regulating wheel axial profile for throughfeed centreless grinding and, from a production standpoint, contributed to a significant increase in set-up time.

- (8) A methodology for gauging the diameter of centreless ground workpieces was established. Consideration was given to the interdependence of size, roundness and geometric form, the relationship between the coordinate system of the workpiece and that of the measurement device, gauging technique, and minimising the impact of temperature variations.
- (9) A basic model of the throughfeed centreless grinding process was developed and a computer program written. The model concentrated on the workpiece sizing mechanism and simulated the effect of regulating wheel system runouts, agreeing closely with experimental observations. An appreciation was gained both of the complexity of modelling the throughfeed centreless grinding process and of the computing power required. In this context, the simulation laid the groundwork for further judicious development.

## Chapter 8.

### 8.0 Further work.

#### (1) Computer simulation.

Further development of the computer simulation of the throughfeed centreless grinding process will depend largely on the nature and objectives of the particular research effort. Potential topics include:

- Using alternative programming practices to reduce the program's run time and make it more efficient.
- Incorporating the effects of incoming workpiece size variations and throughfeed stoppages.
- Investigating the feasibility of determining experimentally a value for  $K$ , the machining-elasticity parameter, for inclusion in the model.
- Incorporating in the model the expressions for the actual regulating wheel form.
- Modelling the effect of sparkout.
- Describing the regulating wheel system runouts in terms of Fourier series.
- Representing each workpiece as a series of slices.
- Developing the roundness generation mechanism.

(2) Regulating wheel contact stiffness.

Investigate the relationship between regulating wheel conditioning and regulating wheel contact stiffness and its effect on the quality of ground workpieces.

(3) Regulating wheel trueing.

Explore alternative regulating wheel trueing systems/philosophies that:

- Create a purer regulating wheel radial form.
- Generate the correct regulating wheel form for throughfeed centreless grinding.
- Recognise production requirements such as shorter set-up times.

(4) Centreless grinding machine design.

Review designs from the viewpoint of improved thermal stability.

(5) Cyclical size variations.

Investigate the cause of the third size variation cycle identified in the plots of consecutively ground workpieces.

## REFERENCES.



## References.

1. 'Centreless grinding - an outline of developments', Lidkopings Mekaniska Verkstads Aktiebolag publication, June 1970.
2. Dall, A.H., 'Rounding effect in centreless grinding', Mechanical Engineering, April 1946, pp 325-329.
3. Yonetsu, S., 'Forming mechanism of cylindrical work in centreless grinding', Proc. of the Fujihara Memorial Faculty of Engineering, Keio University, Vol. 12, No. 47, 1959, pp 27-45.
4. Rowe, W.B. and Barash, M.M., 'Computer method for investigating the inherent accuracy of centreless grinding', Int. J. Mach. Tool Des. Res., Vol. 4, pp 91-116, Pergamon Press 1964.
5. Gurney, J.P., 'An analysis of centreless grinding', ASME Journal of Engineering For Industry, Vol. 86, May 1964, pp 163-174.
6. Reeka, D., 'The relationship between the geometry of the grinding gap and the roundness error at centreless grinding', PhD. Thesis, Aachen, 1967.
7. Furukawa, Y., Miyashita, M. and Shiozaki, S., 'Vibration analysis and work rounding mechanism in centreless grinding', Int. J. Mach. Tool Des. Res., Vol. 11, pp 145-175, Pergamon Press 1971.
8. ISO Standards ISO 3002 1982(E), 'Basic quantities in cutting and grinding'.
9. DIN 69718, Part 3, February 1977, 'Machine Tools, Centreless External Cylindrical Grinding Machines, Definitions and Terms'.
10. Subramanya Udupa, N.G., Shunmugam, M.S. and Radhakrishnan, V., 'Three dimensional geometric analysis of the plunge centreless grinding process', Proc. Instn. Mech. Engrs., Vol. 201, No. C5, 1987, pp 309-320.
11. Smits, C.A., 'In house seminar on grinding theory', The Torrington Company/Cincinnati Milacron Products Division, November 1987.

12. Stroud, K.A., 'Fourier Series and Harmonic Analysis', Stanley Thornes Ltd., 1984, pp 23-25.
13. Dagnall, H., 'Lets talk roundness', Rank Taylor Hobson Publications, List No. 600-5, 1976, pp 5-8.
14. Loxham, J., 'The potentialities of accurate measurement and automatic control in production engineering', The Production Engineer, pp 3-32, Dec. 1960.
15. British Standards BS 3730 Parts 1, 2 and 3 1982, 'Assessment of departures from roundness'.
16. British Standards BS 5773 Part 6: 1980, ISO 6193 - 1980(E), 'Metric needle roller bearings - Part 6 - Specification for tolerances of needle rollers', ISO title 'Roller bearings - Needle rollers - Tolerances'.
17. Murphy, T., Chatfield, H. and Pete, W.S., 'Temperature stability tests of roller diameter gauges', Torrington Internal Report, Oct. 1981, Unpublished.
18. Meis, F.U., Hoenscheid, W. and Koenig, W., 'Increasing the output of centreless throughfeed grinding', Report No. 2540, Aachen University, 1980.
19. Slonimski, W.I., 'Theorie und praxis des spitzenlosen schleifens', Veb Verlag Technik Berlin, 1956.
20. 'Centreless grinding - machine setting and correction of grinding errors', Lidkopings Mekaniska Verkstads Aktiebolag, Publication T1-8/E, December 1980.
21. Hashimoto, F., Kanai, A., Miyashita, M. and Okamura, K., 'High precision trueing method of regulating wheel and effect on grinding accuracy', Annals of the CIRP, Vol. 32, No. 1, 1983, pp 237-239.
22. 'Centreless grinding; Theory, principles, applications', Cincinnati Milacron, Publication No. G-758-6, 1979.
23. Willmore, J.I., Rowe, W.B. and Loxham, J., 'A note on the saw tooth pattern in centreless grinding', Dec. 1970, Unpublished.
24. Summerfield, P.H., 'An analysis of industrial centreless grinding practices', B.Sc. Project 1973, Unpublished, Department of production engineering, Lanchester Polytechnic.



25. Yokogawa, K., 'Einfluss der abricht-und schließbedingungen auf die rauheit und rundheit geschliffenen oberflächen', Werkstatt und Betrieb 107, 1974, pp 513.
26. Nakkeeran, P.R. and Radhakrishnan, V., 'Role of regulating wheel form errors on the quality of the workpiece in centreless grinding', ASME, PED-Vol. 39, 1989, pp 369-381.
27. 'Specifications and tests of metal cutting machine tools', Vols. 1 and 2, Section A, Proc. UMIST Conference, 19-20 February 1970, Untitled.
28. Bhateja, C.P. and Pine, R.D., 'The rotational accuracy characteristics of the preloaded hollow roller bearing', Trans. of the ASME, Paper A9-64, Vol. 103, 1981.
29. Rowe, W.B., 'Research into the mechanics of centreless grinding', Precision Engineering, pp 75-84, 1979.
30. Maden, H. and Fletcher, N.P., 'The influence of diamond geometry on the stability of the grinding wheel dressing process', MTDR, Vol. 19, 1978, pp 607-614.
31. Kaliszer, H. and Trmal, G., 'Effect of dressing upon the grinding performance', CIRP Technical reports, pp 541-544, 1976/77.
32. Bhateja, C.P. and Lindsay, R.P., 'The importance of abrasive grinding wheel hardness control for the productivity of production grinding operations', Annals of the CIRP, Vol. 30, No. 1, 1981, pp 247-249.
33. Rowe, W.B., Spraggett, S. and Gill, R., 'Improvements in centreless grinding machine design', Annals of the CIRP, Vol. 36, No.1, 1987, pp 207-210.
34. 'Grinding Performance - Record, Analyse, Predict', Cincinnati Milacron Publication.
35. 'The language of rubber', Elastomer Chemicals Dept., E.I. du Pont de Nemours and Co.(inc), 1963, Untitled.
36. McCalmont, P., 'Machine evaluation', Cincinnati Milacron, 1987, Unpublished.

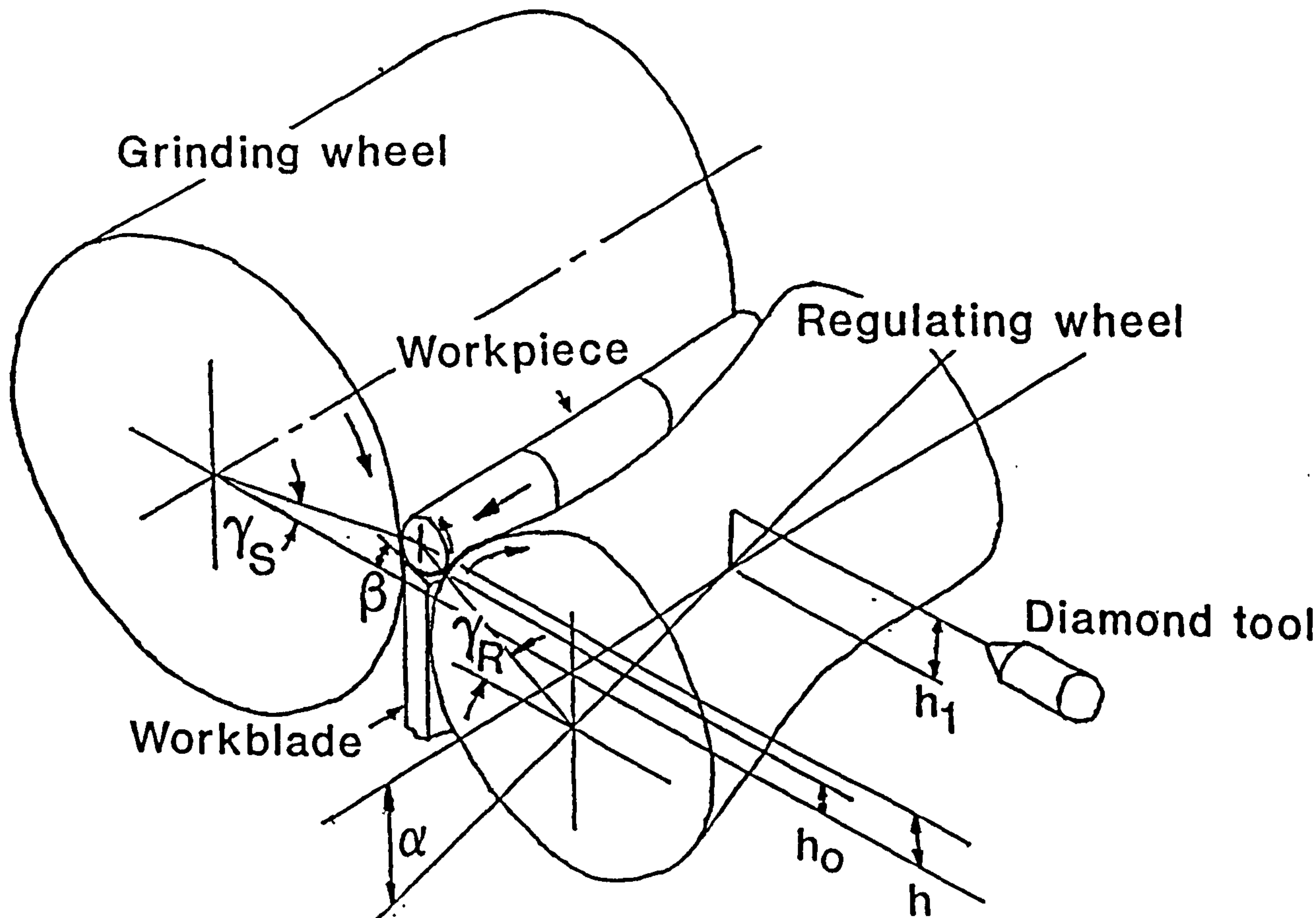
37. Subramanya Udupa, N.G., Shunmugam, M.S. and Radhakrishnan, V., 'Workpiece movement in centreless grinding and its influence on the quality of the ground part', Journal of Engineering for Industry, May 1988, Vol. 110, pp 179-186.
38. Subramanya Udupa, N.G., Shunmugam, M.S. and Radhakrishnan, V., 'Frictional behaviour and its influence on quality in centreless grinding', Wear, 118, 1987, pp 147-160.
39. Rowe, W.B., Barash, M.M. and Koenigsberger, F., 'Some roundness characteristics of centreless grinding', Int. J. Mach. Tool Des. Res., Vol. 5, pp 203-215, Pergamon Press 1965.
40. Becker, E.A., 'Forces and roundness errors in centreless plunge grinding', PhD. Thesis, Aachen, 1965.
41. Furukawa, Y., Miyashita, M. and Shiozaki, S., 'Chatter vibration in centreless grinding', JSME Bulletin, Vol. 13, No. 64, 1970, pp 1274-1283.
42. Miyashita, M., Hashimoto, F. and Kanai, A., 'Diagram for selecting chatter free conditions of centreless grinding', Annals of the CIRP, Vol. 31, No. 1, 1982, pp 221-223.
43. Chien, A.Y., 'The rounding off theory of centreless grinding', Int. J. Mach. Tool Des. Res., Vol. 21, 1981, pp 49-55.
44. Frost, M. and Fursdon, P.M.T., 'Towards optimum centreless grinding', ASME, PED-Vol. 16, 1985, pp 313-328.
45. Frost, M., Horton, B.J. and Tidd, J.L., 'Lobing control in centreless grinding', SME Paper MR88-610, 1988.
46. Subramanya Udupa, N.G., Shunmugam, M.S. and Radhakrishnan, V., 'Influence of workpiece position on roundness error and surface finish in centreless grinding', Int. Mach. Tools Manufact., Vol. 27, No. 1, 1987, pp 77-89.
47. Subramanya Udupa, N.G., Shunmugam, M.S. and Radhakrishnan, V., 'Optimising the workpiece position in centreless grinding by roundness profile analysis', Precision Engineering, Vol. 9, No. 1, 1987, pp 23-30.



48. Spragget, S. and Rowe, W.B., 'Stiffness requirements of the centreless grinding process', Joint Int. Prod. Res. Conf., Leicester Poly., 1983.
49. Schreitmuller, H., 'Kinematic analysis of the practical application of centreless high performance grinding', PhD. Thesis, Aachen, 1971.
50. Meis, F.U., 'Geometric and kinematic basics for centreless throughfeed grinding', PhD. Thesis, Aachen, 1980.

## FIGURES.

Figure 1. The throughfeed centreless grinding system.



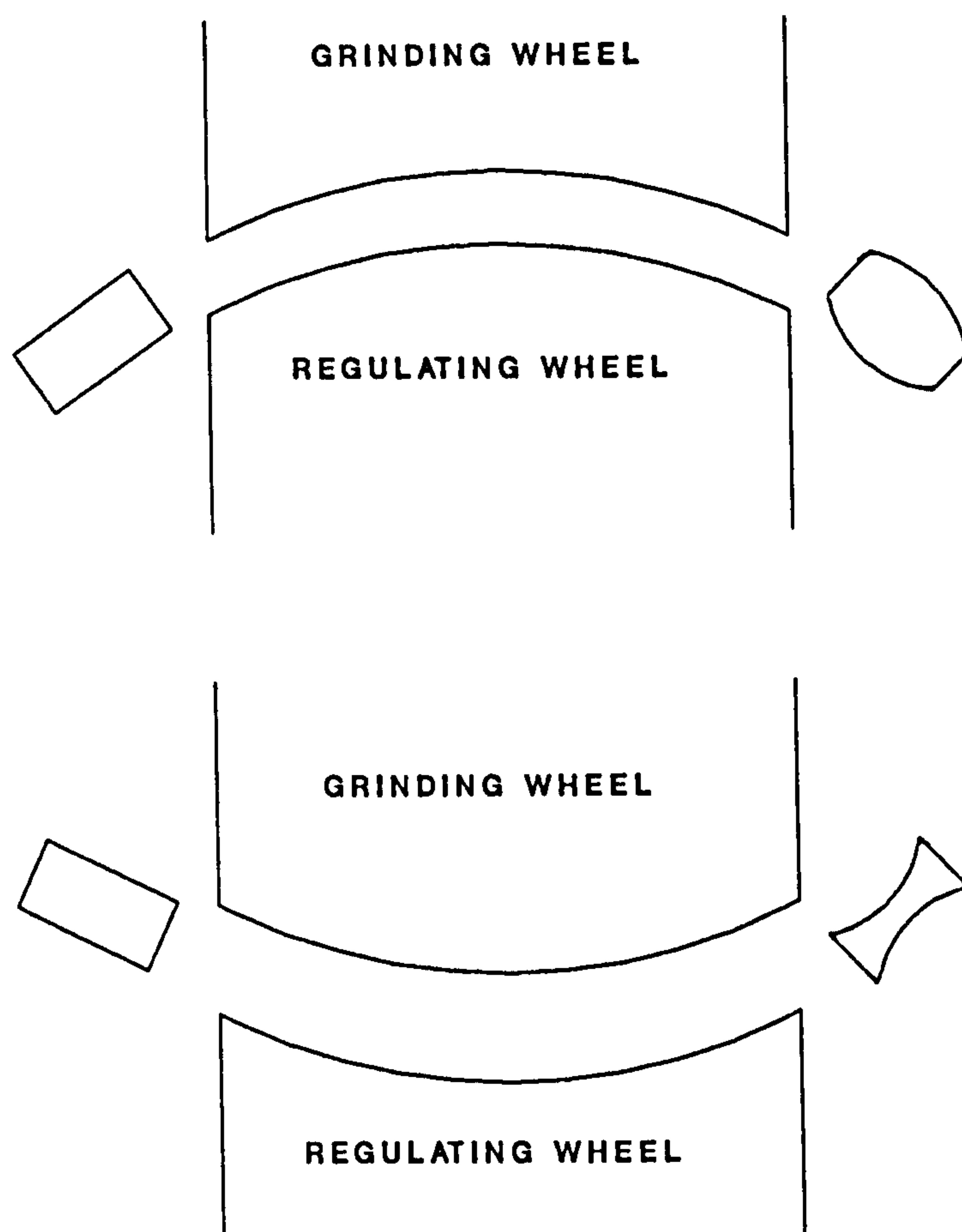
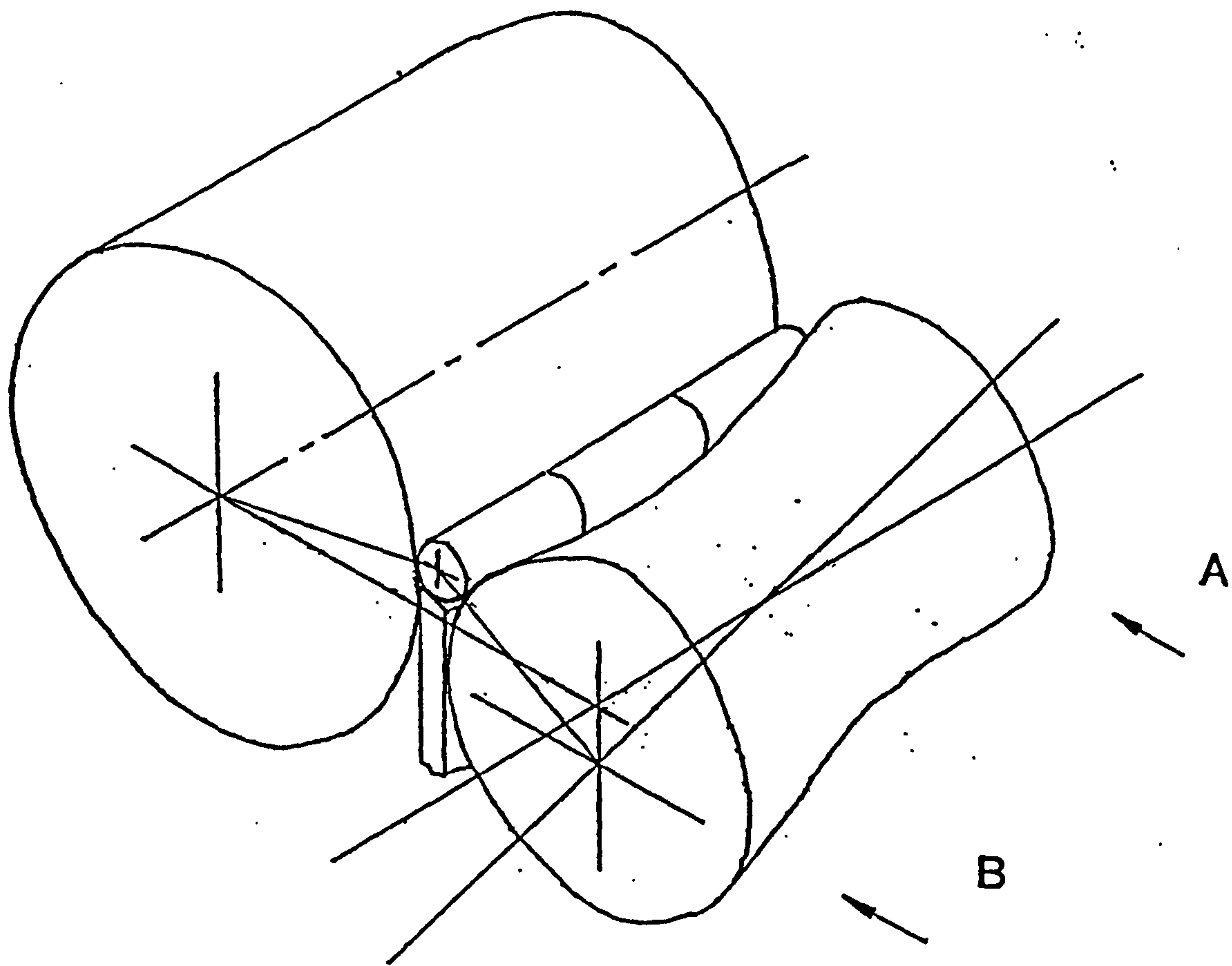


Figure 2. Effect of grinding gap geometry on workpiece axial form.

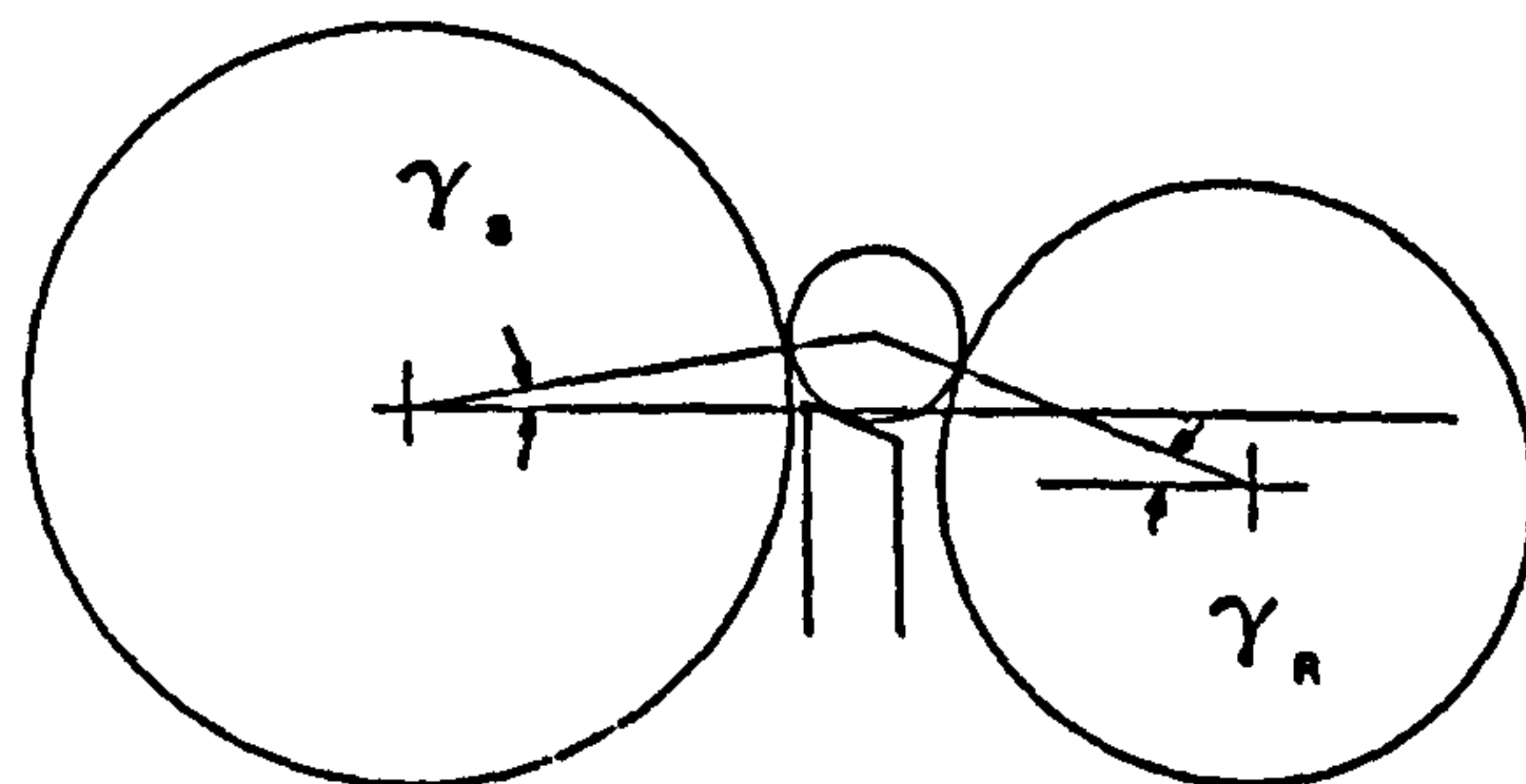
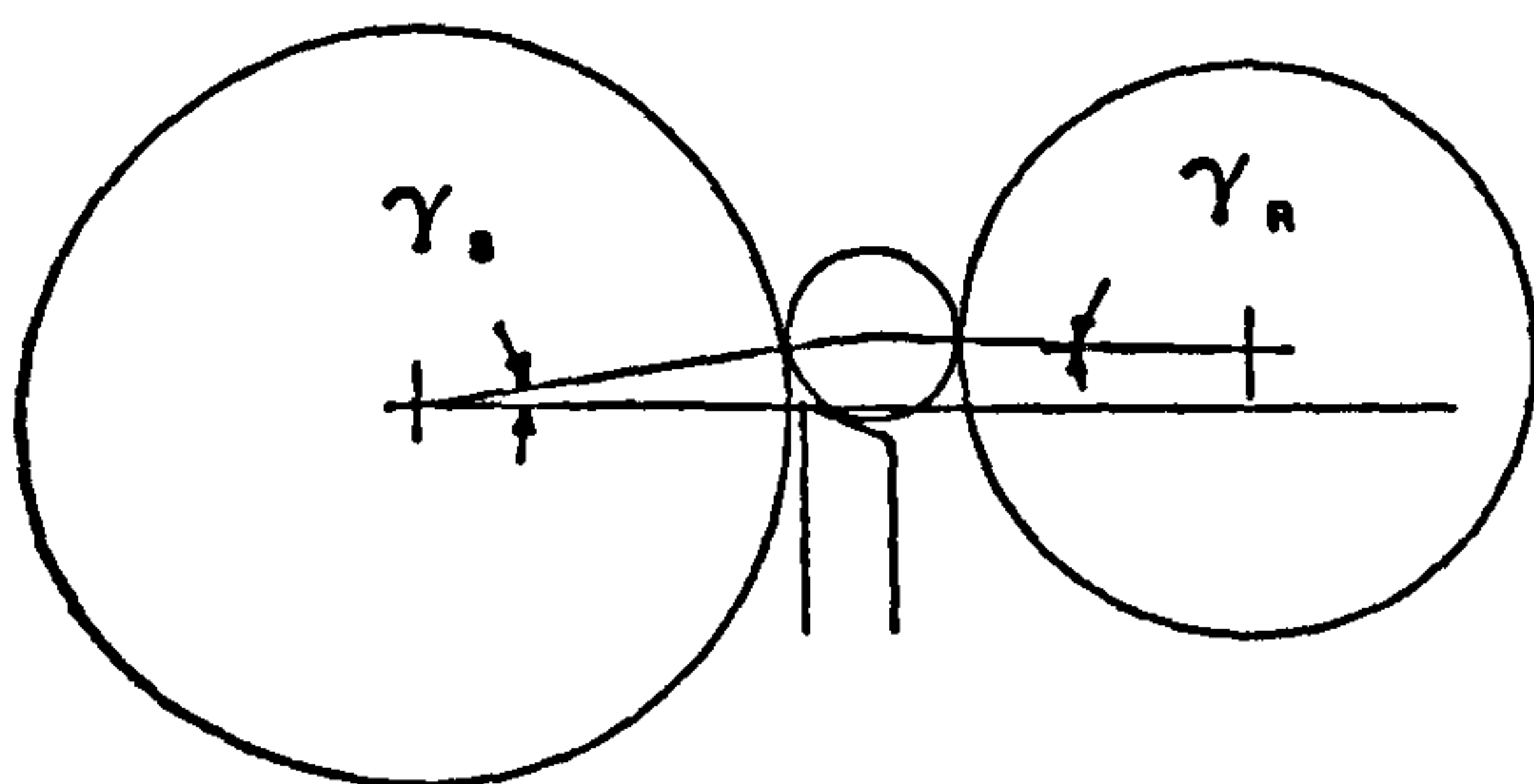


Figure 3. Variation in throat angle in throughfeed centreless grinding.



View A

View B



$\gamma_s = \text{Constant}$

$\gamma_R = \text{Variable}$

Figure 4. Regulating wheel housing pivot point in relation to regulating wheel centre - 'below offset' effect.

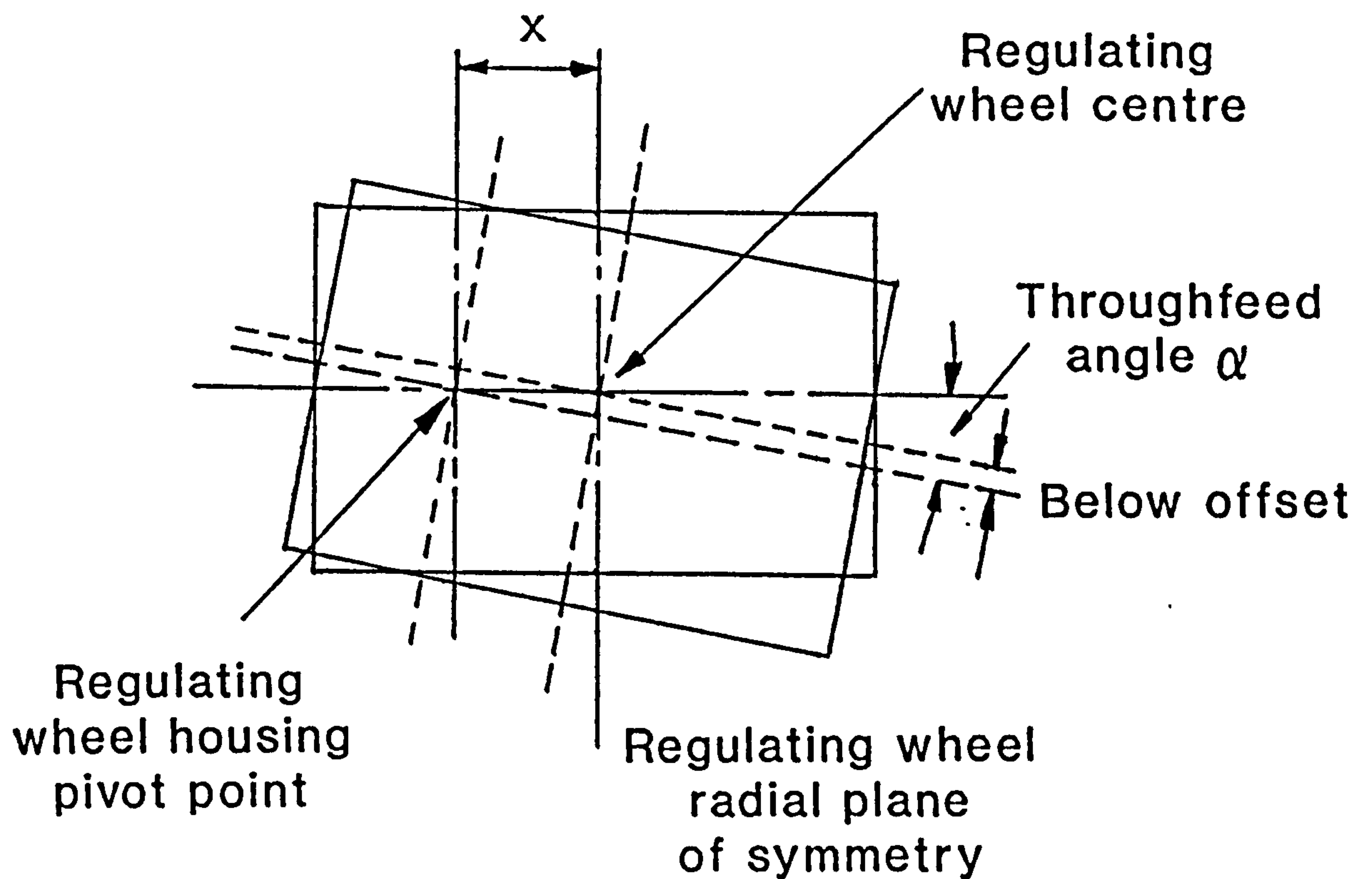








**Figure 6. Plot of consecutive workpiece size variation.**

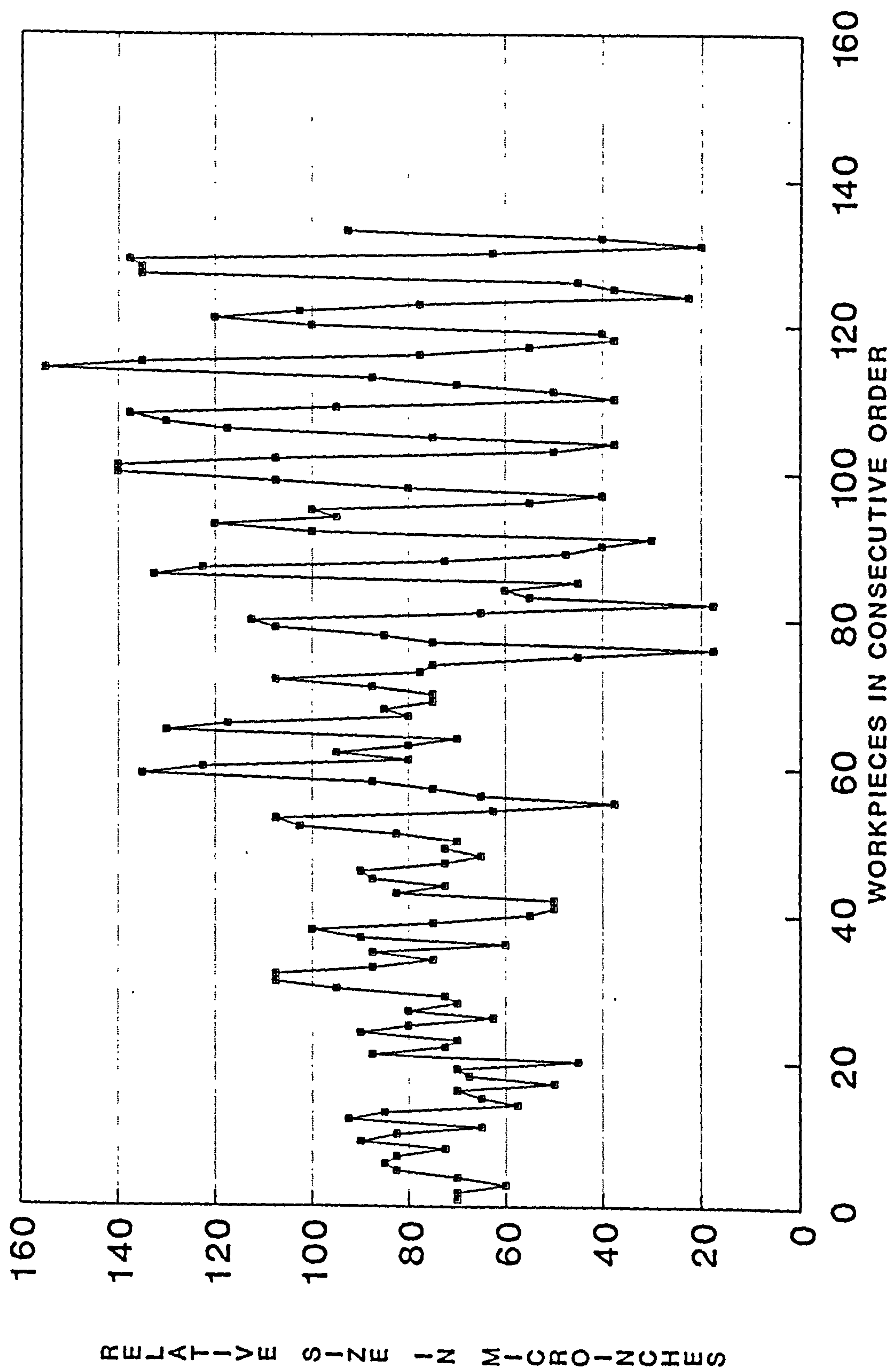
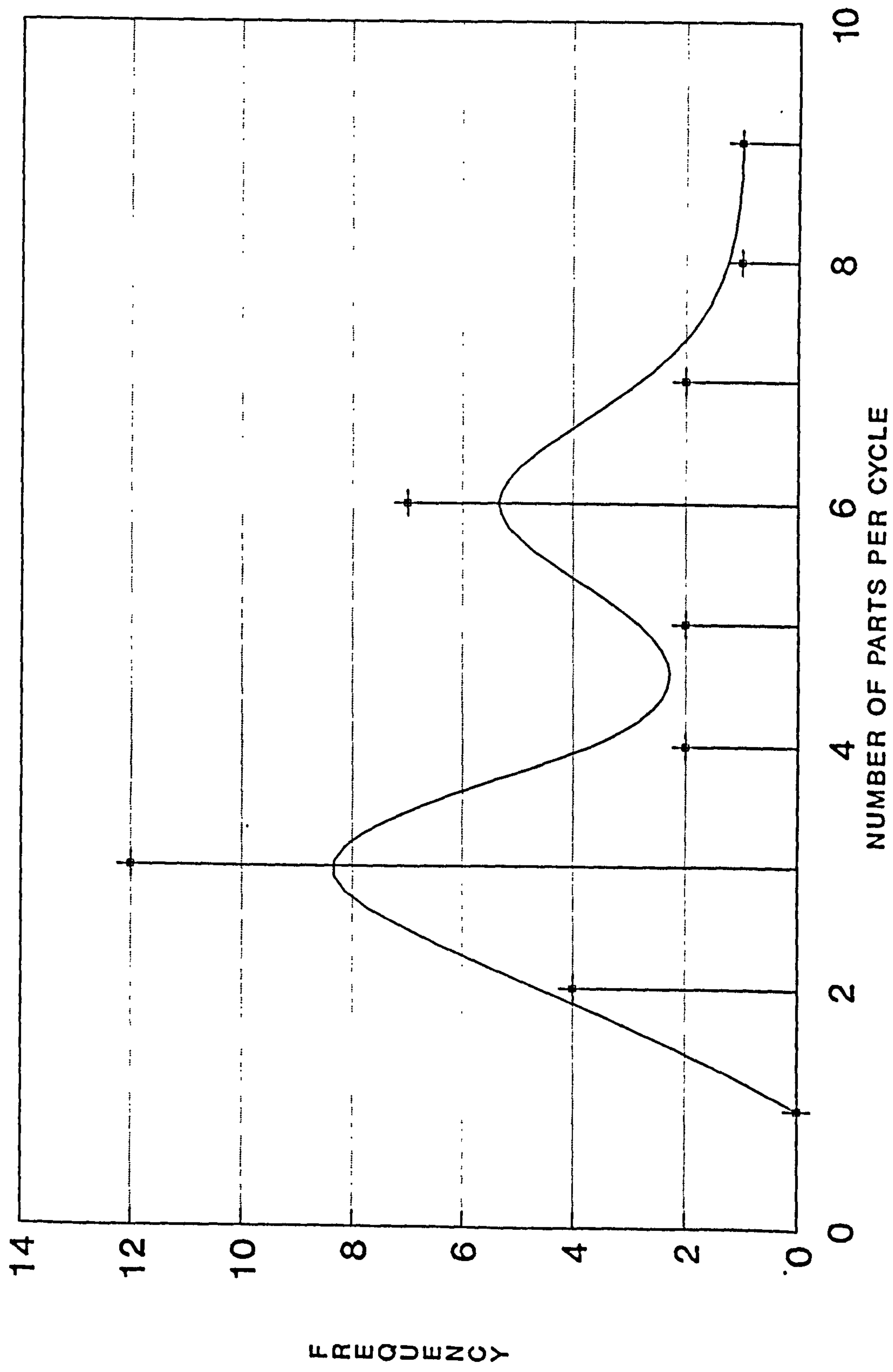


Figure 7. Plot of number of consecutive workpieces per size variation cycle versus frequency of occurrence.



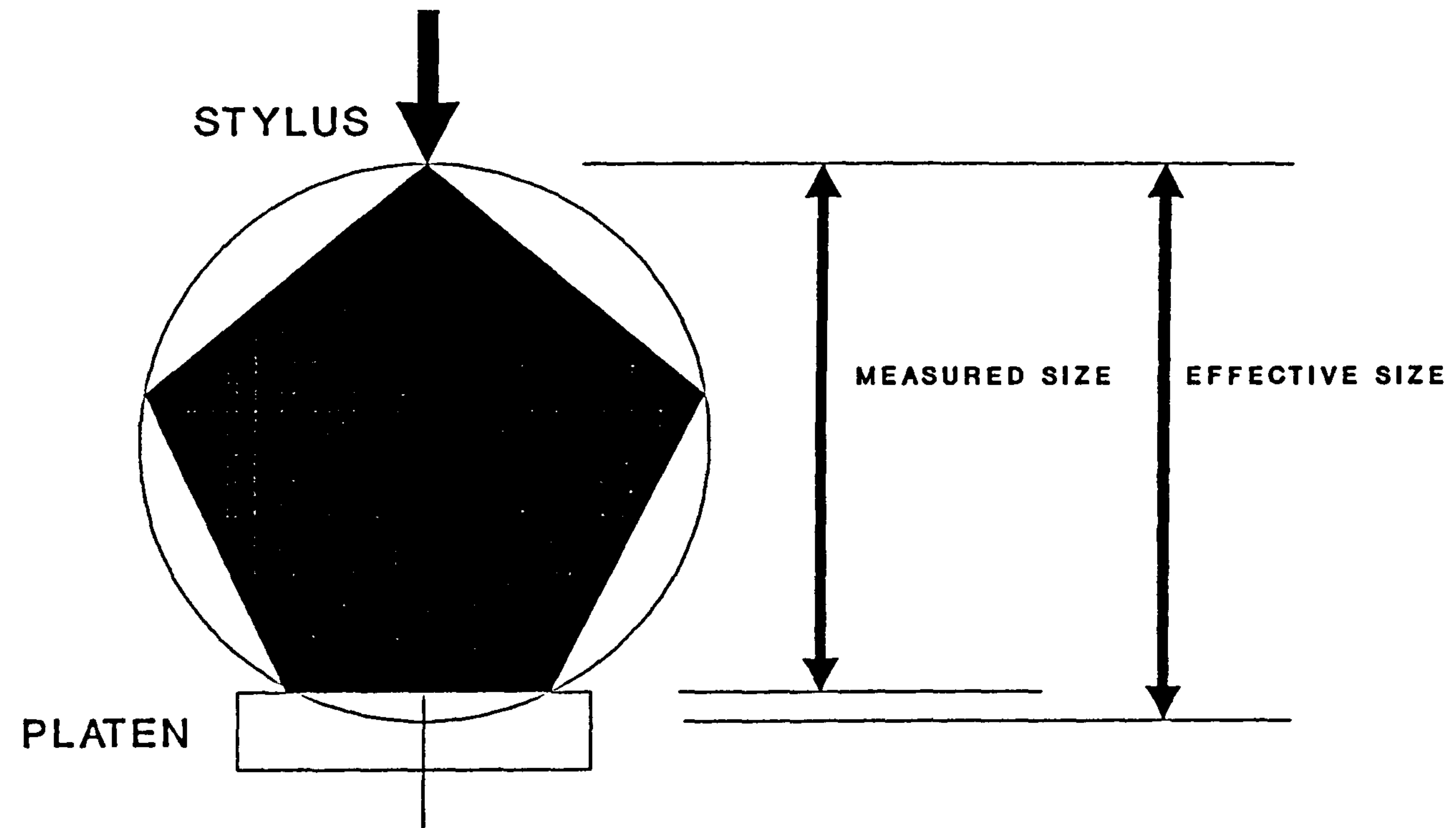


Figure 8. Measurement of an iso-diametric shape (5 lobed).

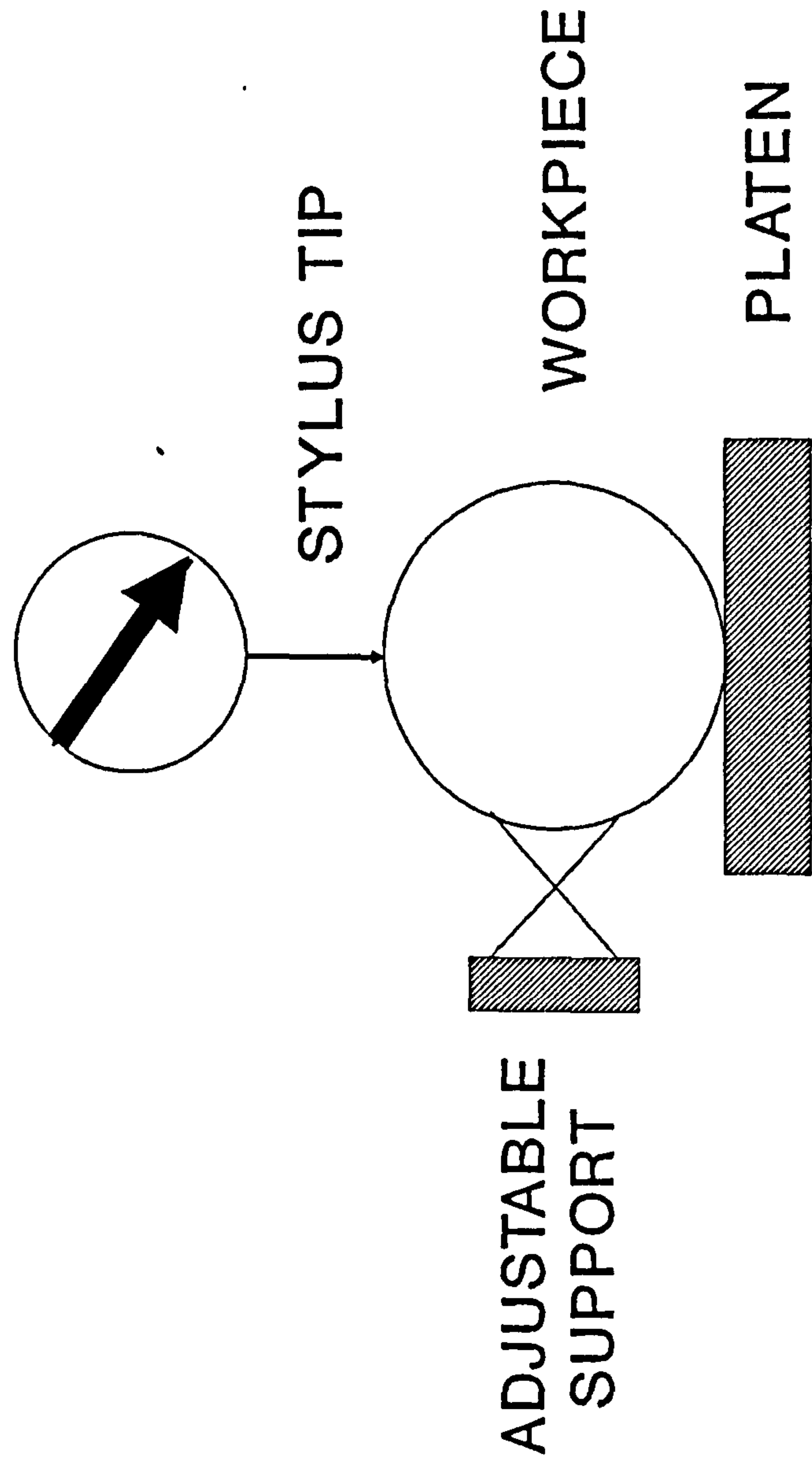


Figure 9. Two-point measurement.



Figure 10. Taylors Principle and iso-diametric workpieces (after Loxham).

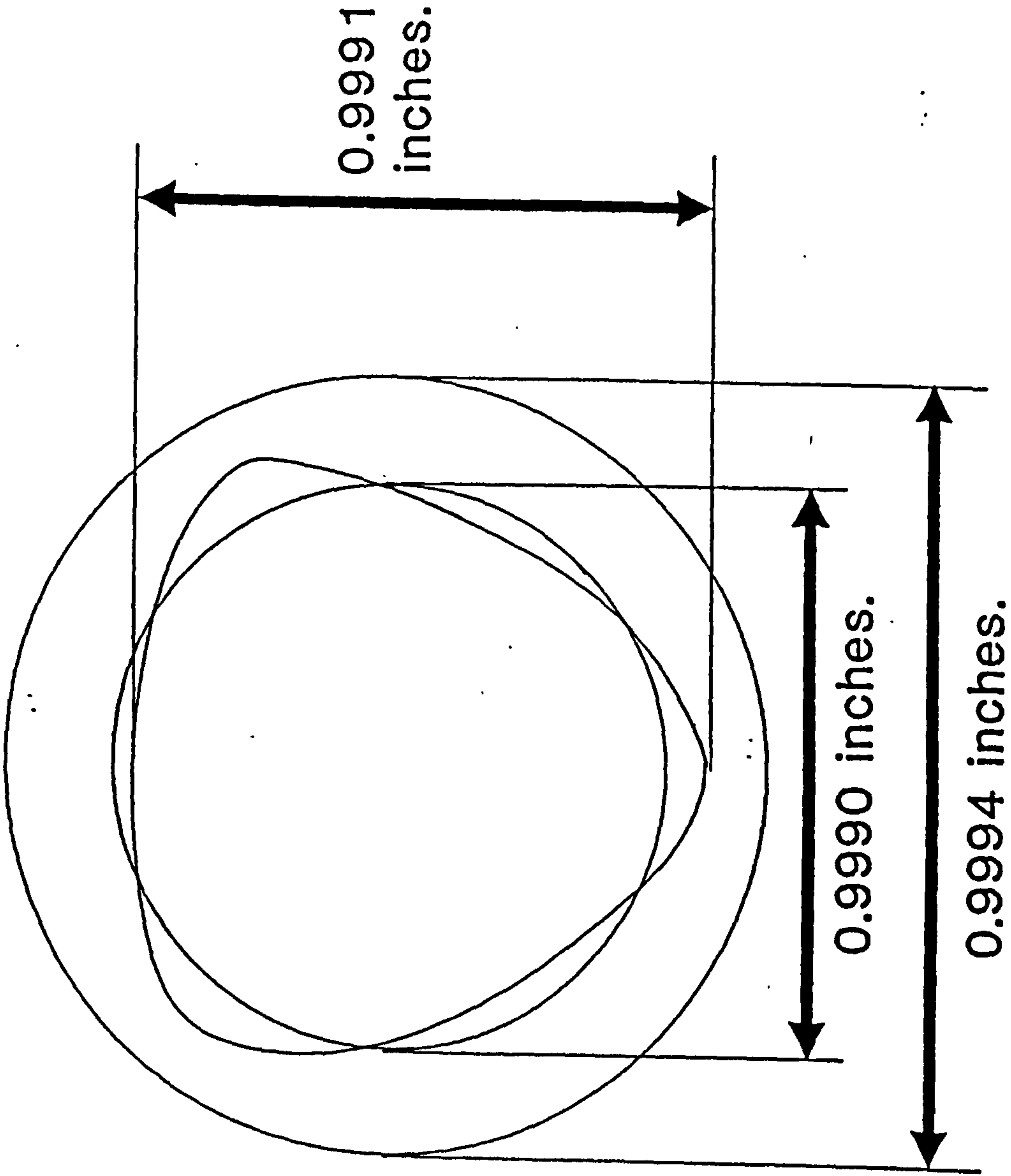


Figure 11. Operator variability -  
Operator 1 versus Operator 2.

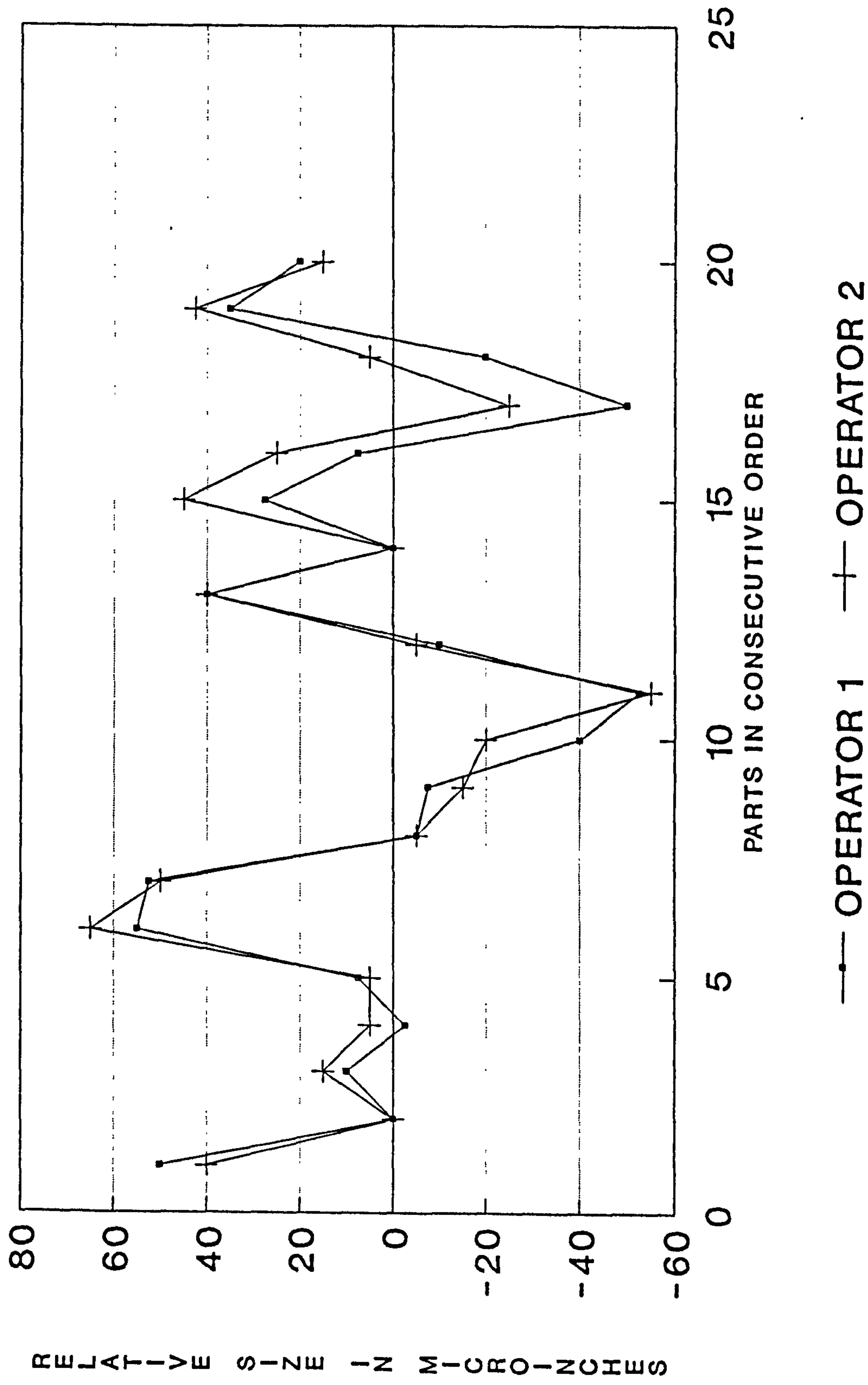


Figure 12. Operator variability -  
Operator 1 versus Operator 3.

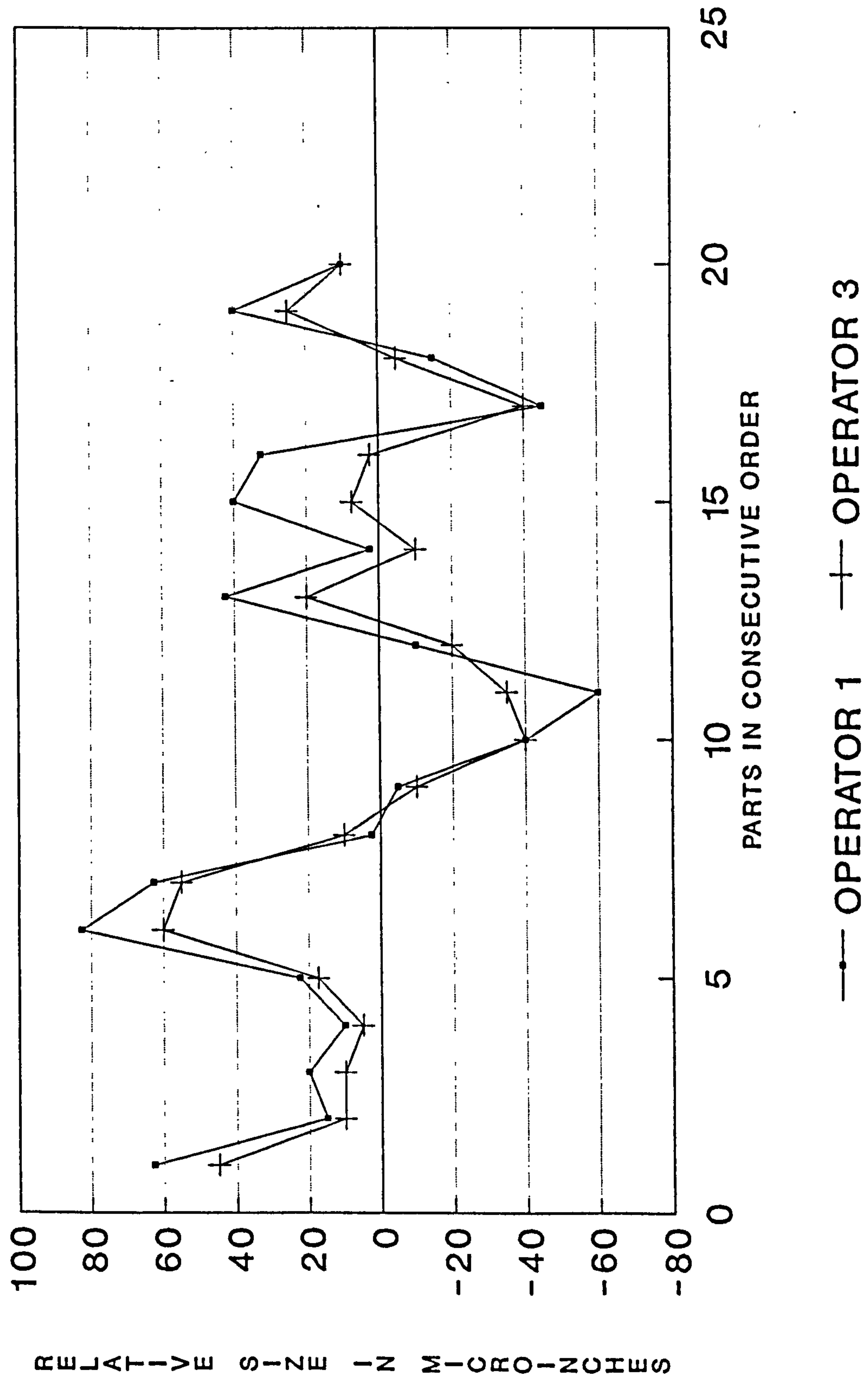


Figure 13. Within workpiece size variation.

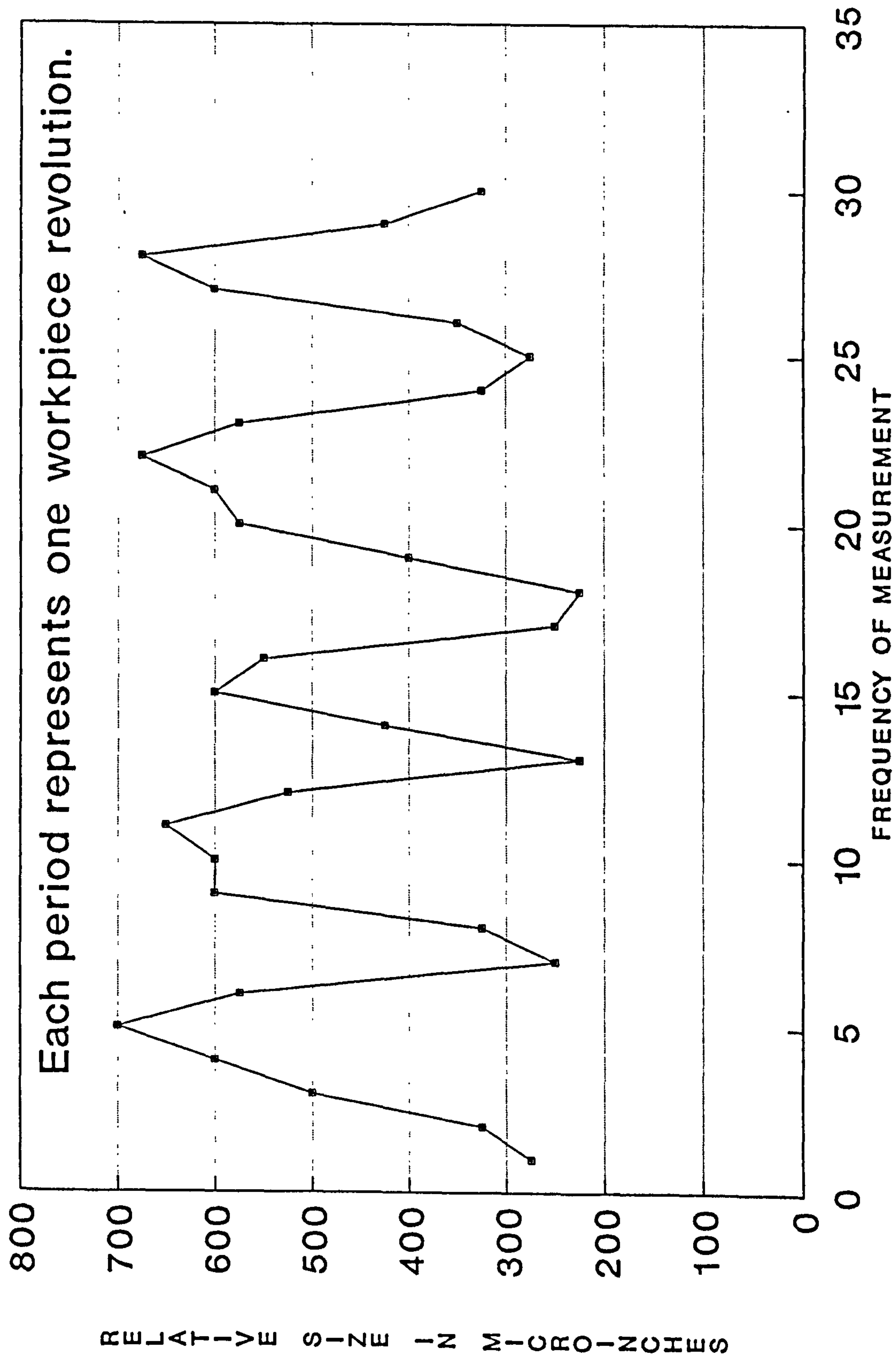




Figure 14. Creation of the shape of the regulating wheel for different height positions (after Meis).

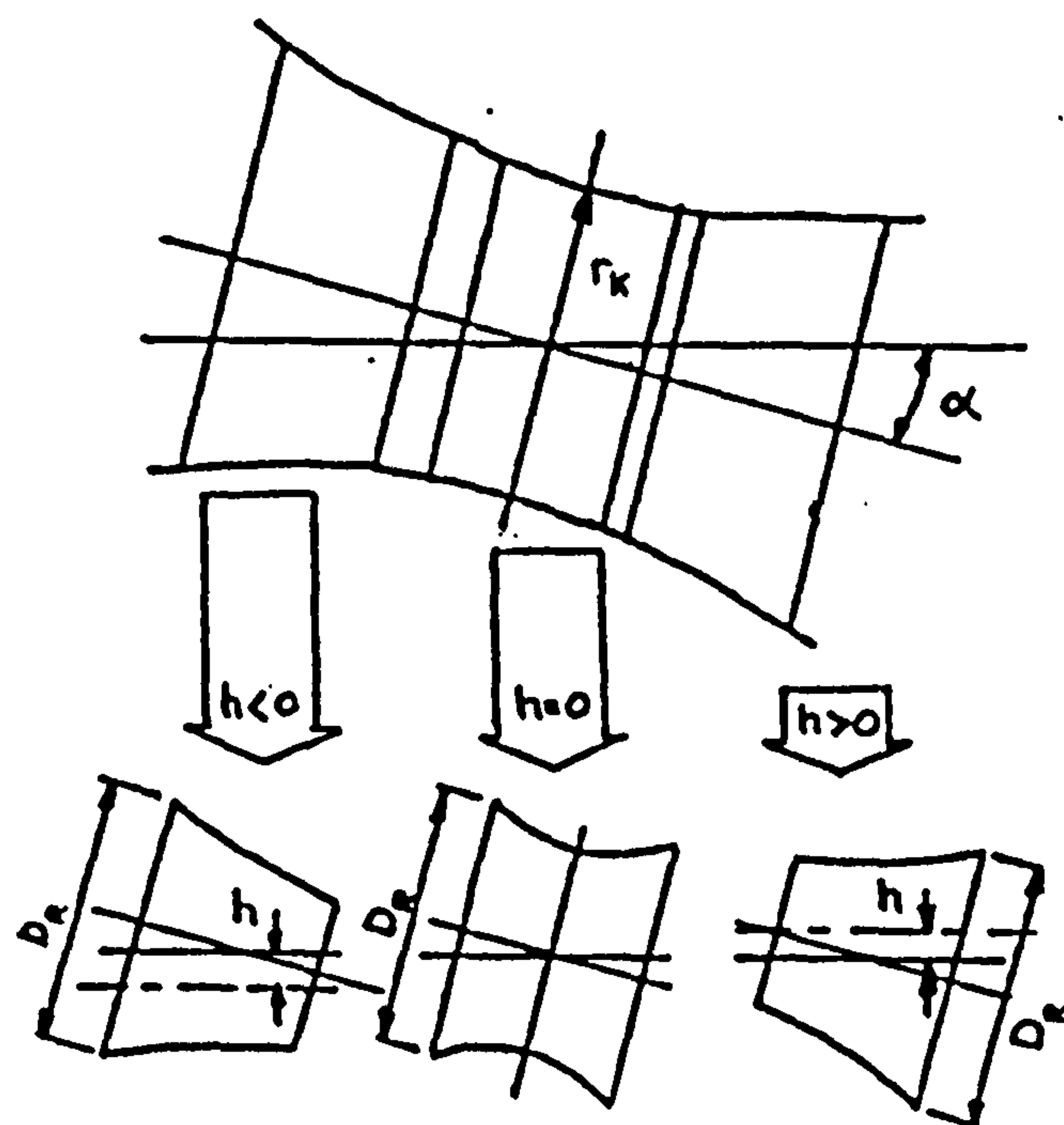
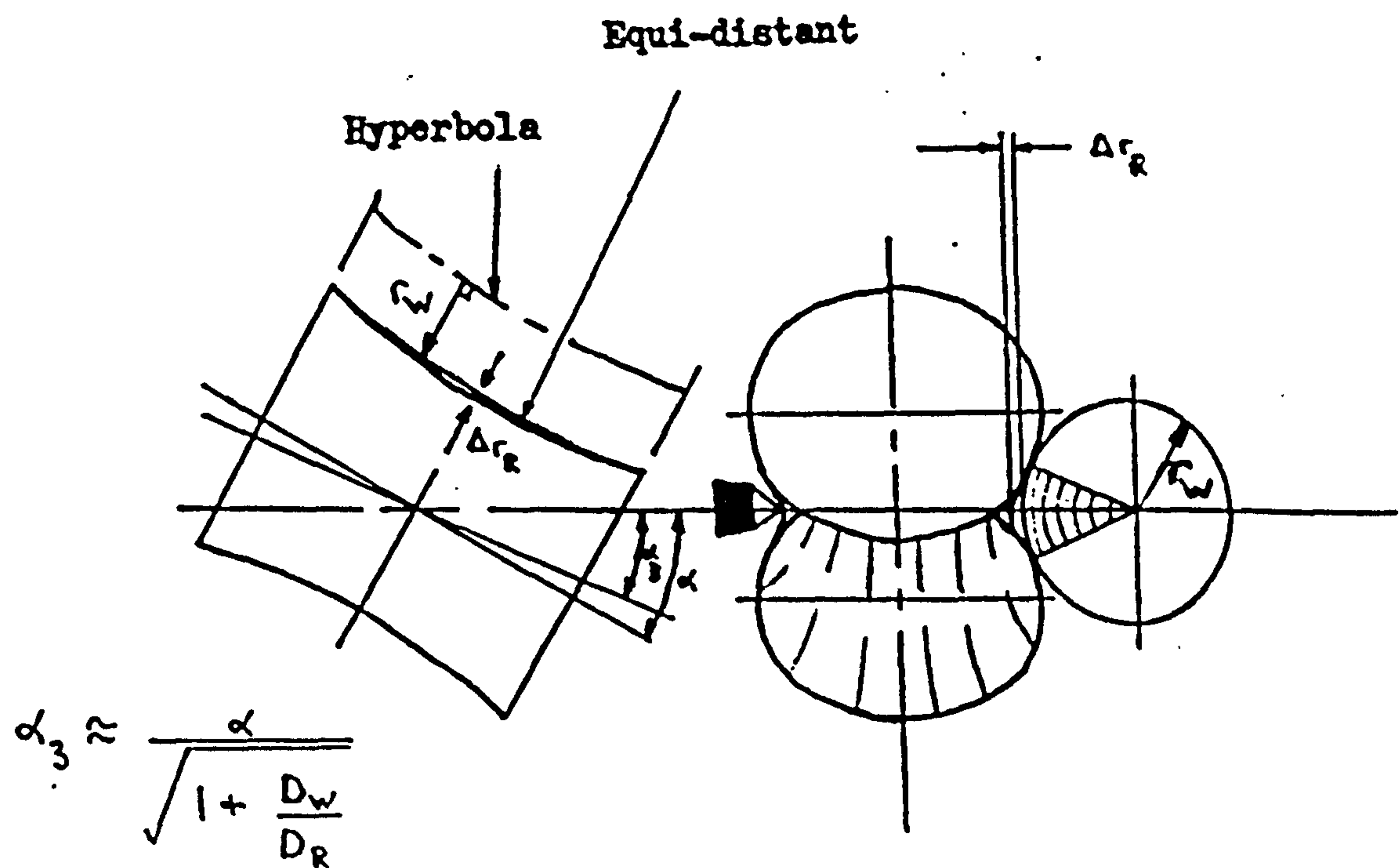
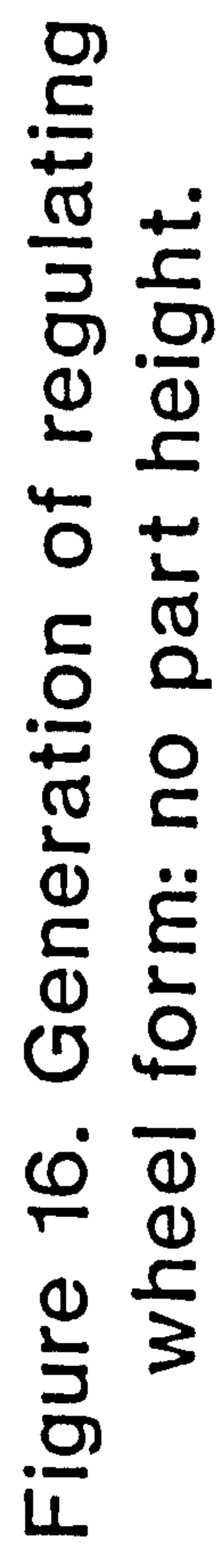


Figure 15. Relationship between workpiece diameter and regulating wheel shape (after Meis).





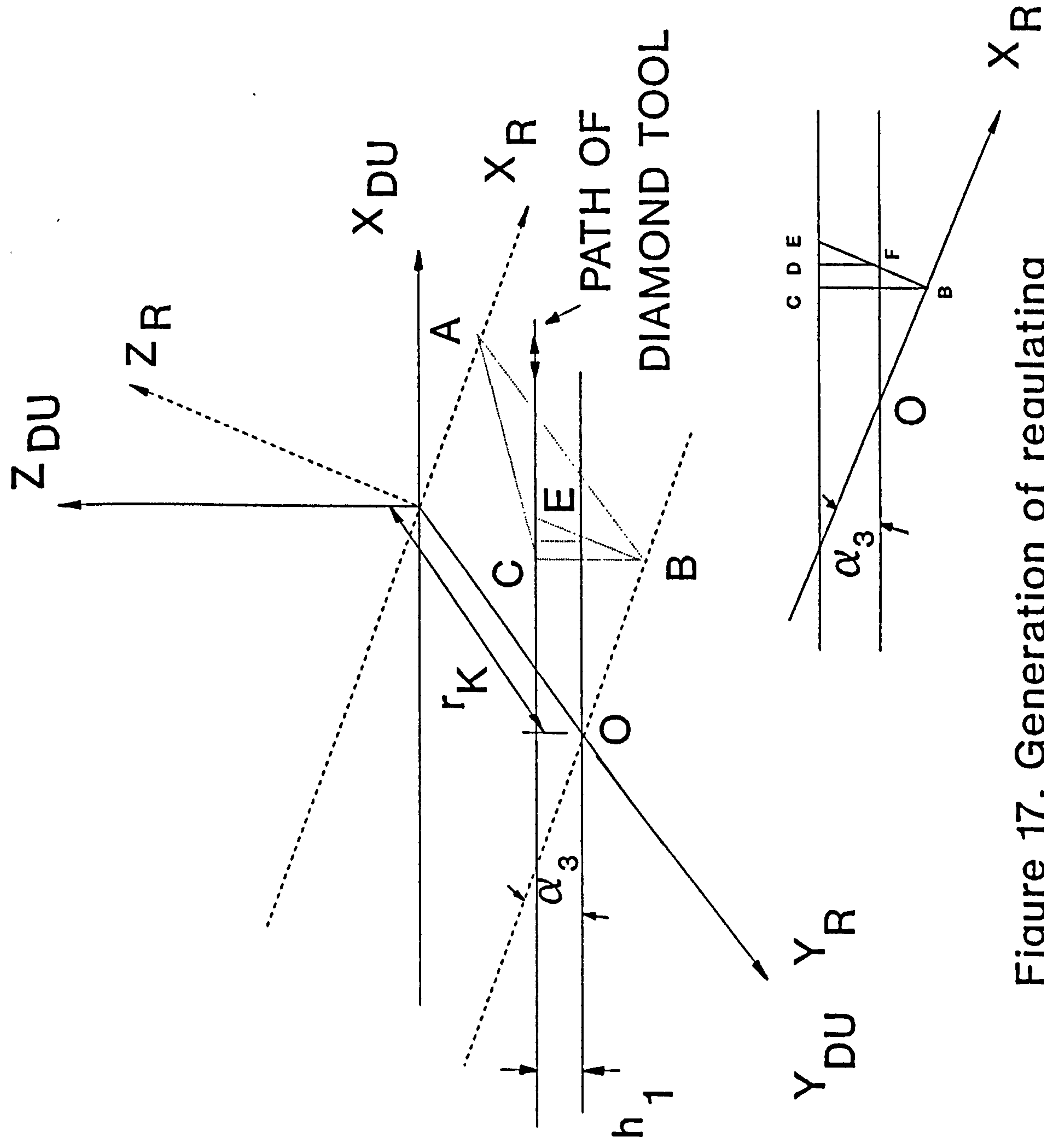


Figure 17. Generation of regulating wheel form: with part height.



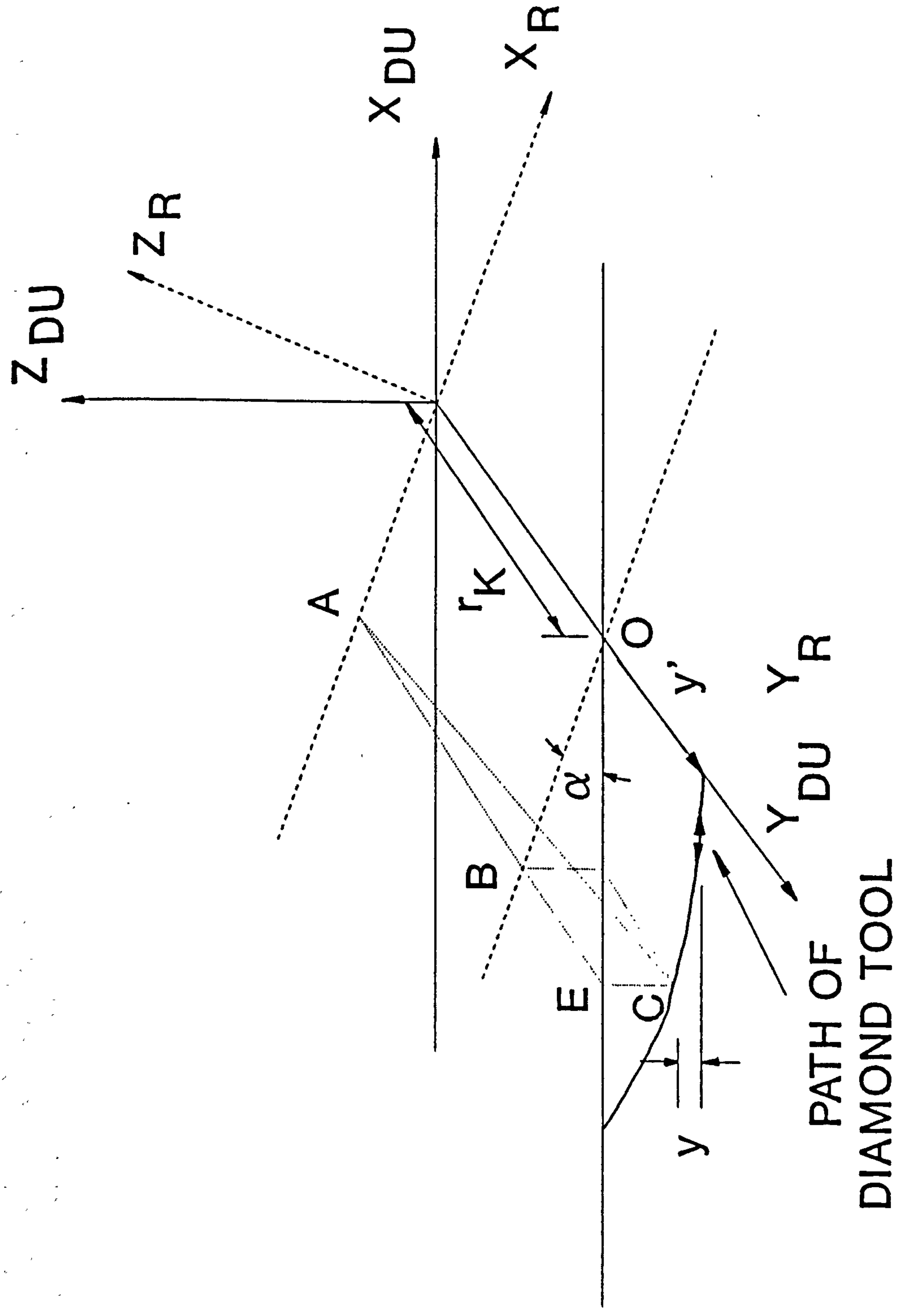


Figure 18. Generation of regulating wheel form when using dresser profile bar.

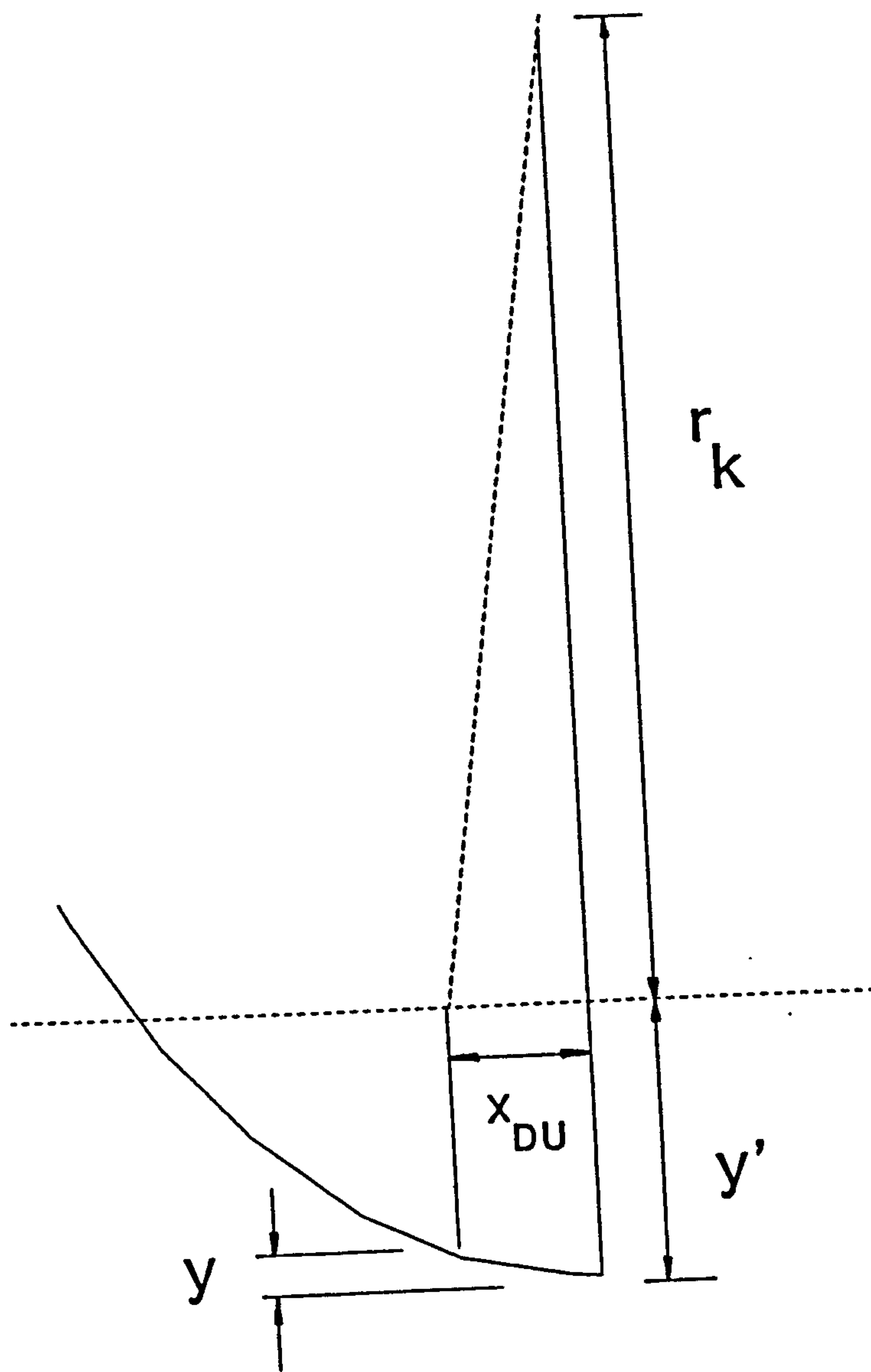


Figure 19. Regulating wheel dresser profile bar.

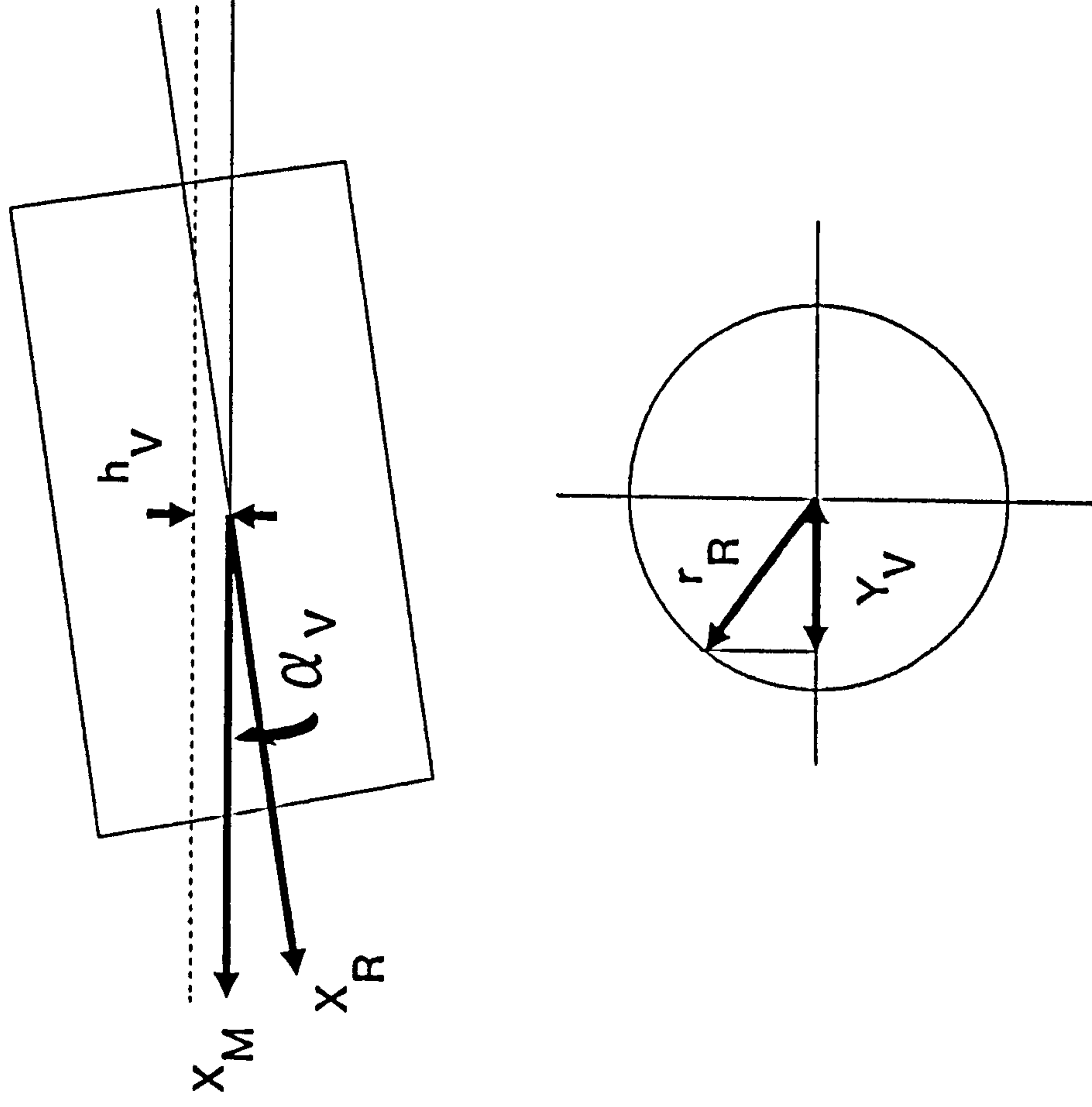


Figure 20. Regulating wheel viewing plane.

Figure 21. Ground regulating wheel axial profile - theoretical shape.

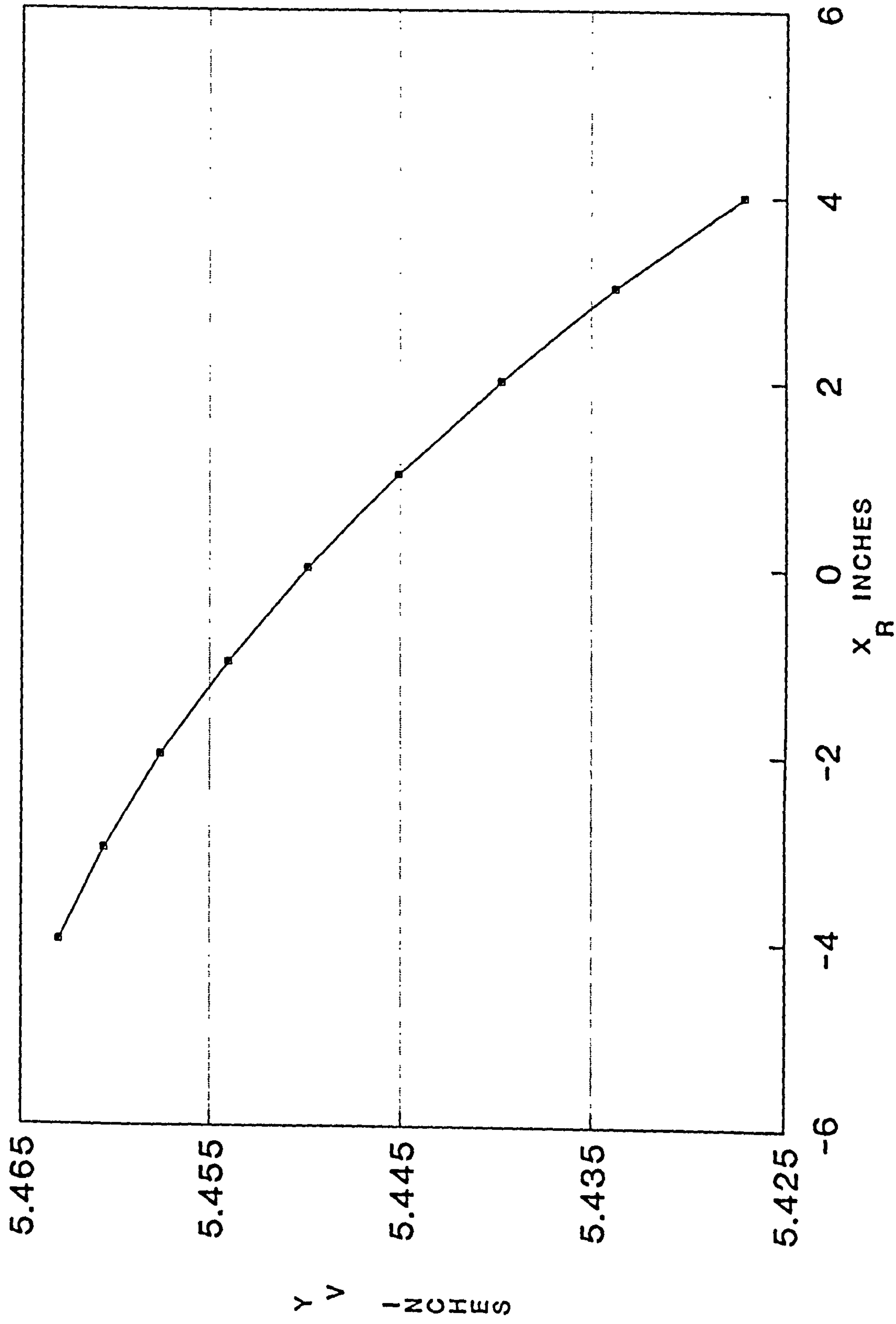




Figure 22. Ground regulating wheel axial  
profile - actual shape.

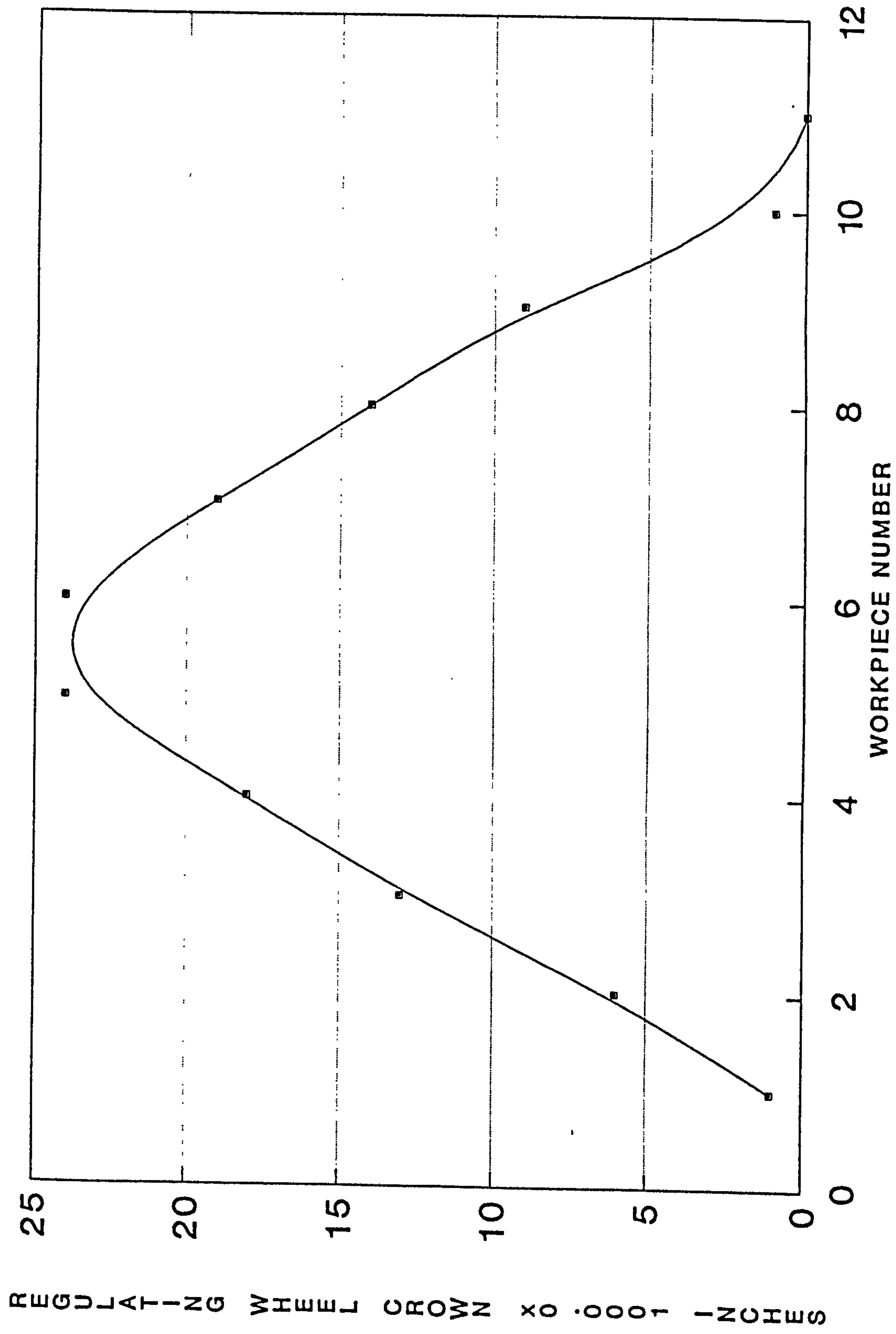


Figure 23. Effect of changing throughfeed angle on regulating wheel axial profile.

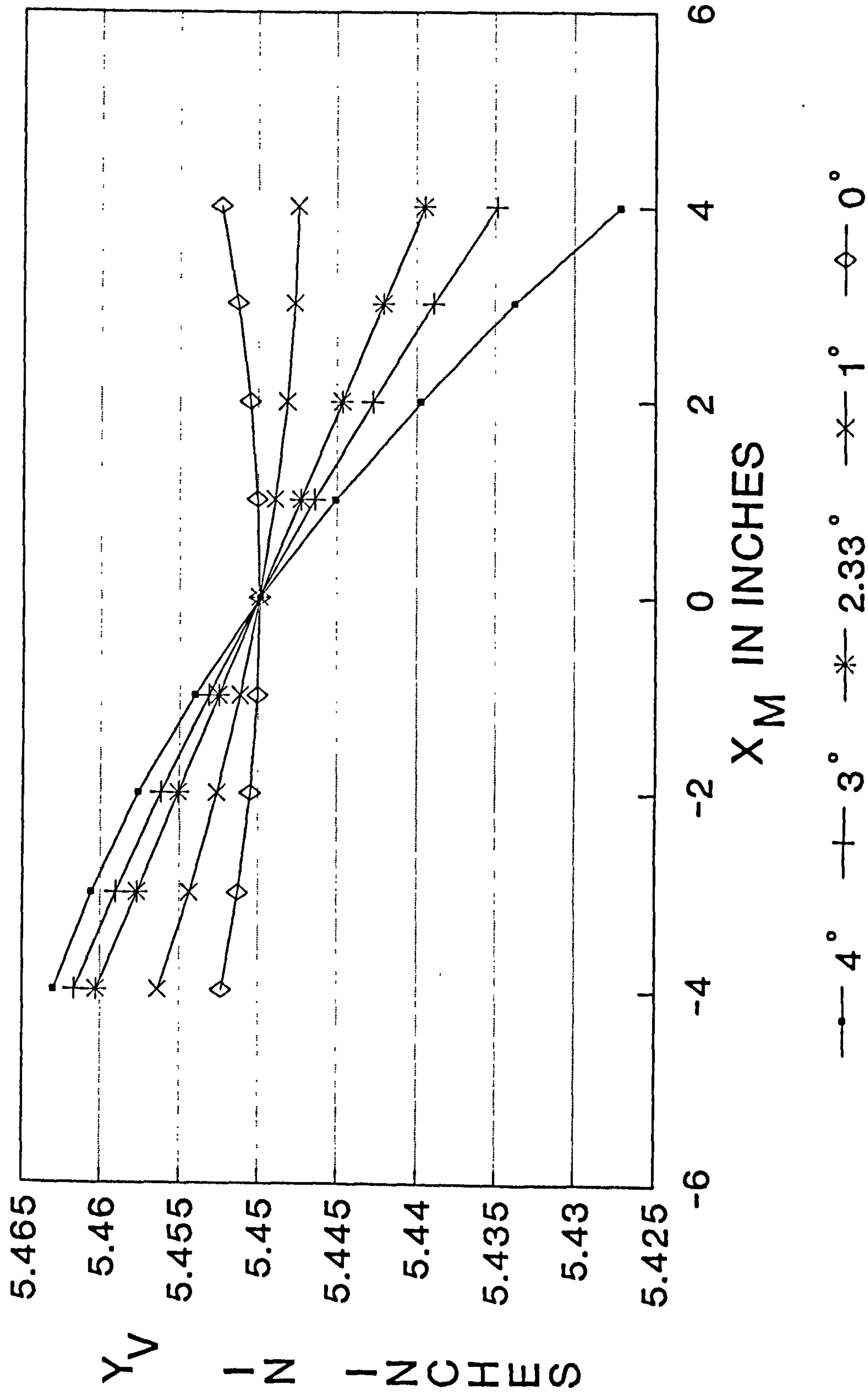


Figure 24. Effect of changing  
truing angle on regulating wheel  
axial profile.

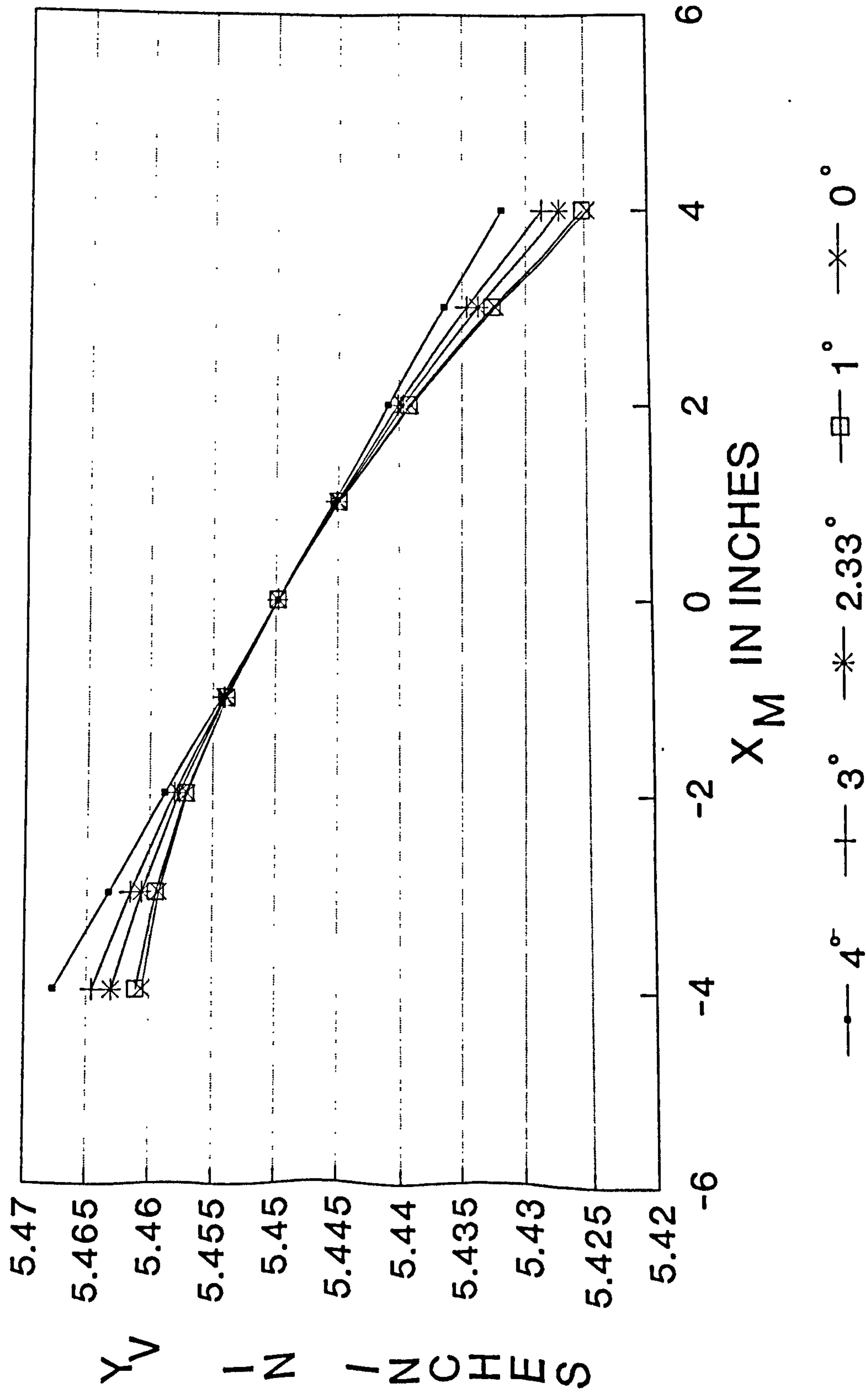
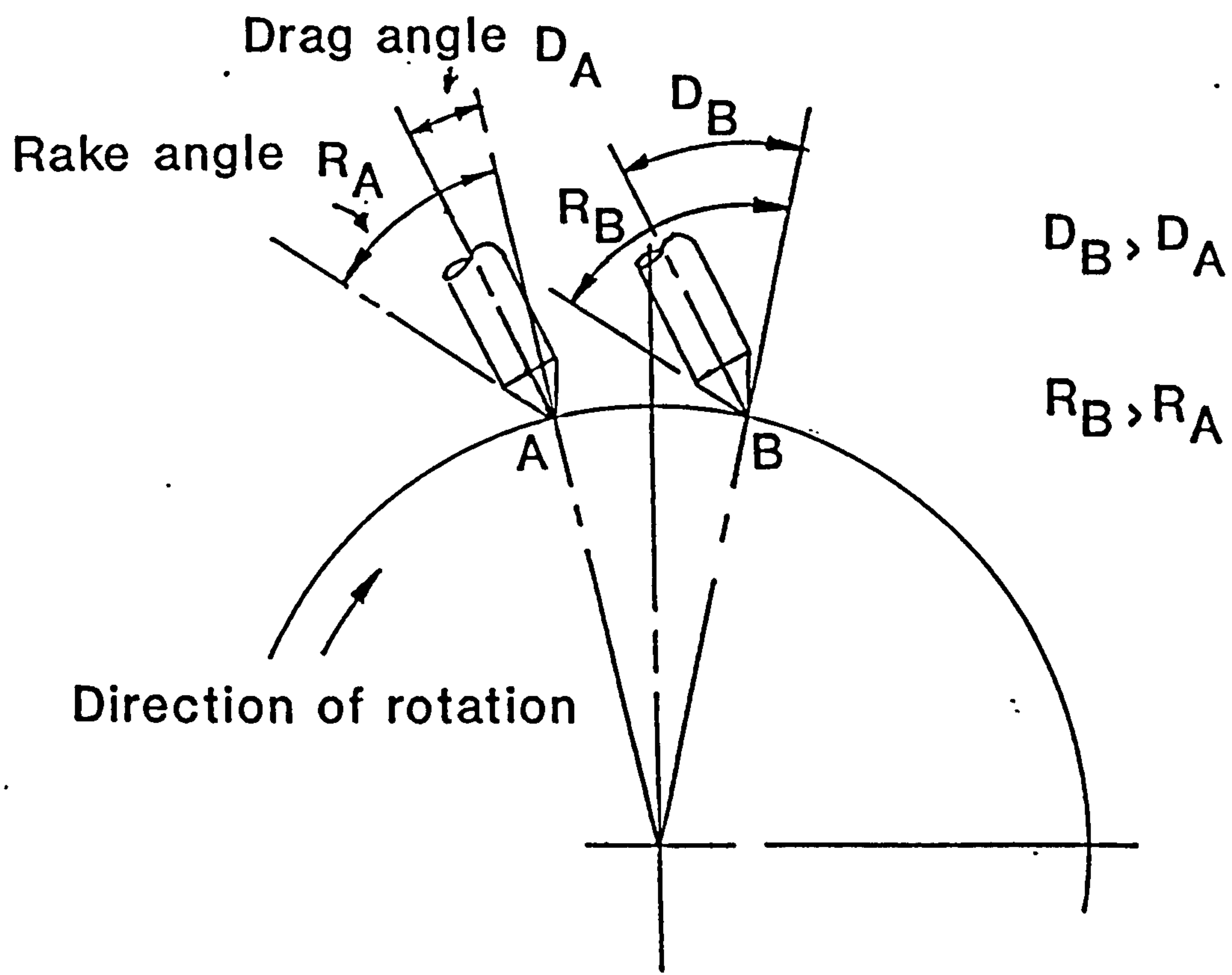


Figure 25. Change in rake and drag angles during regulating wheel trueing.



Path taken by  
trueing tool

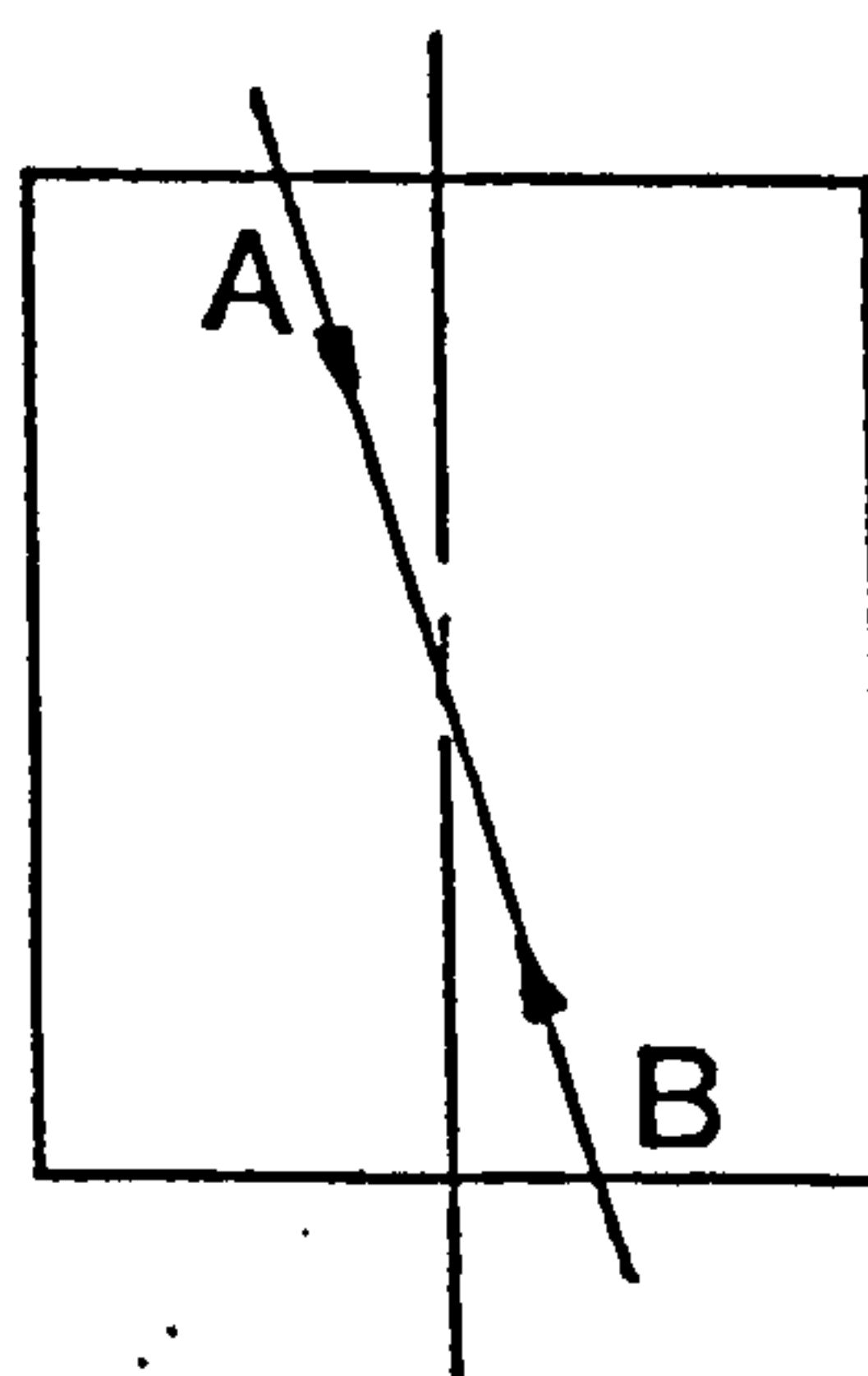




Figure 26. Regulating wheel surface runout (outboard) and outboard bearing temperature against time.

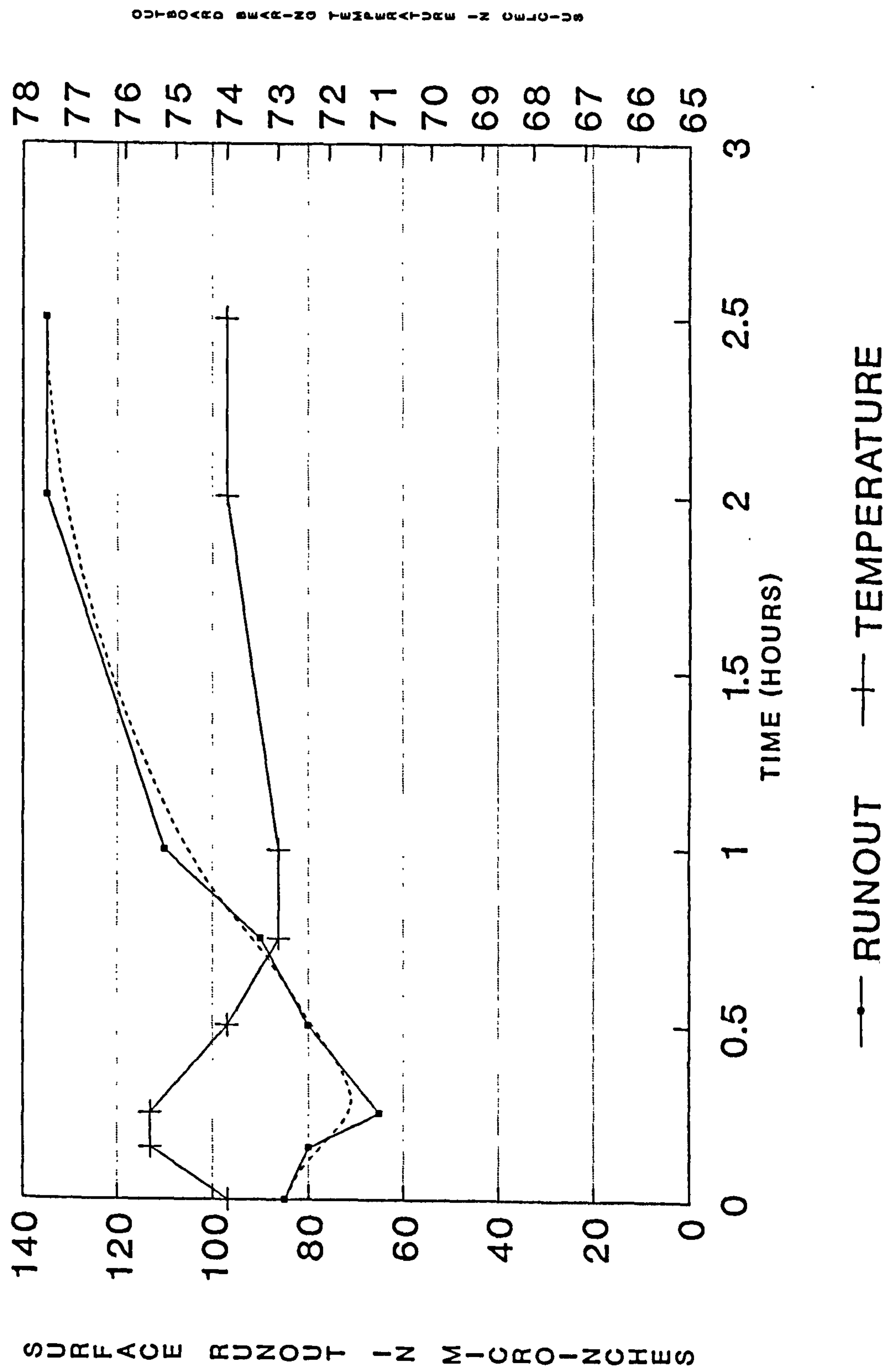


Figure 27. Regulating wheel surface runout (outboard) against time.

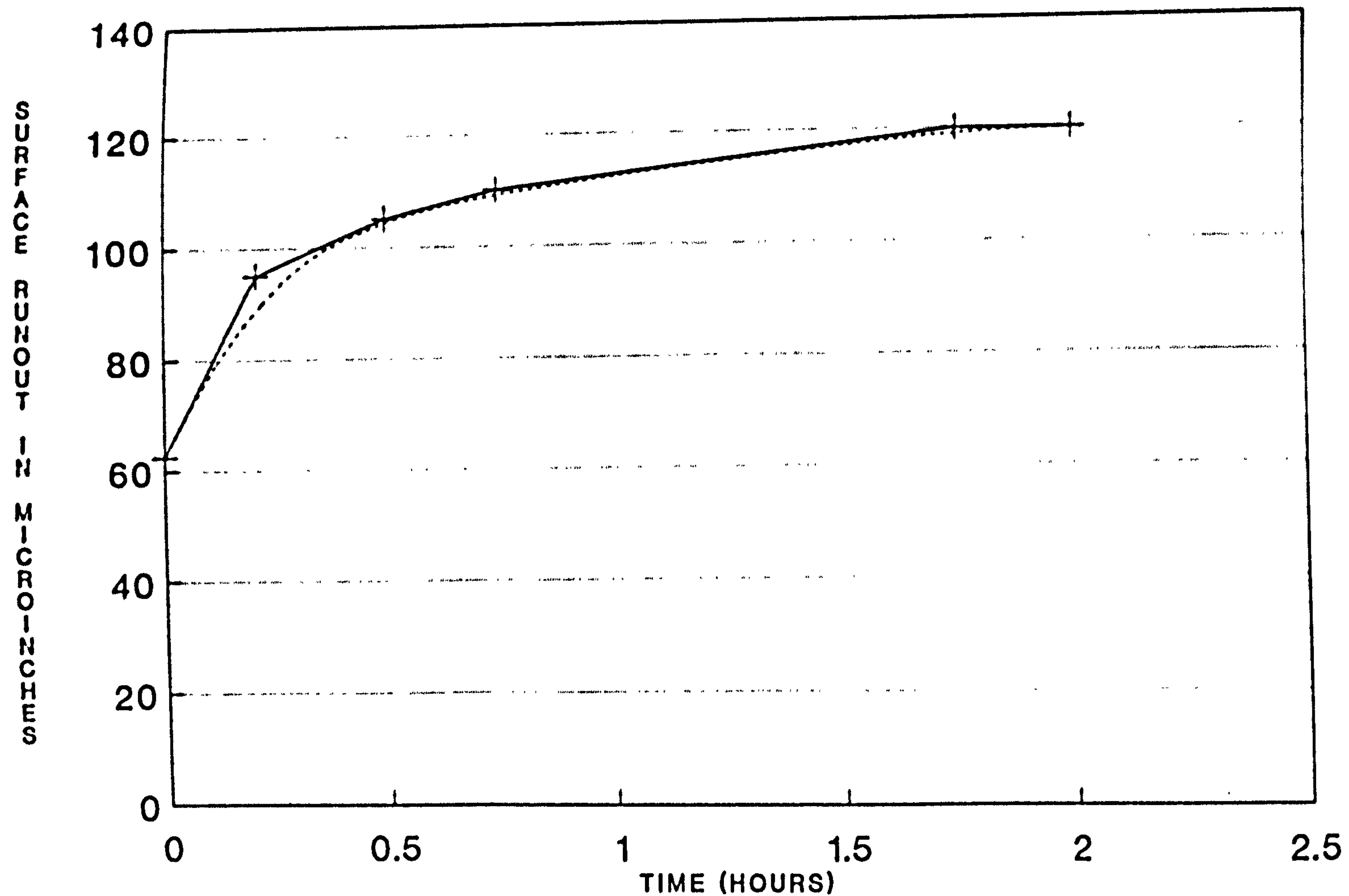


Figure 28. Effect of a three minute feed  
stoppage.

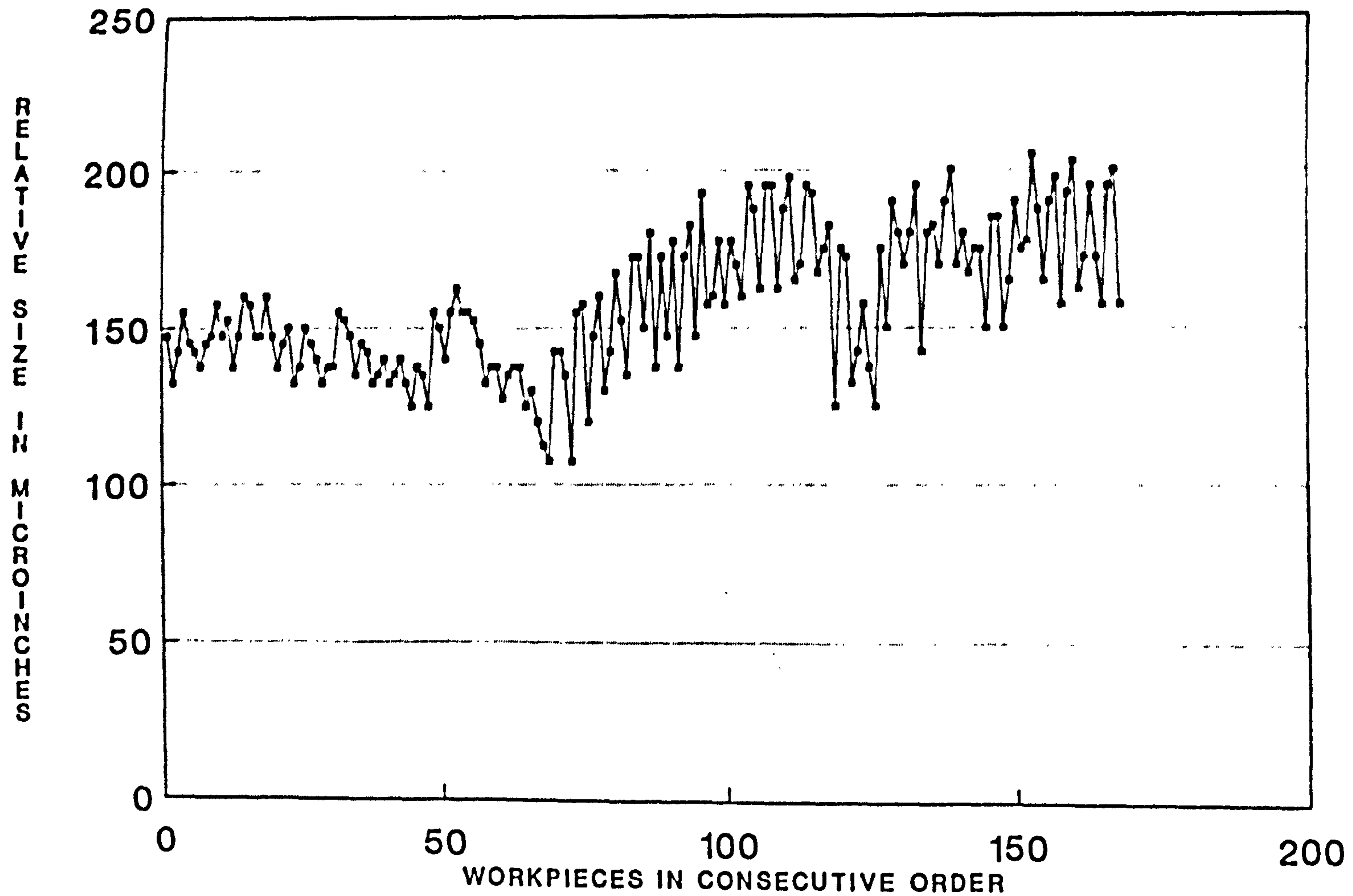


Figure 29. Effect of a momentary feed  
stoppage.

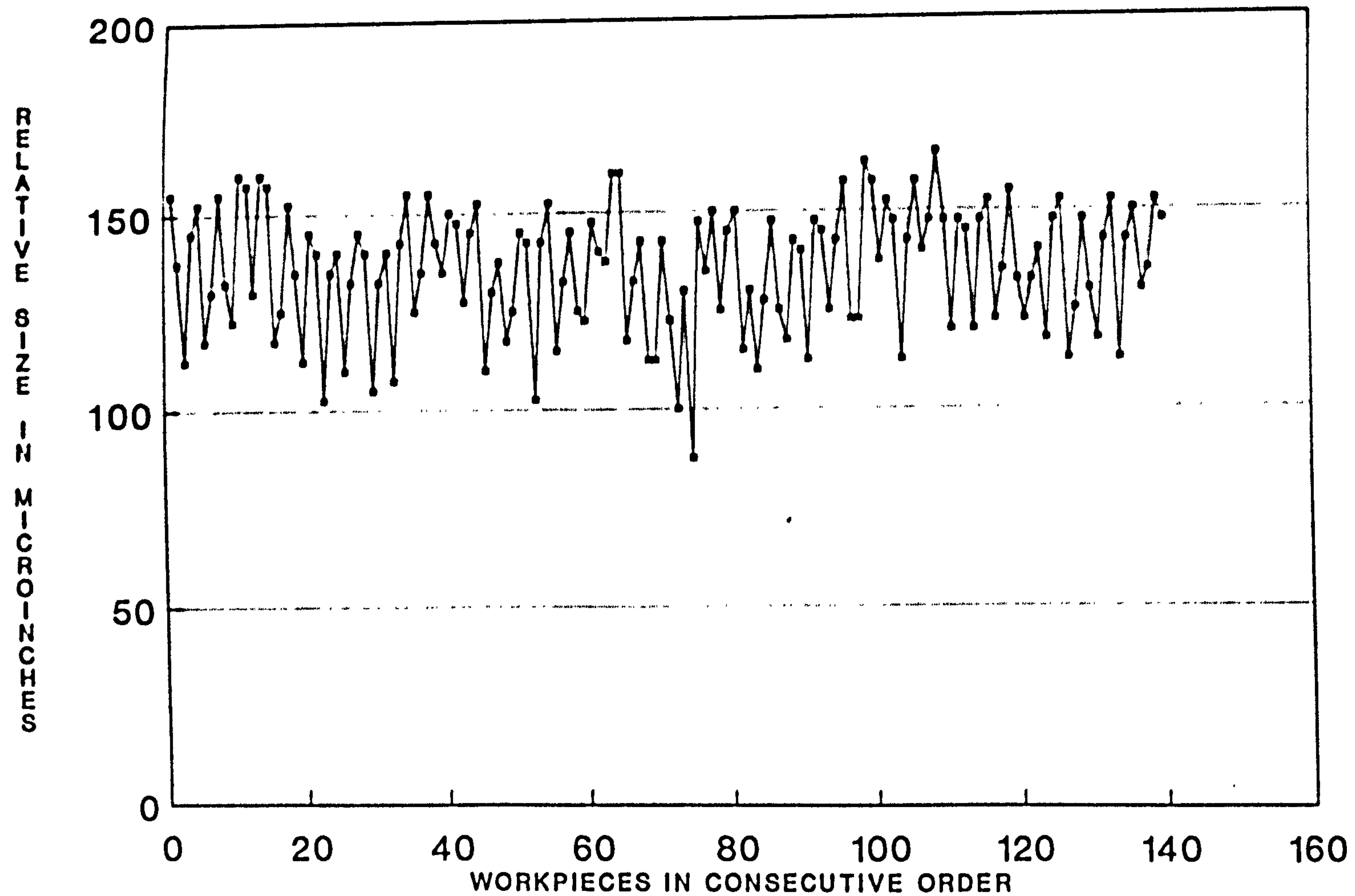




Figure 30. Rough cut size variation.

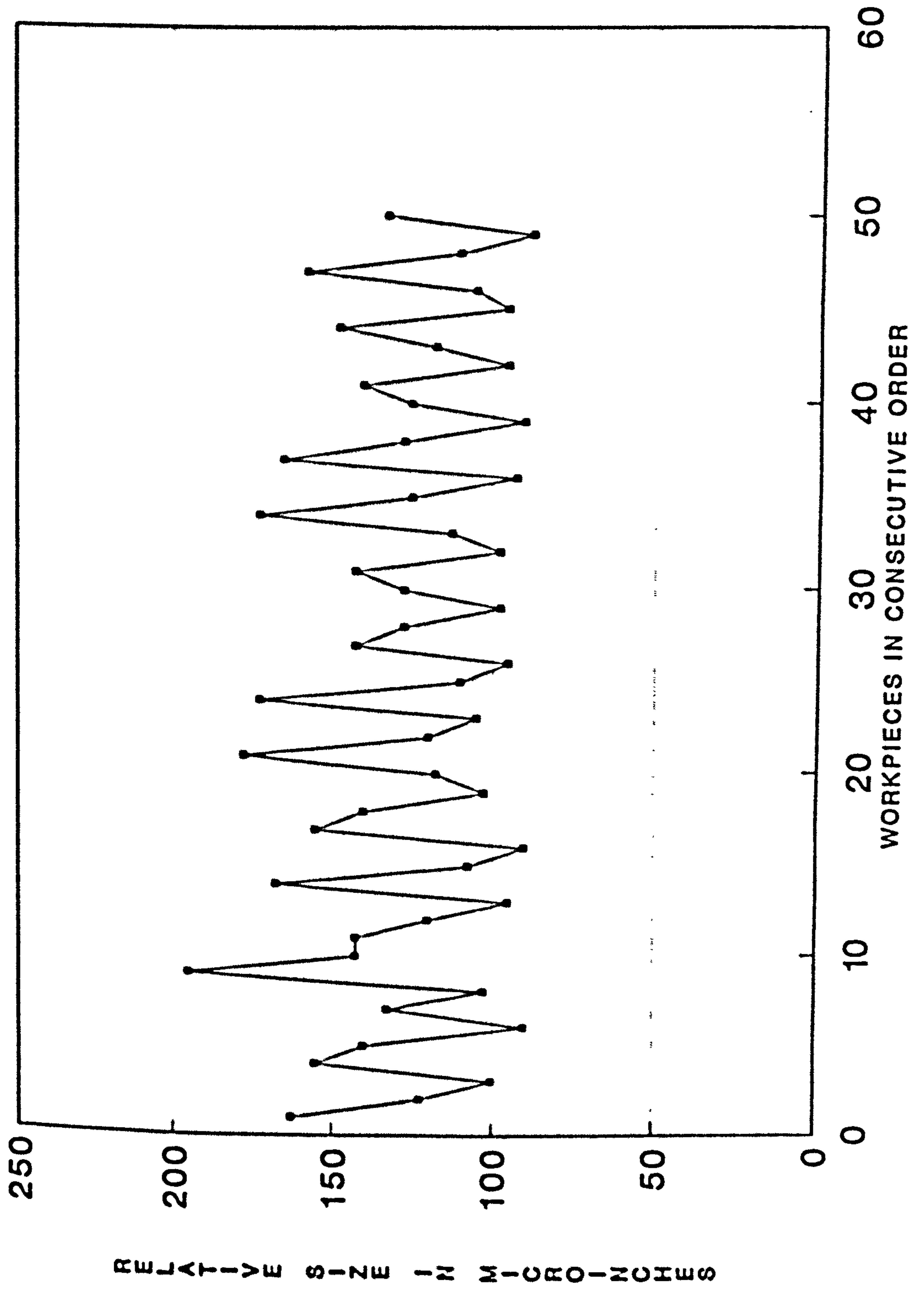


Figure 31. Finish cut size variation.

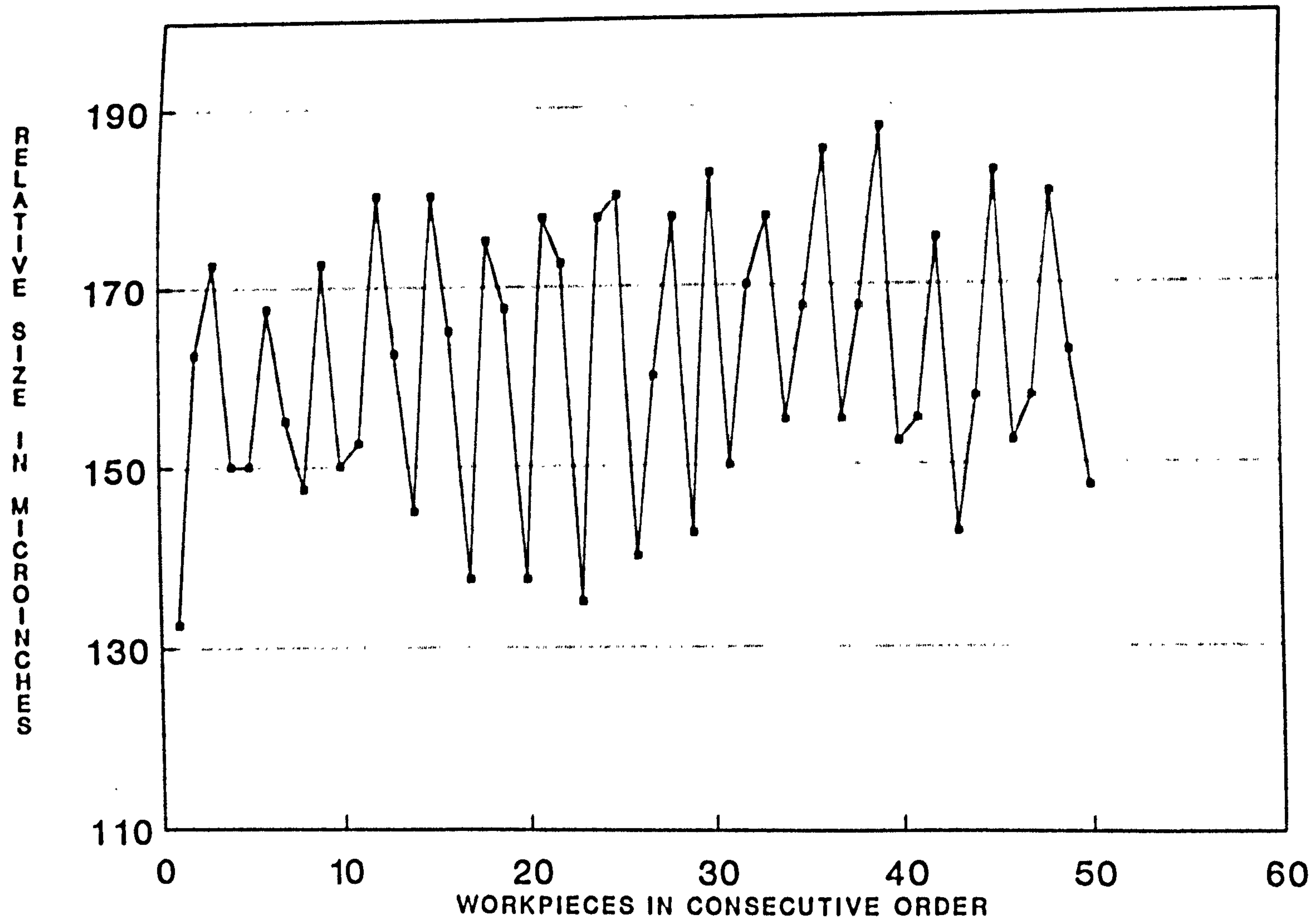


Figure 32. Size variation with  
conventionally dressed regulating wheel.

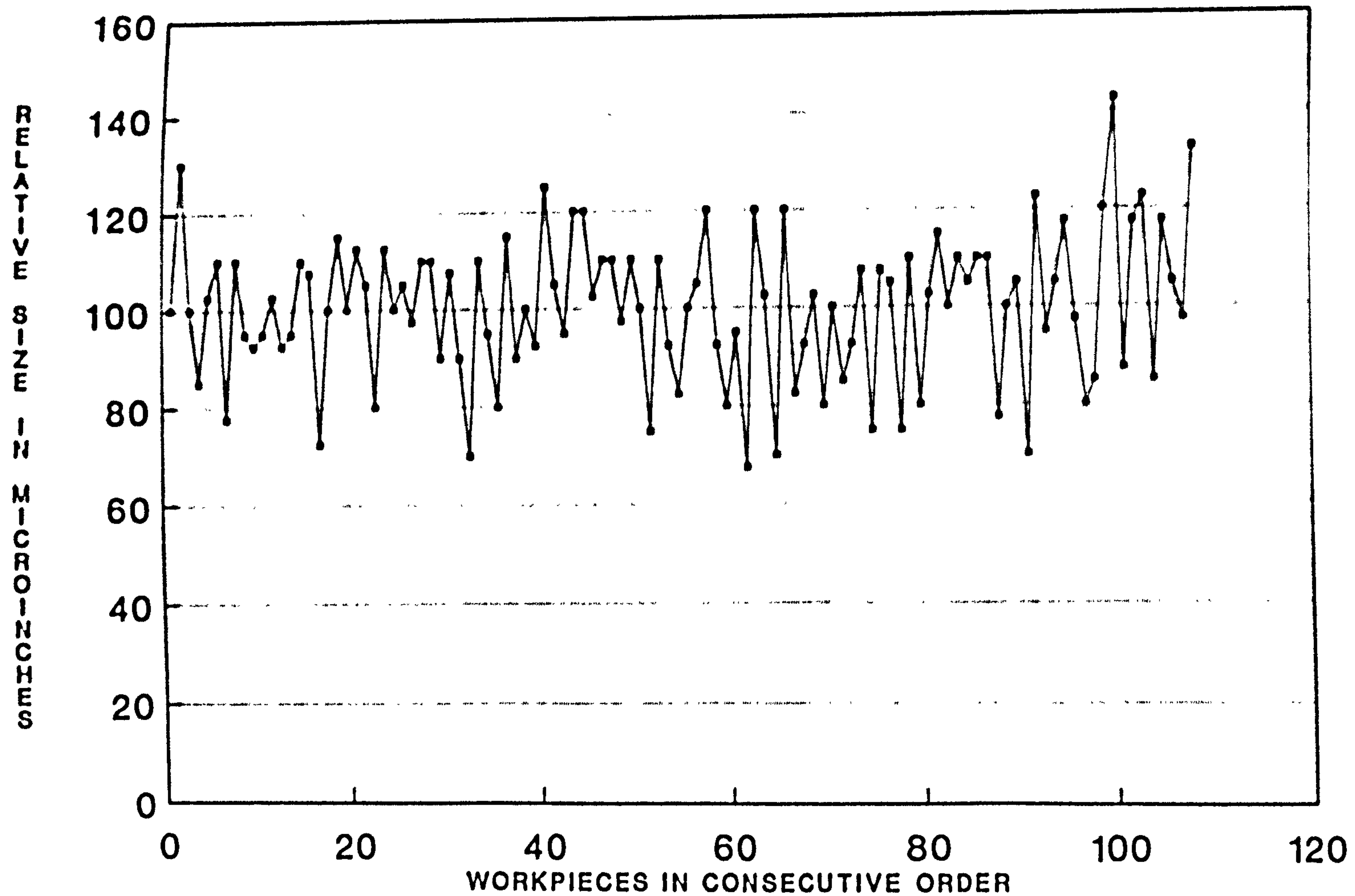
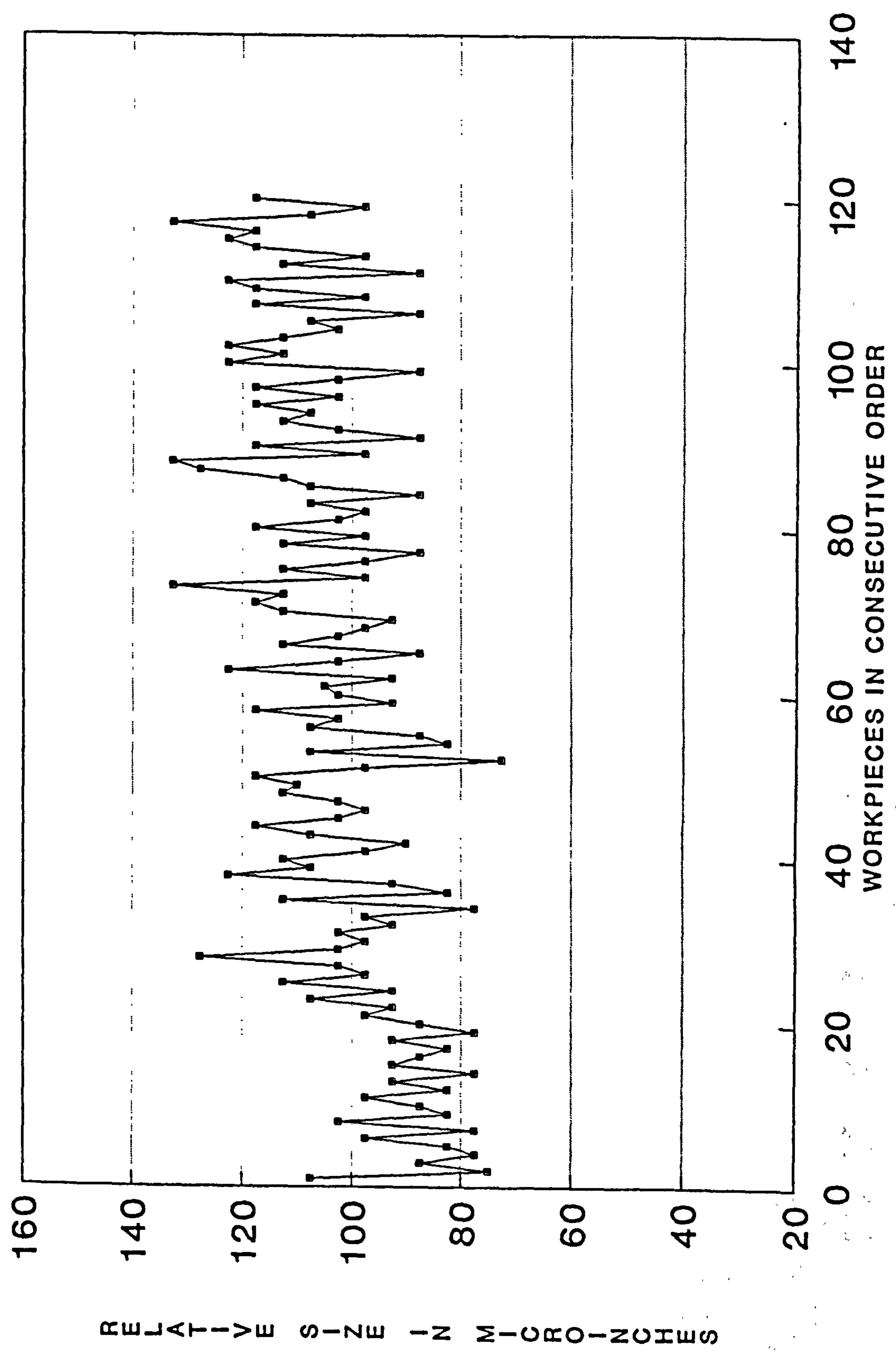


Figure 33. Size variation with  
plunge ground dressed regulating wheel.





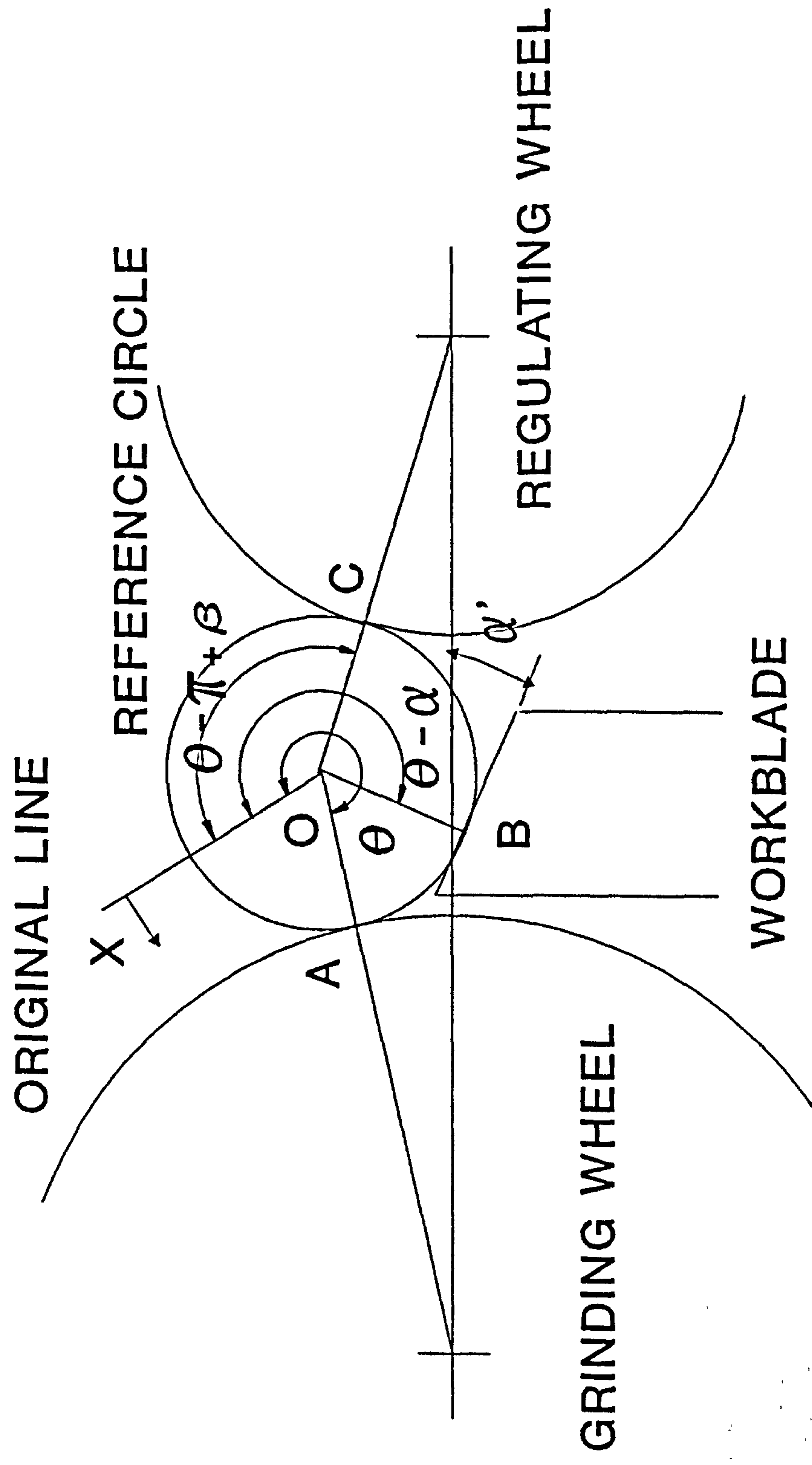
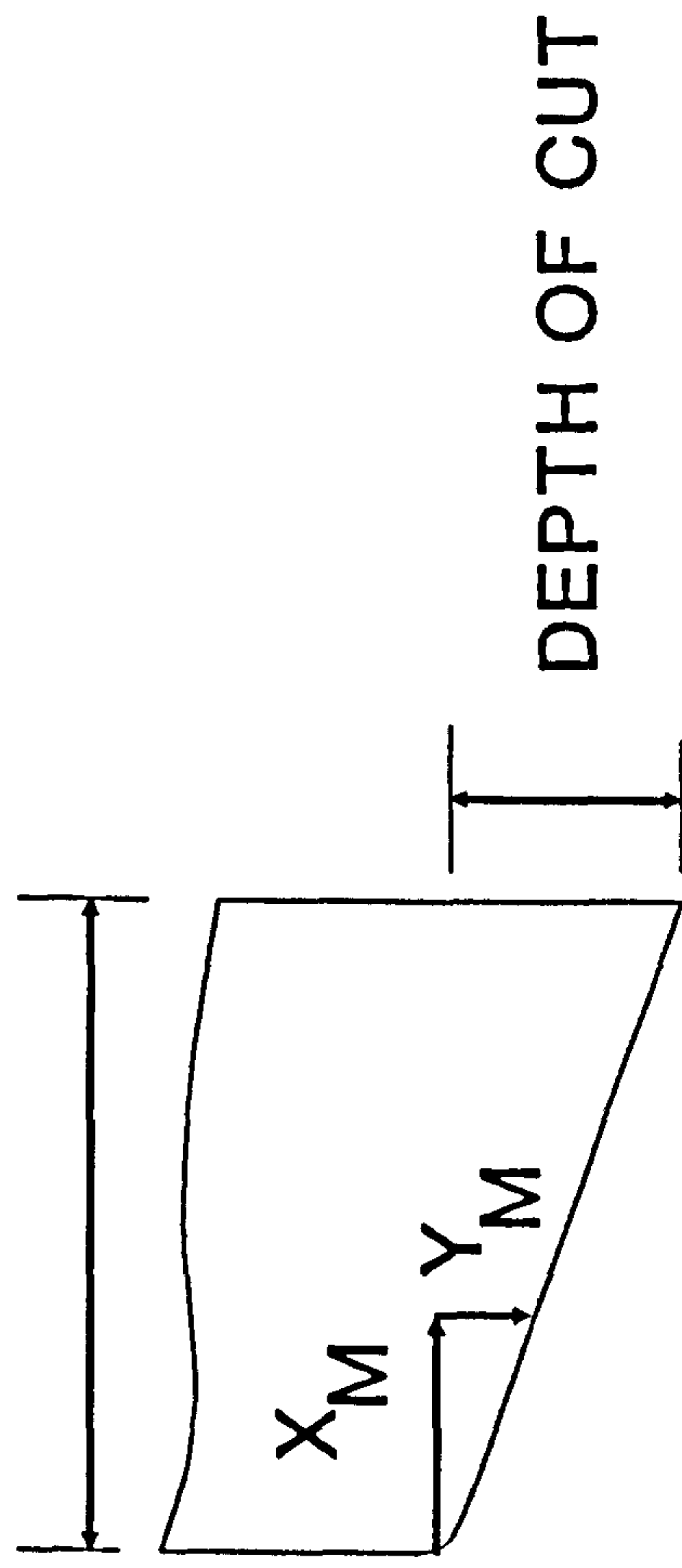
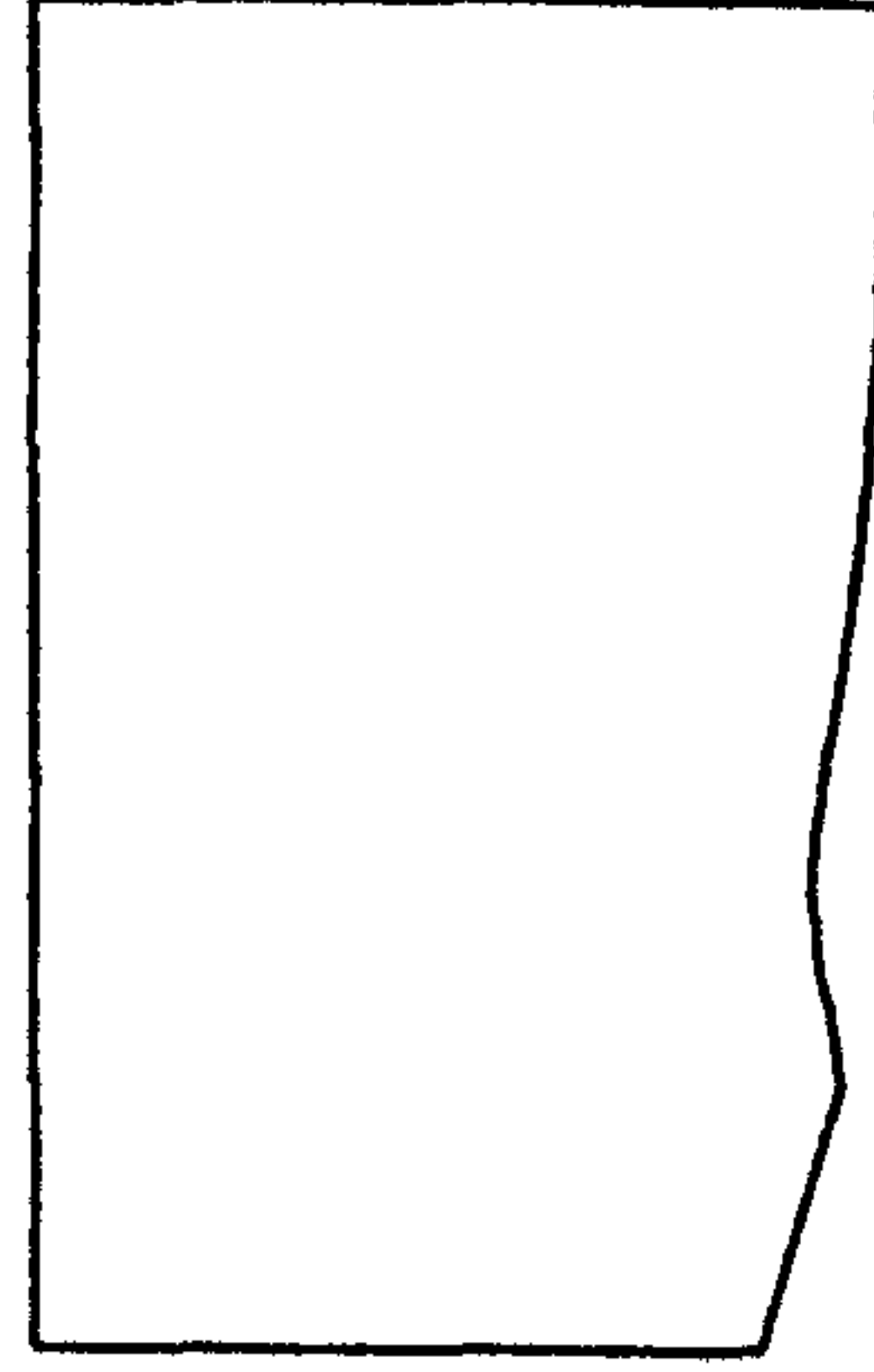


Figure 34. Visual representation of the equation of constraint (after Rowe).

EFFECTIVE REGULATING  
WHEEL WIDTH



DEPTH OF CUT



GRINDING WHEEL

Figure 35. Condition for tapered regulating wheel.

Figure 36. Flowchart of the computer simulation of the throughfeed centreless grinding process.

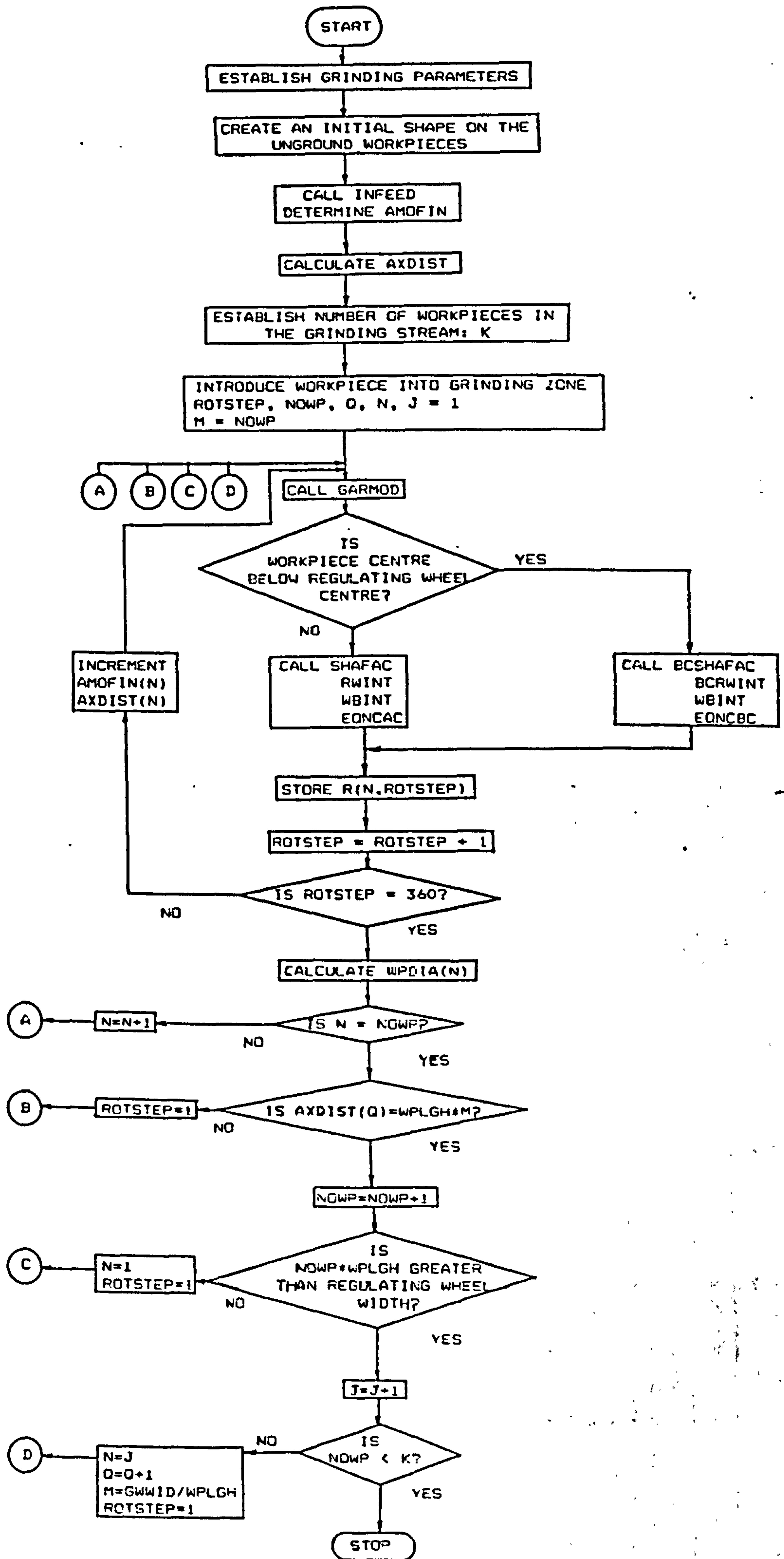


Figure 37. Graphical results  
of computer simulation for  $K = 0.3$ .

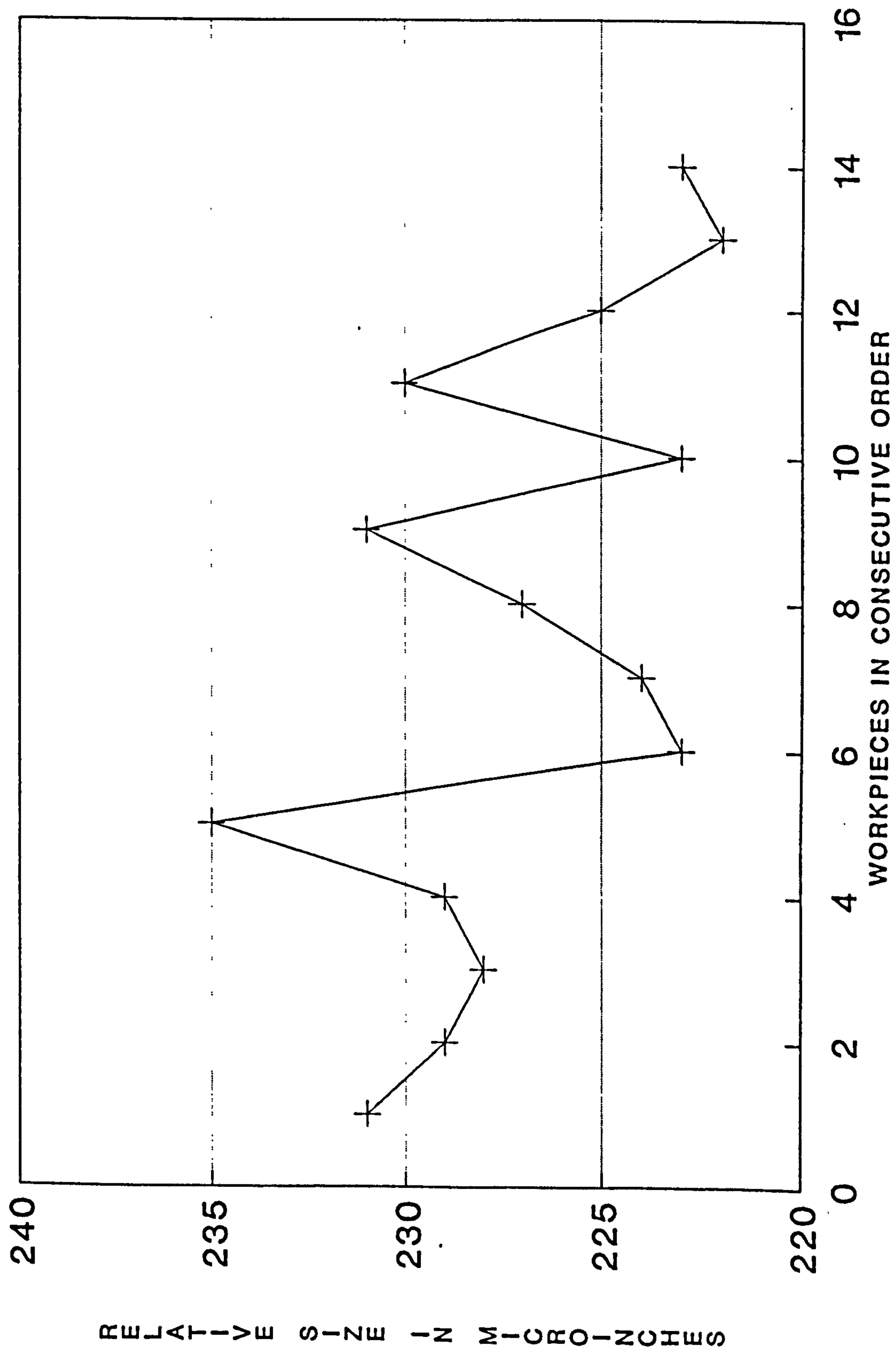
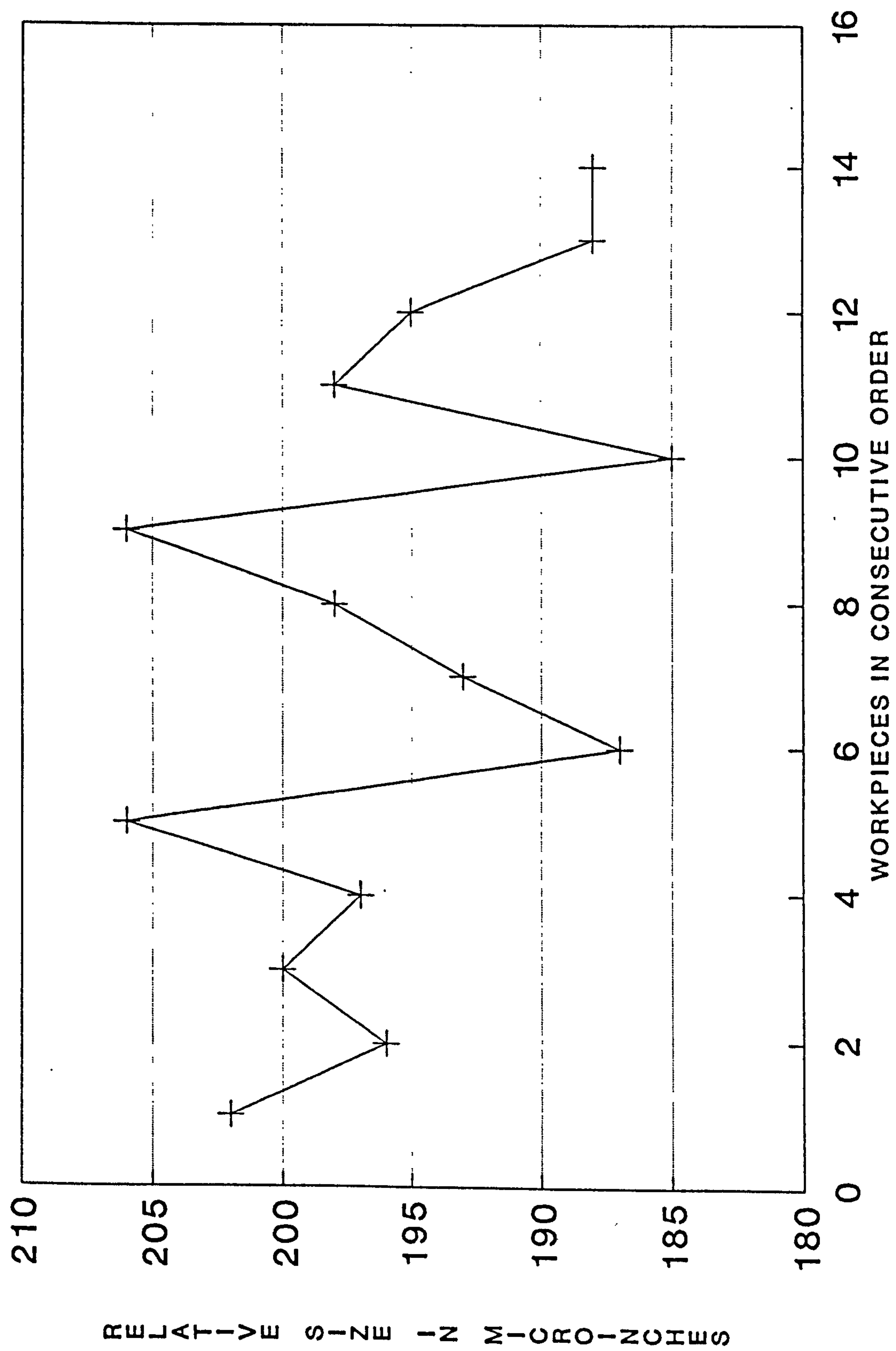


Figure 38. Graphical results  
of computer simulation for  $K = 0.7$ .





## TABLES.

Table 1. Back-pressure evaluation.  
Number of workpieces in 5 seconds.

	<u>TUBE</u>	<u>NON-TUBE</u>
	87	82
	85	86
	81	81
	84	84
	82	88
AVERAGE	83.8	84.2

Table 2. Surface roughness of Tube and Non-Tube parts (early runs).

<u>PART NUMBER</u>	<u>TUBE</u>	<u>NON-TUBE</u>
1	22 $\mu\text{in}$ ( $R_a$ )	13 $\mu\text{in}$
2	24 $\mu\text{in}$	13 $\mu\text{in}$
3	26 $\mu\text{in}$	11 $\mu\text{in}$
AVERAGE	24 $\mu\text{in}$	12.33 $\mu\text{in}$

Table 3. Surface roughness of Tube and Non-Tube parts (later runs).

<u>PART NUMBER</u>	<u>TUBE</u>	<u>NON-TUBE</u>
1	13 $\mu\text{in}$ ( $R_a$ )	13 $\mu\text{in}$
2	13 $\mu\text{in}$	13 $\mu\text{in}$
3	12 $\mu\text{in}$	13 $\mu\text{in}$
AVERAGE	12.66 $\mu\text{in}$	13 $\mu\text{in}$

Table 4. Out-of-roundness of Tube and Non-Tube parts (early runs).

<u>PART NUMBER</u>	<u>TUBE</u>	<u>NON-TUBE</u>
1	56 $\mu$ in	32 $\mu$ in
2	72 $\mu$ in	28 $\mu$ in
3	68 $\mu$ in	24 $\mu$ in
AVERAGE	63.5 $\mu$ in	28 $\mu$ in




Table 5. Out-of-roundness of Tube and Non-Tube parts (later runs).

<u>PART NUMBER</u>	<u>TUBE</u>	<u>NON-TUBE</u>
1	51 $\mu$ in	47 $\mu$ in
2	67 $\mu$ in	59 $\mu$ in
3	51 $\mu$ in	75 $\mu$ in
4	59 $\mu$ in	35 $\mu$ in
5	-	55 $\mu$ in
AVERAGE	57 $\mu$ in	54 $\mu$ in

**Table 6. Size measurements over one workpiece revolution.**

Part rotation  
(degrees)  
Part size  
over datum  
(microinches)

0		360
75	80 80 95 85	75
75	85 95 85	75

**Maximum diameter: 95 microinches + datum**

**Minimum diameter: 75 microinches + datum**

**Average diameter: 85 microinches + datum**

**Table 7. Multiple shot measurement of a  
needle roller.**

<b>MEASUREMENT NUMBER</b>	<b>SIZE OVER DATUM (MICROINCHES)</b>
-------------------------------	--

1	85
2	80
3	80
4	80
5	90
6	85
7	85
8	90
9	95
10	90
11	80
12	95
13	85
14	95
15	85

Table 8. Operator variability - 20 piece sample size: Operator 1 versus Operator 2.

***** S T A T G R A P H I C S *****			
Twosample Analysis			
	Sample 1	Sample 2	Pooled
Sample Statistics: Number of Obs.	20	20	40
Average	6.125	11	8.5625
Variance	1037.81	875.263	956.538
Std. Deviation	32.2151	29.5848	30.9279
Median	3.75	5	5
Conf. Interval For Diff. in Means:	95	Percent	
(Equal Vars.) Sample 1 - Sample 2	-24.6787	14.9287	38 D.F.
(Unequal Vars.) Sample 1 - Sample 2	-24.6834	14.9334	37.7 D.F.
Conf. Interval for Ratio of Variances:	0	Percent	
Sample 1 ÷ Sample 2			
Hypothesis Test for H0: Diff = 0	Computed T statistic = -0.498452		
vs alt: NE	Sig. Level = 0.621038		
at Alpha = 0.05	so do not reject H0.		

Table 9. Operator variability - 20 piece  
sample size: Operator 1 versus Operator 3.

```

***** S T A T G R A P H I C S *****
              Twosample Analysis

Sample Statistics: Number of Obs.      Sample 1      Sample 2      Pooled
                        Average          13.5          5.75          9.625
                        Variance        1366.05        761.25        1063.65
                        Std. Deviation  36.9601        27.5908        32.6137
                        Median          12.5           8.75           10

Conf. Interval For Diff. in Means:      95      Percent
(Equal Vars.)   Sample 1 - Sample 2    -13.1331  28.6331      38 D.F.
(Unequal Vars.) Sample 1 - Sample 2    -13.1887  28.6887      35.2 D.F.

Conf. Interval for Ratio of Variances:  0      Percent
                        Sample 1 ÷ Sample 2

Hypothesis Test for H0: Diff = 0          Computed T statistic = 0.751453
                        vs alt: NE          Sig. Level = 0.457009
                        at Alpha = 0.05     so do not reject H0.

```



Table 10. Operator variability - 20 piece  
sample size: Operator 2 versus Operator 3.

***** S T A T G R A P H I C S *****				
Twosample Analysis				
		Sample 1	Sample 2	Pooled
Sample Statistics: Number of Obs.		20	20	40
Average		11	5.75	8.375
Variance		875.263	761.25	818.257
Std. Deviation		29.5848	27.5908	28.6052
Median		5	8.75	6.25
Conf. Interval For Diff. in Means:		95	Percent	
(Equal Vars.)	Sample 1 - Sample 2	-13.0664	23.5664	38 D.F.
(Unequal Vars.)	Sample 1 - Sample 2	-13.0693	23.5693	37.8 D.F.
Conf. Interval for Ratio of Variances:		0	Percent	
Sample 1 ÷ Sample 2				
Hypothesis Test for H0: Diff = 0		Computed T statistic = 0.580383		
vs alt: NE		Sig. Level = 0.565083		
at Alpha = 0.05		so do not reject H0.		

Table 11. Operator variability - 20 piece  
sample size: Operator 1 versus Operator 1.

***** S T A T G R A P H I C S *****				
Twosample Analysis				
		Sample 1	Sample 2	Pooled
Sample Statistics: Number of Obs.		20	20	40
Average		6.125	13.5	9.8125
Variance		1037.81	1366.05	1201.93
Std. Deviation		32.2151	36.9601	34.6689
Median		3.75	12.5	8.75
Conf. Interval For Diff. in Means:		95	Percent	
(Equal Vars.)	Sample 1 - Sample 2	-29.5741	14.8241	38 D.F.
(Unequal Vars.)	Sample 1 - Sample 2	-29.5877	14.6377	37.3 D.F.
Conf. Interval for Ratio of Variances:		0	Percent	
Sample 1 ÷ Sample 2				
Hypothesis Test for H0: Diff = 0		Computed T statistic = -0.672701		
vs alt: NE		Sig. Level = 0.505208		
at Alpha = 0.05		so do not reject H0.		

Table 12. Operator variability - 10 piece  
sample size: Operator 1 versus Operator 2.

```

***** S T A T G R A P H I C S *****
              Twosample Analysis

Sample Statistics: Number of Obs.      Sample 1      Sample 2      Pooled
                          10              10              20
                          Average         12.5           14             13.25
                          Variance        1012.5          810            911.25
                          Std. Deviation  31.8198         28.4605        30.1869
                          Median          3.75            5              5

Conf. Interval For Diff. in Means:      95      Percent
(Equal Vars.)   Sample 1 - Sample 2    -29.8694  26.8694      18 D.F.
(Unequal Vars.) Sample 1 - Sample 2    -29.8945  26.8945     17.8 D.F.

Conf. Interval for Ratio of Variances:  0      Percent
                          Sample 1 ÷ Sample 2

Hypothesis Test for H0: Diff = 0        Computed T statistic = -0.111111
      vs alt: NE                        Sig. Level = 0.912758
      at Alpha = 0.05                  so do not reject H0.

```

Table 13. Operator variability - 10 piece  
sample size: Operator 1 versus Operator 3.

***** S T A T G R A P H I C S *****				
Twosample Analysis				
		Sample 1	Sample 2	Pooled
Sample Statistics: Number of Obs.		10	10	20
Average		23.25	15.75	19.5
Variance		1341.74	886.181	1113.96
Std. Deviation		36.6297	29.7688	33.376
Median		17.5	10	12.5
Conf. Interval For Diff. in Means:		95	Percent	
(Equal Vars.)	Sample 1 - Sample 2	-23.8665	38.8665	18 D.F.
(Unequal Vars.)	Sample 1 - Sample 2	-23.9608	38.9608	17.3 D.F.
Conf. Interval for Ratio of Variances:		0	Percent	:
Sample 1 ÷ Sample 2				
Hypothesis Test for H0: Diff = 0		Computed T statistic = 0.502472		
vs alt: NE		Sig. Level = 0.621427		
at Alpha = 0.05		so do not reject H0.		

Table 14. Operator variability - 10 piece sample size: Operator 1 versus Operator 1.

***** S T A T G R A P H I C S *****			
Twosample Analysis			
	Sample 1	Sample 2	Pooled
Sample Statistics: Number of Obs.	10	10	20
Average	12.5	23.25	17.875
Variance	1012.5	1341.74	1177.12
Std. Deviation	31.8198	36.6297	34.3092
Median	3.75	17.5	10
Conf. Interval For Diff. in Means:	95	Percent	
(Equal Vars.) Sample 1 - Sample 2	-42.9934	21.4934	18 D.F.
(Unequal Vars.) Sample 1 - Sample 2	-43.0387	21.5387	17.7 D.F.
Conf. Interval for Ratio of Variances:	0	Percent	
Sample 1 ÷ Sample 2			
Hypothesis Test for H0: Diff = 0	Computed T statistic = -0.700621		
vs alt: NE	Sig. Level = 0.492497		
at Alpha = 0.05	so do not reject H0.		



Table 15. Computed regulating wheel shape when  
ground with grinding wheel.

$D_R$	$D_W$	$\alpha$	$\alpha_3$	$H_1$	$X_R$	$R_R$	$Y_V$
10.922	21.188	4	2.33	0	4	5.463426	5.427149
10.922	21.188	4	2.33	0	3	5.462365	5.433724
10.922	21.188	4	2.33	0	2	5.461606	5.439698
10.922	21.188	4	2.33	0	1	5.461151	5.445071
10.922	21.188	4	2.33	0	0	5.461000	5.449846
10.922	21.188	4	2.33	0	-1	5.461151	5.454024
10.922	21.188	4	2.33	0	-2	5.461606	5.457606
10.922	21.188	4	2.33	0	-3	5.462365	5.460594
10.922	21.188	4	2.33	0	-4	5.463426	5.462989

Table 16. Workpiece diameter change as a function of axial location.

Workpiece number	Roller diameter pre-ground (inches)	Roller diameter post-ground (inches)	Difference (inches)
1	0.0960	0.0959	0.0001
2	0.0961	0.0955	0.0006
3	0.0960	0.0947	0.0013
4	0.0959	0.0941	0.0018
5	0.0960	0.0936	0.0024
6	0.0960	0.0936	0.0024
7	0.0959	0.0940	0.0019
8	0.0959	0.0945	0.0014
9	0.0961	0.0952	0.0009
10	0.0961	0.0960	0.0001
11	0.0960	0.0960	0.0000

Workpiece number 1 was at grinding gap exit.

Workpiece number 11 was at grinding gap entrance.

Table 17. Effect of changing throughfeed angle  
on regulating wheel axial profile.

$X_M$	$\alpha_3$	$Y_V$				
		$4^\circ$	$3^\circ$	$2.33^\circ$	$1^\circ$	$0^\circ$
4		5.427149	5.434845	5.439473	5.447422	5.452332
3		5.433724	5.438906	5.442077	5.447669	5.451268
2		5.439698	5.442763	5.444679	5.448163	5.450508
1		5.445071	5.446417	5.447281	5.448906	5.450052
0		5.449846	5.449870	5.449882	5.449897	5.449900
-1		5.454024	5.453120	5.452482	5.451135	5.450052
-2		5.457606	5.456168	5.455080	5.452622	5.450508
-3		5.460594	5.459016	5.457678	5.454356	5.451268
-4		5.462989	5.461662	5.460275	5.456337	5.452332

Table 18. Effect of changing trueing angle  
on regulating wheel axial profile.

$X_M$	$\alpha_3$	$Y_V$				
		$4^\circ$	$3^\circ$	$2.33^\circ$	$1^\circ$	$0^\circ$
4	5.431877	5.428744	5.427149	5.425155	5.424706	
3	5.436381	5.43462	5.433724	5.432604	5.432352	
2	5.440878	5.440096	5.439698	5.439201	5.439089	
1	5.445366	5.44517	5.445071	5.444947	5.444919	
0	5.449846	5.449846	5.449846	5.449846	5.449846	
-1	5.454318	5.454123	5.454024	5.4539	5.453872	
-2	5.458782	5.458003	5.457606	5.45711	5.456999	
-3	5.463238	5.461486	5.460594	5.45948	5.459228	
-4	5.467686	5.464573	5.462989	5.461008	5.460562	